The Effect of Non-Ionic Surfactants on the Potentiometric Response of Ion Selective Electrodes

Morten Karlsen

9. juni 2009

Resumé

I dette speciale undersøges ikke-ioniske overfladeaktive stoffers indvirkning på Ionselektive Elektroders (ISE) potientiometriske respons.

Specialet bygger på et samarbejde med firmaet Radiometer Medical Aps., hvor eksperimenterne er udført. Radiometer bruger ISE-teknologi til blodgasmålinger. Deres eksperimentelle platform benyttes til eksperimenterne i dette speciale.

Den interfererende effekt af overfladeaktive stoffer er tidligere blevet observeret af forskere på Radiometer. De overfladeaktive stoffer ændrer potentialet med op til 5 mV, svarende til en ændring i ionkoncentration på 20%. Dette er interessant, da det involverede overfladeaktive stof ikke er ladet.

Overfladeaktive stoffers påvirkning af Ionselektive Elektroder er generelt ikke underbygget teoretisk, og der mangler forståelse på området. Dette speciale gennemgår grundlæggende elementer af de fremherskende etablerede teorier og præsenterer en model der beskriver surfaktantresponset under særlige forhold.

Overfladeaktive stoffers generelle egenskaber bliver undersøgt, og relateret til problemstillingen. Responset bliver undersøgt ved forskellige koncentrationer af de overfladeaktive stoffer, for at finde mønstre og mulige forklaringer. Der er fokuseret på surfaktanter af typen "ethoxylerede acetylenske dioler", og særligt på en magnesiumselektiv elektrode.

Ionselektive Elektroders virkemåde og funktion undersøges gennem eksperimenter, og det undersøges om surfaktanter har en indvirkning på de karakteristiske parametre for en elektrode: Følsomhed og Selektivitet. Dernæst undersøges responsets koncentrationsafhængighed i detaljer.

Der observeres en klar koncentrationsafhængighed. For sensorer der ikke tidligere har været udsat for surfaktanter ses en meget markant effekt. Dette respons kan fittes til en model.

For sensorer, der har været i brug et stykke tid, observeres en lineær relation mellem potentiale og koncentration. Dette er overraskende, da gængse modeller forudsiger en logaritmisk relation.

Der observeres desuden fænomener med en tidskonstant, der er meget længere end normalt observeret.

Specialet sandsynliggør at responset skyldes kompleksering med ioner på overfladen af den Ionselektive Elektrode.

Abstract

This thesis investigates the interfering effects of certain non-ionic surfactants on the potentiometric response of polymer-membrane based Ion Selective Electrodes (ISE). It is focused on the surfactant type "ethoxylated acetylenic diol".

The interfering effect of certain surfactants has been observed by researchers at Radiometer Medical Aps.. They have measured a change in potential of 5mV, corresponding to a change in ion concentration of 20%, when changing surfactant concentration. This is fundamentally interesting, since the surfactant itself is not charged.

The technology of ISE's for Blood Gas measurement is introduced and fundamental theoretical models of ISE systems are introduced. General properties of non-ionic surfactants in relation to ISE technology are introduced. A model describing the interfering effect through the complexating behavior of surfactants is introduced and adapted.

Experiments are performed to investigate the influence of the surfactant on the standard parameters of a sensor, i.e. ion sensitivity and selectivity, and investigates the direct potential change caused by a change in surfactant concentration, i.e. the surfactant sensitivity. The experiments are performed on magnesium-selective sensors and dummy-sensors with the same membrane composition but without ionophore.

The sensors with membranes without ionophores demonstrate a very high sensitivity towards changes in surfactant concentration.

For new sensors without previous exposure to surfactant, a nernstian response to changes in surfactant concentration is observed, and fitted to a theoretical model.

For pre-exposed sensors a linear relation between potential an concentration is observed. This is surprising since all theoretical models predict a logarithmic relation.

The results indicate that the interference is caused by complexation of surfactant and ions at the surface of the sensor membrane. The data can be fitted to a model model describing this behavior.

The existence of two phenomena with different timescales is documented.

The thesis is based on a cooperation with the company Radiometer Medical Aps., where the experiments have been performed. Radiometer uses ISE technology for blood gas measurements. Their experimental platform is used for the experiments in this thesis.

Acknowledgements

I would like to thank my external supervisor Poul Sørensen, without whom this project would never have happened, for his open minded approach to all my thoughts and ideas. And to Thomas Heimburg at NBI for his patience.

I would like to thank everybody working at the research and development department at Radiometer for their support and open-mindedness, and willingness to discuss my ideas. Especially Thomas, Thomas and Thomas for the many discussions, model-constructions and feedback.

Radiometer

This thesis is based on a project proposed by Radiometer Medical Aps., 2700 Brønshøj, Denmark. Throughout this thesis the company will be referred to simply as "Radiometer".

Due to the nature of the project, some information is confidential. This is generally contained in appendices which are not publicly available. For access to the appendices, please contact the author of the present thesis.

Notation and Abbreviations

As is customary in technology-oriented scientific literature, a wide range of acronyms will be used throughout this thesis. They will be introduced as they appear, and are summarized in table 1 below.

Table 1: Acronyms

ABL	A blood gas analyser developed by Radiometer
CWE	Coated Wire Electrode
FIM	Fixed Interference Method
ISE	Ion Selective Electrode
IUPAC	International Union of Pure and Applied Chemistry
LMSC	Liquid Membrane Solid Contact electrode

The notation for chemical properties and physical constants will follow IUPAC's recommendations [1] for Ion Selective Electrode-related papers.

Table 2: Terms

c_i	Concentration of substance i
$[K]$	Concentration of substance K
a_i	Activity of substance i
a_{aq}	Activity in Aquatic Phase
a_{org}	Activity in Organic Phase
E	Electric Potential
ϕ	Electric Field
G	Gibbs Free Energy
z_i	Charge of ion of species i
μ	Chemical Potential
$\overline{\mu}$	Electrochemical Potential
J_i/f_i	Flux of particles of species i
D_i	Diffusion coefficient of species i
δ	Nernst Diffusion Layer
S	Slope of Nernstian Response ($61.57m\mathrm{V}/z_i$ at 37°C)
K_{ij}^{pot}	Interference Coefficient

A wide range of chemicals are used, and will typically be referred to by their trivial abbreviation. Table A.1 in Appendix A includes most substances mentioned in this thesis. Structural diagrams can also be found in Appendix A.

Contents

Chapter 1

Introduction

1.1 Thesis Topic

In this thesis, the influence of non-ionic surfactants on the potentiometric response of Ion Selective Electrodes (ISE) is investigated.

The focus of the research will be a specific Magnesium-selective electrode and a non-ionic surfactant of the *acetylenic diol*-family.

The response of the ISE at different surfactant concentrations will be analyzed in detail to find patterns and possible explanations.

The thesis is written in cooperation with the company Radiometer Medical Aps., and is based on experiments performed at Radiometer.

1.2 Motivation

The company Radiometer produces and uses Ion Selective Electrodes (ISE), for blood gas measurements. Using several different techniques, they can measure the concentration of 15 different ions and other substances dissolved in the blood.

Recently, they have begun a process of miniaturization of the ISE which has presented them with problems, that are generally not well described in existing theory. Certain effects arise from macromolecules like proteins in the blood sample, while others arise when rinsing the Ion Selective Electrode between two samples.

Specifically, they have discovered that certain non-ionic surfactants in the rinse liquid may cause a shift in the measurement on some sensors, corresponding to a change in concentration of ions of up to 20%.

1.3 Introduction

My goal is to research why and how a non-ionic surfactant can effect the measurement on a specific Ion Selective Electrode (ISE).

Since the surfactant itself is not charged, this phenomenon is a bit of a mystery.

The theory describing the response of ion selective electrodes towards charged particles is quite developed, and can account for most observed phenomena, but no theory exists that adequately explains the response to neutral surfactant molecules.

The initial analysis performed by Radiometer showed that the magnitude of the response is dependent on the surfactant concentration; the higher the concentration of surfactant, the higher the potential difference

1.4 Theoretical Foundation

The theoretical foundation for describing the response to charged particles was laid in the early 20th century. Two schools have arisen, with continuous, and still ongoing, development of the theory. One school focuses on dynamical aspects of the process, such as ion transfer rates, while the other focuses on thermodynamical aspects, such as the difference in the electrochemical potential of an ion between two immiscible phases.

In many cases, the two schools have reached the same descriptive equations, even though they are fundamentally different in approach.

The strength of the thermodynamic school, is that the involved parameters are thermodynamic quantities, which are readily accessible experimentally, while a weakness of the theory is that the system must be at or near equilibrium.

The strength of the dynamic school, is that one does not need assumptions of equilibrium, and it is possible to describe time dependent phenomena. The disadvantage is that the models rely on knowledge of e.g ionic mobilities in all parts of the system, parameters which are not readily measureable, or possible to predict from theory.

This thesis will build on both schools. I will attempt to relate them to my own understanding from biophysics.

1.5 General Introduction to Ion Selective Electrodes

Ion Selective Electrodes (ISE) are a class of instruments used to measure ion concentrations in a solution containing several species of ions. In figure 1.5 the conventional construction of an Ion Selective Electrode is illustrated.

Several types exist, but the relevant for this project is the Liquid Bulk Membrane type, which consists of a thick ($\approx 100\mu m$) plasticized hydrophobic PVC membrane, containing ionophore molecules, that is, molecules with a higher complexation rate for a specific ion than for any other ion. See figure 1.2 for an example of a K^+ specific ionophore.

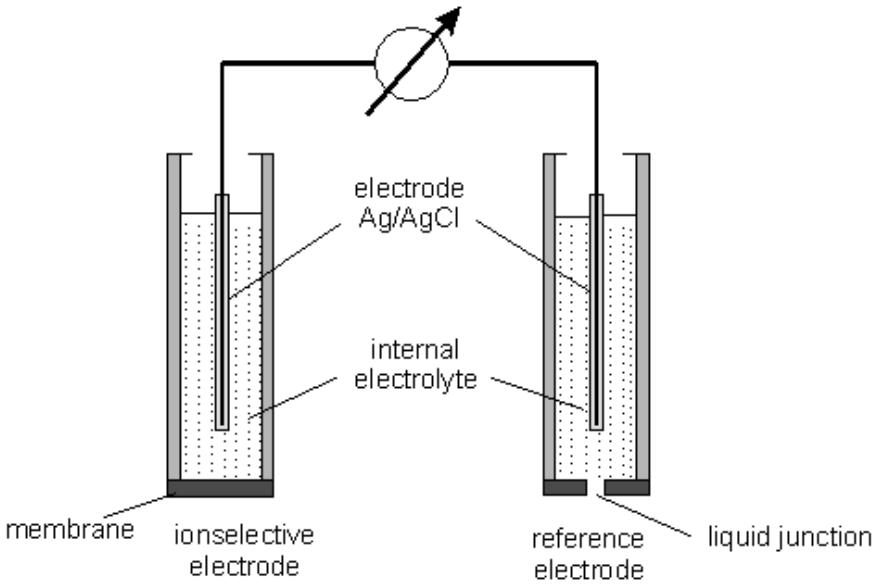

Figure 1.1: Schematic drawing of an ISE. Both electrodes are immersed in the sample.

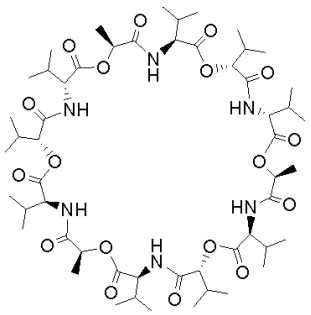

Figure 1.2: Valinomycin, a K^+ specific ionophore.

In the most simplified case, the potential can be described by the Nernst equation for Zero Current Potential (EMF) [2, eq.(6.4)];

$$E = E_i^\circ + \frac{RT}{z_i F} \ln a_i', \tag{1.1}$$

where a_i is the activity of the ion for which the sensor is specific.

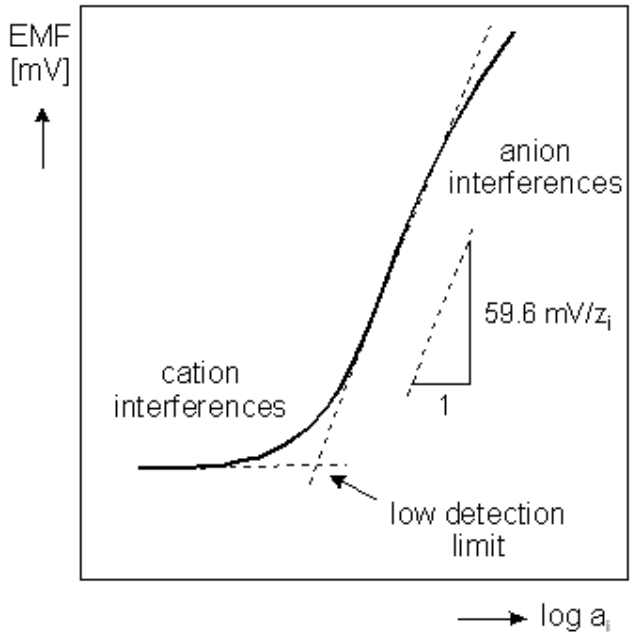

Figure 1.3: Illustration of the response of an ISE. The linear activity range is called the *Nernstian regime*, and follows equation (1.1).

1.6 Problem Description and Method

An interfering effect of a non-ionic surfactant had been observed by researchers at Radiometer. This effect changed the potential of an ion selective electrode by up to 5 mV, corresponding to a change in ion-activity of 20%.

This effect was found to be proportional to the concentration of the surfactant. Furthermore it was reversible and reproducible.

Not all sensors show a response towards the non-ionic surfactant.

To simplify the problem, I have chosen to analyze a single type of Magnesium selective sensor. The composition of this sensor is simplified, to identify key interactions.

Inspection of the Nernst equation equation (1.1), shows that a positive change in potential follows from a higher positive charge at the membrane surface. How this is related to the non-ionic surfactant is not clear.

There do not seem to be any generalized results in this area, and this thesis will analyze a single example of the challenges in this field.

To establish et baseline, a series of experiments will be performed to verify the ISE's response towards ions without surfactant present.

These experiments will then be repeated with surfactant present.

Furthermore, experiments will be performed where the surfactant con-

centration is changed, but where the ion concentration is kept constant.

1.7 Outline of Research

A sensor is chosen to be the target of the research. A Magnesium-sensitive ISE is chosen, as it displays the interference phenomena clearly.

This sensor is tested and compared with similar sensors. It is compared with a sensor with the same composition, but without lipophilic salt, and without ionophore.

The influence of a single type of surfactant on the potential is investigated.

1.7.1 Theoretical Foundation

The theoretical description of an ISE's response to charged particles is examined. The two main approaches are exemplified and compared, and their applicability is analyzed.

A model developed to explain the response of a specific sensor towards certain non-ionic surfactants will be analyzed.

This is documented in Chapter 2.

1.7.2 Practical Foundation

The concept of ISE's can be implemented in many ways. I will present and explain the technology as it is developed by Radiometer, in order to understand and be able to perform experiments. The "state of the art" of ISE technology will be described in Chapter 3.

1.7.3 Understanding of Surfactants

To understand the effect of surfactants in ISE systems, it is first necessary to understand the general properties of surfactants, their behavior, and the reasons for having surfactants in the system. This is done in Chapter 4.

1.7.4 Standard Response

An ISE is characterized by some standard parameters, i.e. sensitivity and selectivity, based on solid theoretical ground. These parameters are found experimentally, and the effect of surfactant on them analyzed.

This is done through experiments described in Chapter 6.

All experiments are performed on Radiometers experimental platform, which will be described in Chapter 5.

1.7.5 Surfactant Response

The direct effect of a change in surfactant concentration will be analyzed. Experiments with varying concentrations of surfactants will be performed, with the aim of reproducing the findings by Radiometer. These experiments are documented in Chapter 7.

1.7.6 Discussion and Modeling

The results from the experiments will be discussed in Chapter 9 and possible correlations and causes will be analysed. The key findings will be summarized, and future research areas to document the validity of the results will be suggested.

Chapter 2

Theory of Ion-Selective Electrodes

This chapter introduces the basic theoretical foundation of Ion Selective Electrodes. Since the field is in constant development, it cannot hope to cover it all .

The chapter describes the conventional ISE system, and the models that have been developed to describe it.

It introduces the two main approaches to modelling of the system: The Thermodynamic approach and the Kinetic approach.

For the description of potentiometric sensors both of these approaches assume a zero current steady state, in which charge builds up at interfaces.

Potentiometric sensors may not always be in a steady state, and some models describing time dependence are introduced.

The interference from non-ionic surfactants is not part of the established theories, but a few models have been developed that may describe it in specific cases. One of these are presented.

It is based primarily on two books, Morf [2] and Silver [3], as well as several recent review articles: Bakker et al. [4], Pretsch [5] and Makarychev-Mikhalov et al. [6]. A model to describe the effect of surfactants, developed by Sak-Bosnar et al. [7], is introduced and adapted.

2.1 Introduction to Ion Selective Electrodes

Ion Selective Electrodes (ISE) are electrochemical sensors that allow potentiometric determination of the activity of certain ions in the presence of other ions. Such an electrode consists of a galvanic half-cell. In the conventional construction, depicted in figure 2.1, it consists of an ion-selective membrane, an internal contacting solution and an internal reference electrode, all housed in a single body. The other half-cell is an external reference electrode, immersed in a reference electrolyte. The reference electrolyte is connected to

the sample through a salt bridge, that maintains a steady potential.

The circuit of an Ion Selective Electrode is illustrated in figure 2.1.

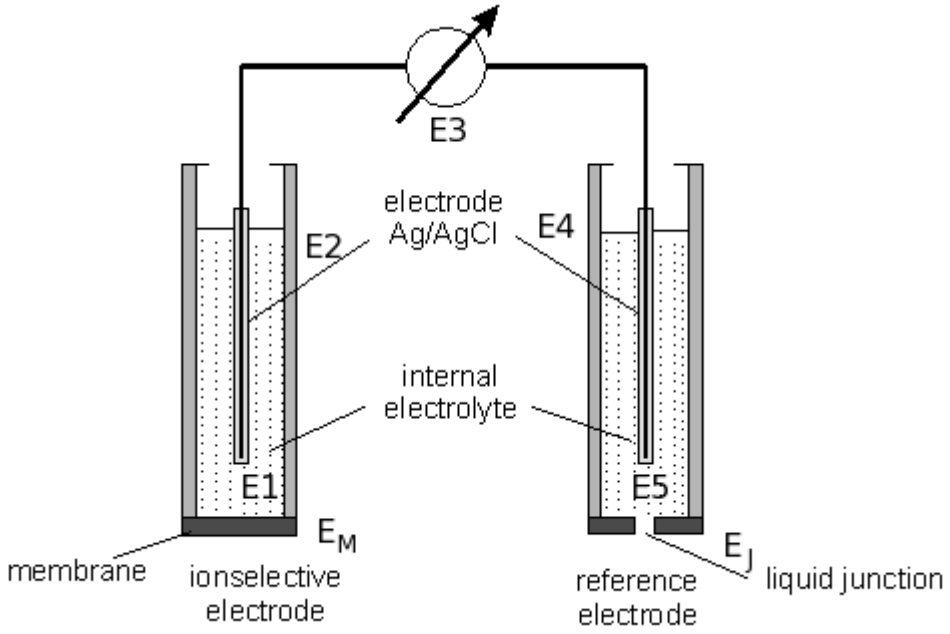

Figure 2.1: Schematic drawing of an ISE measuring circuit. E_1-E_5 are contributions that are assumed constant. E_M is the membrane potential, and E_J is the liquid junction potential of the reference electrode.

Each phase boundary may give rise to a potential.

The total potential can be separated into a contribution from each interface in the system, as they may give rise to a potential difference, whether it is a liquid/liquid, a liquid/membrane, a liquid/solid or a solid/solid interface, see figure 2.1 for identification of the potentials.

$$E_{Total} = E_1 + E_2 + E_3 + E_4 + E_5 + E_M + E_J, \tag{2.1}$$

where E_1 to E_5 are contributions that are assumed to be constant, E_M is the Membrane Potential, and E_J is the so-called Liquid Junction Potential. The total potential is rewritten as

$$E_{Total} = E_0 + E_M + E_J, \quad E_0 = \sum_{i=1}^{5} E_i. \tag{2.2}$$

2.1.1 Nernstian Response

In the most simplified case, we make the following assumptions, and get an expression for the membrane potential which is surprisingly fundamental.

i) The membrane is ideal, i.e. infinitely thin and only permeable to one ion (denoted with the subscript i)

ii) The system is in equilibrium

iii) The standard chemical potential of the ion is the same on each side of the membrane

This system is shown in figure 2.2.

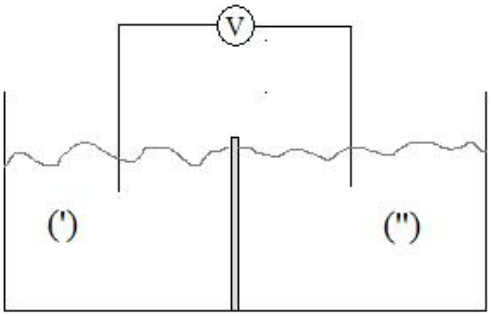

Figure 2.2: Infinitely thin membrane, with solutions (') and (").

From the equilibrium assumption follows,

$$\overline{\mu}_i' = \overline{\mu}_i'' \tag{2.3}$$

since the electrochemical potential must be the same at each side of the membrane. Writing this as the chemical potential plus a contribution from the electrostatic field (elaborated in section 2.2.1), we get:

$$\mu_i^{0\prime} + RT \ln a_i' + z_i F \phi' = \mu_i^{0\prime\prime} + RT \ln a_i'' + z_i F \phi''. \tag{2.4}$$

This gives the potential difference,

$$\phi'' - \phi' = \frac{\mu_i^{0\prime} - \mu_i^{0\prime\prime} + RT(\ln a_i' - \ln a_i'')}{z_i F}, \tag{2.5}$$

and since $\mu_i^{0\prime} - \mu_i^{0\prime\prime} = 0$ from assumption iii), the membrane potential is identified as

$$E_M = \phi'' - \phi' = \frac{RT}{z_i F} \ln \frac{a_i'}{a_i''}. \tag{2.6}$$

Inserting this in equation (2.2), and assuming that E_J is constant, we get:

$$E = E_0 + E_M = E_0 + \frac{RT}{z_i F} \ln \frac{a_i'}{a_i''} \approx E_0 + 2,303 \frac{RT}{z_i F} \log \frac{a_i'}{a_i''}. \tag{2.7}$$

If we furthermore assume that a_i'' is unchanged, this becomes the central Nernst equation for Zero Current Potential [2, eq.(6.4)]:

$$E = E_i^0 + \frac{RT}{z_i F} \ln a_i'. \tag{2.8}$$

2.1.2 Membrane Models

The model above is very simplified, yet it describes the response of a typical ISE surprisingly well within a certain concentration range, called the *Nernstian Response Regime*.

To allow for non-ideal behavior, more advanced models have been proposed, each with it's own set of approximations and limitations. There are generally two approaches to modeling: a thermodynamic and a kinetic approach.

The difference can be illustrated in the following extensions to the model above:

Membrane with thickness d:

Set up: Consider a membrane of thickness d, with an internal electrolyte on one side (noted $'$), and a sample on the other (noted $''$). This can be seen in figure 2.3. The total membrane potential can be divided into three contributions:

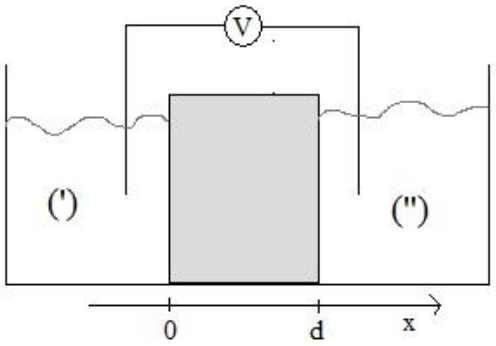

Figure 2.3: Membrane with thickness d, with solutions ($'$) and ($''$).

$$E_M = \phi'' - \phi' = \underbrace{(\phi(0) - \phi')}_{E_B'} - \underbrace{(\phi(d) - \phi'')}_{E_B''} + \underbrace{(\phi(d) - \phi(0))}_{E_D}. \tag{2.9}$$

The first two contributions are boundary potentials similar to the one described in equation (2.8), and will be named E_B' and E_B''. The third contri-

bution is a diffusion controlled potential, which will be described later, in section 2.2.2.

There are two approaches to calculating the boundary potentials:

Thermodynamic Approach: The boundary can be considered as a semipermeable membrane, and modeled similarly to previously, with the exception that the standard chemical potentials do not need to be the same. Rewriting equation (2.5) we get:

$$E_B = \phi'' - \phi' = \frac{\mu_i^{0\prime} - \mu_i^{0\prime\prime} + RT(\ln a_i' - \ln a_i'')}{z_i F} = \frac{RT}{z_i F} \ln \frac{k_i a_i'}{a_i''}, \tag{2.10}$$

where

$$k_i := \exp^{(\mu_i^{0\prime} - \mu_i^{0\prime\prime})/RT}. \tag{2.11}$$

Here k_i is an equilibrium constant between the chemical standard potentials at each side of the boundary. It is called the distribution coefficient.

Kinetic Approach: In this approach, the rate of transfer of ions through the membrane from each side are compared. The total flux density J_i is the sum of the flux in each direction, and may be formulated as[2]:

$$J_i := \overrightarrow{k}_i a_i' exp\left(-\alpha \frac{z_i F}{RT}(\phi(0) - \phi')\right) - \overleftarrow{k}_i a_i' exp\left(1 - \alpha \frac{z_i F}{RT}(\phi(0) - \phi')\right), \tag{2.12}$$

where $\alpha \approx 0.5$ is an exchange parameter. Since the system is in equilibrium, the total flux is zero ($J_i = 0$), and we get

$$a_i(0) = k_i a_i' exp\left(-\frac{z_i F}{RT}(\phi(0) - \phi')\right), \text{with} \quad k_i = \frac{\overrightarrow{k}_i}{\overleftarrow{k}_i}. \tag{2.13}$$

This can be rearranged to the form of equation (2.10), except that k_i now is defined kinetically.

2.1.3 General Assumptions

All membrane models share a number of assumptions about the system, in order to simplify the system enough to make a theoretical treatment feasible. These are summarised by Morf [2]:

i) There are no gradients of pressure and temperature across the membrane. The only driving forces to be considered are differences in concentrations and in electrical potential.

ii) A thermodynamic equilibirum exists between the membrane and each of the outside solutions at the respective phase boundaries.

iii) The same solvent is used for the electrolyte solutions on either side of the membrane.

iv) Within the membrane, all chemical standard potentials of all particles are invariant with space and time.

v) The effect of solvent flow over the membrane is negligible, i.e. there s no convective distribution to the flow of particles.

vi) every cell component is homogenous with respect to a direction perpendicular to the cell axis; therefore, concentration gradients and the concomitant potential differences are possible only along this cell axis.

vii) The system is in a zero-current steady-state.

viii) The mobilities of all particles within the membrane are invariant.

Furthermore, since the ion-selective membrane measures single-ion activities, some assumptions regarding these are needed:

ix) a) The local activity coefficients are the same for all ions in the membrane (McInnes convention) *or*

b) The individual activity coefficients in the membrane are the same for all cations and for all anions, respectively (Debye-Hückel convention).

For more information on the calculation of individual ion activities, see Appendix B.

2.2 Conventional Models

This section introduces the two conventional approaches and relates them to the potentials described in equation (2.2).

First the thermodynamic approach is used to describe the membrane potential, E_M, by the *Phase Boundary Potential* model.

Then the kinetic approach is used to describe the liquid junction potential, E_J.

2.2.1 Thermodynamic approach

The thermodynamic approach generally neglects ionic mobilities, including selective permeability of the membrane, and concentrates solely on differences is standard electrochemical potential. This requires that diffusive and other non-equilibirum effects are very slow compared to the modeled phenomena.

Electrochemical Potential

The chemical potential, μ, is defined as the change in Gibbs Free Energy, when the number of particles of a species change, with temperature, pressure and number of other species of particles kept constant [8]:

$$\mu_i' = \left(\frac{\partial G}{\partial n_i}\right)_{T,P,n_{j\neq i}}$$

where μ_i' is the chemical potential of species i in phase ($'$).

Chemical equilibrium is thus characterised by the equality of chemical potential.

Under constant pressure and temperature, the chemical potential can be calculated using the activity:

$$\mu_i' = \mu_i^{0\prime} + RT \ln a_i'$$

For a system involving charged particles, the electrochemical potential can be defined as

$$\overline{\mu}_i = \mu_i + z_i F\phi = \mu_{i,0} + RT \ln a_i + z_i F\phi \tag{2.14}$$

At this point it should be noted that:

- The separation of the electrochemical potential $\overline{\mu}$ into a chemical term (μ) and an electrical term ($z_i F\phi$) is artificial, since any change in potential would cause a change in local concentration of charged species and vice versa. Hence the terms μ and $z_i F\phi$ cannot be determined independently, while $\overline{\mu}$ is measurable in principle. The separation is, however, useful in deriving various electrochemical relationships.
- The inner potential ϕ' of a single phase $'$ cannot be measured.
- The inner potential difference across a single phase boundary is also not measurable, as any measurement necessarily involves at least two interfaces (e.g. two electrodes).
- The quantity usually measured is the change in internal potential. Under suitable conditions this can indeed be measured, and is the basic working mechanism of Ion Selective Electrodes.

Phase Boundary Potential

The 'Phase Boundary Potential' approach[9], assumes that the membrane potential is determined solely by the change in the boundary potential between the sample and the membrane, as described in section 2.1.2, i.e.

$$E_M = E_B' + E_B'' + E_D \approx E_B', \tag{2.15}$$

which leads to the membrane potential described in equation (2.10):

$$E_M = \frac{RT}{z_i F} \ln \frac{k_i a_i'}{a_i''}, \qquad k_i := \exp^{(\mu_i^{\circ\prime} - \mu_i^{\circ\prime\prime})/RT} . \tag{2.16}$$

This model is equal to the assumption of two semiinfinite phases with constant C_∞'s and a single boundary.

The modeling consists in describing k_i, a_i' and a_i'' in the desired case.

This model can account for a wide range of the phenomena observed in relation to ISE, especially in the recent development of polymeric membrane-based electrodes, for which the validity of the assumptions have been verified experimentally, i.e. by Umezawa [10].

Interference.

An ideally selective ISE will not respond to changes in activity of other ions in the sample. This, however, is usually not a valid assumption. The response from other ions than the sensors primary ion is called *Interference*.

The recommended method by IUPAC for describing interference is the semiempirical *Nikolsky-Eisenmann* equation, [1, eq. 1];

$$E_M = E_i^\circ + \frac{RT}{2F} \ln \left(a_i' + \sum_j K_{ij}^{Pot} a_j'^{z_i/z_j} \right) \tag{2.17}$$

where K_{ij}^{Pot} is the potentiometric selectivity coefficient for ion j with respect to the primary ion i

In 1999 Nagele and Bakker extended the description of interference using the phase boundary model[11]. They modelled interference effects through fairly simple thermodynamic arguments and reaction equilibriums, using models of polymeric membranes containing uncharged carriers (ionophores) and lipophilic ion exchangers (ionic sites) (see section 2.4).

The result was the following impressive equation, describing the response of a sensor towards a sample containing any number of mono-, di- and trivalent ions.

$$\begin{aligned} E &= E_I^0 + \frac{RT}{F} \ln \left\{ \frac{1}{3} \sum_{i1} K_{i1}^{pot} a_{i1} \right. \\ &\left. + \frac{2^{1/3}\theta}{3\left(\vartheta + \sqrt{-4\theta^3 + \vartheta^2}\right)^{1/3}} + \frac{3\left(\vartheta + \sqrt{-4\theta^3 + \vartheta^2}\right)^{1/3}}{\left(3 \times 2^{1/3}\right)} \right\} \end{aligned} \tag{2.18}$$

where

$$\theta = \left(\sum_{i1} K_{i1}^{pot} a_{i1} \right)^2 + 3 \sum_{i2} K_{i2}^{pot\,2/z_I} a_{i2} \tag{2.19}$$

and

$$\vartheta = 2\left(K_{i1}^{pot\,1/z_I} a_{i1}\right)^3 + 9\left(K_{i1}^{pot\,1/z_I} a_{i1}\right) \times \left(\sum_{i2} K_{i2}^{pot\,2/z_I} a_{i2}\right) + 27\sum_{i3} K_{i3}^{pot\,3/z_I} a_{i3} \tag{2.20}$$

Although this equation looks rather impressive, it summarizes the response of a sensor into a single equation, whereas the more traditional Nikolsky-Eisenmann approach would require 7 separate equations for the same description.

Introducing a new selectivity coefficient,

$$k_{ij}^{Psel} = (K_{ij}^{pot})^{z_i/z_j} e^{(E_M - E_i^0)(z_i - z_j)F/(RT)} \tag{2.21}$$

equation (2.18) can be rewritten as

$$E_M = E_i^\circ + \frac{RT}{z_i F} \ln\left(a_i' + \sum_j k_{ij}^{Psel} a_j'\right). \tag{2.22}$$

which is similar in form to the regular Nikolsky-Eisenmann equation (2.17).

The Nikolsky-Eisenmann equation is known to fail only in cases where the primary and interfering ion both give significant contributions to the potential, and are of different valency. Since this will not be the case in any experiments performed in this thesis, the selectivity coefficient K_{ij}^{pot} will be used throughout.

2.2.2 Kinetic Approach

The potential of the reference electrode is a so-called liquid junction potential, that arises where two identical phases with different ion activities meet. This leads to diffusive fluxes across the interface, even in a zero-current state.

These fluxes, and their corresponding potentials have been calculated through Kinetic Transport models.

The diffusive flux of a species due to concentration and potential gradients, can be considered to be proportional to the gradient of the standard electrochemical potential[3], i.e.

$$J_i = -c_i u_i \frac{\partial \overline{\mu}_i}{\partial x}, \tag{2.23}$$

where u_i is the mobility pr. mol. This means that when equilibrium is reached, flow will cease. It is called the Nernst approach. Calculating the differential, we get

$$\frac{\mathrm{d}\overline{\mu}_i}{\mathrm{d}x} = \frac{\mathrm{d}}{\mathrm{d}x}\left(\mu_i^0 + RT \ln a_i + z_i F \phi\right). \tag{2.24}$$

At constant pressure and temperature and $a_i \approx c_i$, this becomes

$$\frac{\mathrm{d}\overline{\mu}_i}{\mathrm{d}x} = \frac{RT}{c_i}\frac{\mathrm{d}c_i}{\mathrm{d}x} + z_i F \frac{d\phi}{\mathrm{d}x}. \tag{2.25}$$

The proportionality also can be identified with the diffusion constant through Fick's law:

$$J_i = -D_i \frac{\partial c_i}{\partial x} \tag{2.26}$$

and we get the so-called *Nernst-Planck equation*[12]:

$$J_i(x,t) = -D_i \left[\frac{\partial c_i(x,t)}{\partial x} - z_i c_i(x,t) \left(\frac{F}{RT} \right) \frac{\partial(\phi(x,t)}{\partial x} \right], \tag{2.27}$$

which when combined with the general Poisson equation, in the form of the displacement current equation,

$$I = F \sum_i z_i f_i(x,t) + \epsilon \frac{\partial E(x,t)}{\partial t}, \tag{2.28}$$

gives a system with $n+1$ equations and $n+1$ unknowns, for a system with n ion types. This approach is called a kinetic approach due to its dependence the knowledge of ionic mobilities, through the diffusion constants.

These coupled equations can either be solved iteratively by computer, or in some specific cases, exactly.

Diffusion Potential

The potential arising from concentration gradients within the membrane is termed the diffusion potential.

The Nernst-Planck equation has benn solved exactly by Planck, to yield the Planck-formulation[2]:

$$E_D = -\frac{RT}{F} \int_0^d \frac{\frac{\partial}{\partial x} \left[|z_m| u_m a_m(x) - \sum |z_x| u_x a_x(x) \right]}{\sum z_m^2 u_m a_m(x) - \sum z_x^2 u_x a_x(x)}, \tag{2.29}$$

which is the traditional way of calculating a diffusion potential.

This result is implicit, so an iterative approach is required to calculate the actual potential. Furthermore it relies on the assumptions no. viii) and no. ix)a) on page 12 that: a) The mobilities of all particles within the membrane are invariant, and, more importantly: b) The local activity coefficients are the same for all ions in the membrane (McInnes Convention).

To obtain an explicit equation, the *Henderson formalism* assumes that the concentration profile of ions in the diffusion layer is linear between each side:

$$\frac{\partial}{\partial x} a_i(x) = \frac{a_i(0) - a_i(d)}{d} = \frac{\Delta a_i}{d}. \tag{2.30}$$

Inserting this in equation (2.29) results in the *Henderson* equation [2, eq. 4.41]:

$$E_D \cong \frac{\sum |z_m| u_m \Delta a_m - \sum |z_x| u_x \Delta a_x}{\sum z_m^2 u_m \Delta a_m + \sum z_x^2 u_x \Delta a_x} \times \frac{RT}{F} \ln \frac{\sum z_m^2 u_m a_m(0) - \sum z_x^2 u_x a_x(0)}{\sum z_m^2 u_m a_m(d) + \sum z_x^2 u_x a_x(d)} \tag{2.31}$$

This approximate equation is explicit, and makes it possible to estimate diffusion potentials. This method is the conventional method of calculating liquid junction potentials.

This solution relies on knowledge of ionic mobilities, it is therefore not generally applicable, since mobilities in membranes are not easy to measure experimentally.

A similar solution has been reached through thermodynamic modeling, using non-equilibrium thermodynamics, but this approach introduces phenomenological constants relating flow and potential gradients, which also have to be measured.

Reference Electrode

Investigation of the Henderson equation (2.31), shows that it may be possible to construct a liquid junction potential that is constant. This is the requirement of a reference electrode.

The potential E_J, comes from a liquid junction, which is an interface where to separate water solutions meet each other. It has the form of a diffusion potential.

In order for a liquid/liquid interface to be constant, the solution at the inside of the interface must be equitransferent, i.e. $\sum |z_m| u_m c_m \cong \sum |z_x| u_x c_x$, where subscript m denotes cations and x anions.

The mobility u_i, is related to the *molar conductivity at infinite dilution* of the ions, which has been measured and tabulated for many ions in aqueous solution. An example of an equitransferent solution contains $0.2M\ KCl$ and $0.2M\ KNO_3$, since $u_{K^+} = 0.8u_{Cl^-} + 0.2u_{NO_3^-}$, as can be seen in table C.1, [from 2, Table 5.1].

The equitransference requirement is not enough, as the relative ionic strength of the inner solution and the sample also makes a difference.

In general, the internal solution should be at a significantly higher concentration than the sample, for the potential to be stable.

2.3 Time Dependent Behavior

The models above all assume that the sensor is in a steady state and the potential E_{total} is stable. When this is not the case, a model of the time-dependent response is necesary.

If it is assumed that diffusion within the membrane does not make a difference, the slowest process involved in the equilibration process, is that of diffusion through a stagnant aqueous layer. An approximate equation describing the response, has been developed[4]:

$$E(t) = E_\infty + \frac{RT}{z_I F} \ln\left(1 - \left(1 - \frac{a_I^0}{a_I}\right)\frac{4}{\pi}\mathrm{e}^{-t/\tau\prime}\right), \tag{2.32}$$

where a_I^0 and a_I are the activities at the membrane surface at $t = 0$ and at equilibrium, respectively, and $\tau\prime$ is a time constant defined as:

$$\tau\prime = \frac{\delta^2}{2D_{aq}}, \tag{2.33}$$

where δ is the thickness of the Nernst Diffusion Layer and D_{aq} is the aqueous diffusion coefficient of ion I.

Due to the logarithmic nature of this response, the response time is significantly longer when a diluted concentration is measured after a more concentrated (by a factor of ≈ 100 in case of a 10-fold activity change). Since the thickness of the Nernst Diffusion Layer is reduced dramatically when the solution is stirred, the response time can change by several orders of magnitude (i.e. from $\tau\prime \approx 1$s (unstirred solution) to $\tau\prime \approx 10^{-3}$s)[4].

Diffusion processes within the membrane have a different effect. According to Morf [2], an inverse square root response is to be expected instead of the exponential decay:

$$E(t) = E_\infty + S\log\left[1 - \left(1 - \frac{a_i^0}{a_i}\right)\frac{1}{\sqrt{t/\tau} + 1}\right], \tag{2.34}$$

where

$$\tau = \frac{DK^2\delta^2}{\pi D_{aq}^2} \approx \tau\prime\frac{D}{D\prime}K^2. \tag{2.35}$$

These equations may be used to estimate the equilibrium response of a slowly responding ISE by extrapolation.

2.4 Polymeric Bulk Membranes

The membranes described in this thesis are all of the liquid bulk polymer type. This consists of a nonpolar liquid of high viscosity, usually a plasticized polymer. They are relatively thick ($\approx 100\mu$m). They differ from bilayer membranes in a number of ways. Notably, the electroneutrality assumption:

$$\sum_j c_j z_j = \frac{\rho}{F} = 0 \tag{2.36}$$

holds in bulk membranes[13]. For a discussion on the possible phenomena in lipid bilayers, see Silver [3], Chap. 14.

Ionophores and *Ionic Sites* are added to the membrane to make it selective. Their role will be explained in this section.

This model is illustrated in figure 2.4.

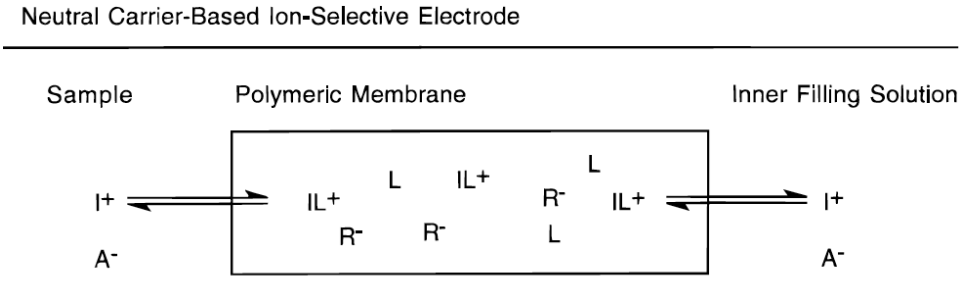

Figure 2.4: Schematic view of the equilibria between sample, ion-selective membrane, and inner filling solution for the special case of equal sample and inner filling solution electrolytes in a membrane containing electrically neutral carrier (L) and anionic sites (R^-)[4].

2.4.1 Ionophores

In water, the water molecules orient themselves around charged particles due to their polarity. If the ion is positive, i.e. a cation, the oxygen atoms are close to the ion, and the hydrogen atoms form a polar "shell". This structure is not trivial to predict, but one important consequence is that the ion has to release the water molecules to enter the apolar phase.

Ionophores (lit. *Ion Carriers*), are molecules with the property that they can substitute some or all the water molecules around an ion with their own polar parts, usually formed by oxygen or nitrogen atoms. These atoms are usually covalently bound to carbon atoms, that do not get polarized like hydrogen.

Ionophores also have highly hydrophobic parts that can shield the polar parts, and make the ionophore/ion complex dissolve into the membrane.

Selectivity

The water molecules arrange differently around different ions, due to differences in ion size, charge etc., and since ionophores must replace the water molecules, altering the geometry of an ionophore may cause it to complex more readily with one ion than with another.

A illustrative example of this is the so-called Crown-Ethers. Their polar parts are ring-shaped molecules with a number of $[CH_2CH_2O]$-links, which

are connected to hydrophobic parts. The number of links in the ring is highly decisive for their complexing behaviour. A clear example is seen in figure 2.5. which shows crown-ether-based ionophores with 4,5,6 and 8 links

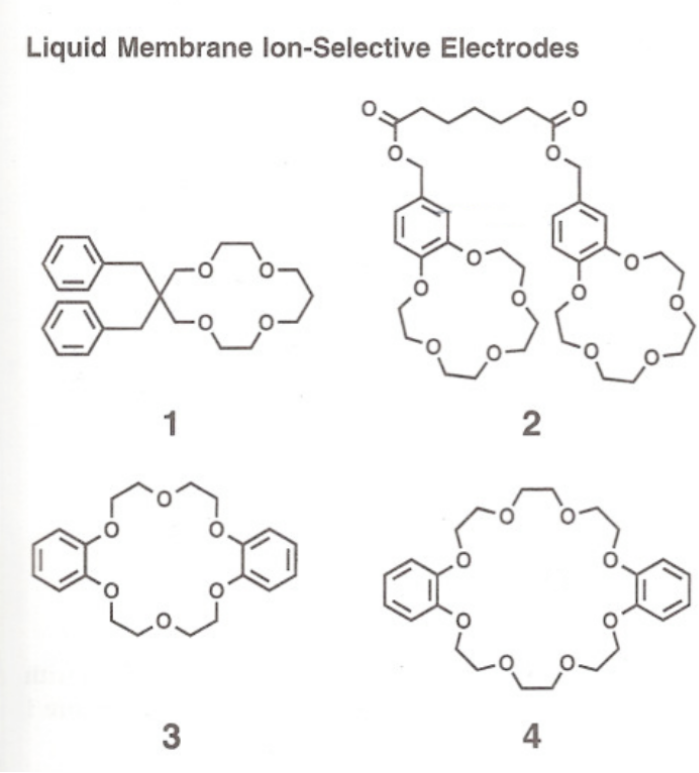

Figure 2.5: 4 Ionophores. Selective towards: 1) Li^+; 2) K^+; 3) K^+; 4) Na^+. [10]

in the ring, which are selective towards Li^+, K^+, K^+ and Na^+ respectively.

The relation between geometry and selectivity is not trivial, and is the focus of the area Coordination Chemistry.

A comprehensive list of ionophores has been compiled by Buhlmann et al. [14].

2.4.2 Lipophilic Salt

In early polymeric-membrane based sensors, the membranes were made without adding additional ionic sites, e.g. in the form of lipophilic counter-ions. Later it was discovered that the response was due to ionic impurities in the polymer, which started a research into what exactly their effect was. Lately, research on highly purified membranes have shown that without ionic sites, they do not respond at all[10].

Salt with lipophilic anions, such as sodium tetra-phenyl-borate (see fig-

ure 2.6) are now added customarily to cations-selective sensors. Some of their primary roles are to ensure electroneutrality and avoid co-ion extraction, a process where the primary ion "drags" a counter-ion with it into the membrane.

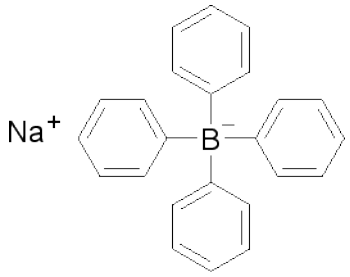

Figure 2.6: Sodium tetra-phenyl-borate, a lipophilic salt used in Ion Selective Electrodes.

In 1993, Eugster et al. [15] made some modelling based on the phase-boundary approach, and found that the ratio between ionic sites and ionophore can have a large influence on the interference from ions of different charge than the primary ion, or on interference from interfering ions with the same charge, but which have a different stoichiometry of the carrier-ion complex. In other words, it is possible to "fine-tune" a sensor by choosing the amount of added lipophilic salt carefully.

2.5 Surfactant Interaction Model

A sensor which reacts in a predictable manner towards concentrations of certain non-ionic surfactants has been developed by Sak-Bosnar, Madunic-Cacic, Matesic-Puac, and Grabaric [7]. A theoretical model has been developed, which describe the response.

The surfactants in the model have long ethoxylated chains. These chains are known to complexate Barium and other metal(II)-ions. An ionophore has been developed through this principle, and can be seen in figure 2.7[14, p. 1624].

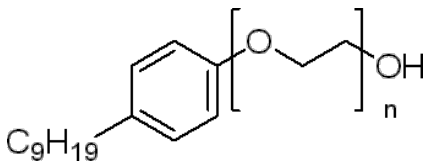

Figure 2.7: Molecular structure of the Barium ionophore Igepal 890. $n \approx 40$.

While the result is interesting, it is not a general description of the effect of non-ionic surfactants, but rather a model of reactions when the sample contains ion carriers that are specific to the primary ion of the membrane. Specifically, it does not relate the response to any surfactant specific properties, such as ambiphilicity, surface adsorption rate, etc..

It does, however, describe the response quite well, and I have adapted the model developed by Sak-Bosnar et al. [7] to the case of this thesis.

In the case of the surfactant investigated in this thesis, it is not known how many molecules form the complexes, or which charge the ions have. The model will thus be generalized to "unknown" ion charge and stoichiometry.

2.5.1 Sensor Response to Non-Ionic Surfactant

Assuming that the surfactant in question (denoted D) complexates with one ion J, with charge z_J, the following equilibrium reaction will describe the situation:

$$J^{z_J} + xD \leftrightharpoons JD_x^{z_J}, \tag{2.37}$$

where x denotes the average number of surfactant molecules pr. ion.

The corresponding formation constant is

$$K_f = \frac{JD_x^{z_J}}{[J^{z_J}][D]^x}. \tag{2.38}$$

If the pseudo-cationic complex is at or in the membrane, it can form a complex with the lipophilic anion, tetra-phenyl-borate (TPB^-). This forms according to

$$JD_x^{z_J} + z_J \cdot TPB^- \leftrightharpoons ID_x(TPB)_{z_J}. \tag{2.39}$$

The solubility product can be defined as

$$K_{sp} = [JD_x^{z_J}][TPB^-]^{z_J} \tag{2.40}$$

The stoichiometry of these reactions are unknown.

Assuming a Nernstian response to the charged particles, $JD_x^{z_J}$ and TPB^-, the sensor potential can be written as

$$E_{TPB^-} = E^0_{TPB^-} - S_{TPB^-} \log[TPB^-] \tag{2.41}$$

and

$$E_{JD_x^{z_J}} = E^0_{JD_x^{z_J}} + S_{JD_x^{z_J}} \log[JD_x^{z_J}] \tag{2.42}$$

Inserting $JD_x^{z_J} = K_f \cdot [J^{z_J}][D]^x$ from equation (2.38), we get

$$\begin{aligned} E_{JD_x^{z_J}} &= E^0_{JD_x^{z_J}} + S_{JD_x^{z_J}} \log(K_f[J^{z_J}][D]^x) \qquad (2.43)\\ &= \underbrace{E^0_{JD_x^{z_J}} + S_{JD_x^{z_J}} \log K_f + S_{JD_x^{z_J}} \log[J^{z_J}]}_{E^0_D} + S_{JD_x^{z_J}} \log([D]^x) \end{aligned}$$

Renaming $E_{JD_x^{z_J}}$ E_D, and assuming E_D^0, as defined above, is constant, we get:

$$E_D = E_D^0 + S_D \log[D], \tag{2.44}$$

where

$$S_D = \frac{x}{z_J} \cdot 2.303 \frac{RT}{F}. \tag{2.45}$$

If this model holds, it makes it possible to extract information about x and z_J, although not independently.

This is coupled to the membrane potential through the solubility product K_{sp} defined in equation (2.40). If the concentrations $[TPB^-]$ and $[J^{z_J}]$ can be assumed constant, the above equation hold.

In Sak-Bosnar et al. [7], J^{z_J} comes from dissociation of the surfactant complex:

$$JD_x^{z_J} \leftrightharpoons J^{z_J} + xD. \tag{2.46}$$

which in turns result from the sparingly soluble ion-excange complex:

$$JD_x(TPB)_{z_J} \leftrightharpoons JD_x^{z_J} + z_J TPB^-. \tag{2.47}$$

Since the concentration of dissolved complex in the plasticizer is constant, the concentration of $JD_x^{z_J}$ is also constant, and defined by the solubility product. Consequently, the concentration of J^{z_J} can be considered constant.

In the sensor described in the article, they keep the concentrations of the organic phase constant by their construction of the membrane. One cannot necessarily assume that the same assumptions are valid in the case of sensors that have not been exposed to surfactant before.

The validity of the assumptions, and conditions of the model, will be adressed in section 4.7.

Chapter 3

Technology of Ion-Selective Electrodes

This chapter introduces the technology of Ion Selective Electrodes and modern applications.

The practical construction of a modern ISE system is described. Several key elements of practical use are covered.

3.1 Introduction to ISE Technology

This section will give a general introduction to the current implementations of Ion Selective Electrodes, as well as a historical overview of the development.

3.1.1 Historical Overview

The development of Ion Selective Electrodes started in 1906 with the discovery by Cremer of a pH-dependent response of thin glass membranes[16]. This electrode is now present in virtually all modern chemical laboratories. Although the performance of such solid-state electrodes is still unsurpassed, the chemical versatility is limited, which imposes limitations on the possible analytes.

In the 1930's the first polymer-based membranes were developed, at first in the form of sulfonated polystyrene membranes. These membrane polymers have either positive or negative functional sites covalently bound, which make the membranes permeable to either anions or cations.

In 1964 it was discovered that certain antibiotics facilitated charge transport over the cell membranes of mithocondria. These molecules were highly selective as to which ions were transported, and their effect was rapidly exploited in ISE technology. One of the first was based on the antibiotic *Valinomycin*, which can be seen in figure 1.2 on page 3.

Other ion selective molecules were discovered soon after, and many new were designed and tested. The versatility of polymer-based membranes doped with ionophores have made them very popular, and it is now possible to construct sensors for a wide range of analytes, among others: metalic cations, organic cat- and anions, alcohols, and may other. For a comprehensive list see Buhlmann et al. [14].

The field has not stagnated, and there is ongoing research in developing new ionophores, as well as development of increased theoretical understanding.

The development of polymer-based membranes in particular will be described in section 3.1.2.

3.1.2 Development of Polymeric-Membrane Based Electrodes

In this thesis, the focus is on the development of sensors with a polymeric membrane. In these electrodes, the membrane is made of a highly plasticized polymer, i.e. PVC, containing the relevant molecules such as ionophores, lipophilic salt etc.. This membrane is solubilized to facilitate production, by adding a solvent when mixing the components. The fluid membrane liquid is called a *membrane cocktail*.

An example of a classical construction can be seen in figure 3.1. This has typically been produced by mixing the membrane components with a solvent, dispensing the resulting membrane cocktail on a surface within a circular frame, waiting for it to dry into a gel, cutting out a circular patch in the middle, where the membrane is the least curved, and fitting this piece within a glass tube. The tube is then filled with an internal solution, and an internal silver/silver-chloride electrode.

As this process is quite complex, and very difficult to automate, several new approaches have been developed.

One of the early examples of an electrode without inner filling solution is the Coated Wire Electrode, see figure 3.2. It is produced simply by dipping a metal wire into a membrane cocktail. This produces an electrode with quite excellent measurement characteristics, but with problems of irreproducible results and low stability. This is now known to be due to a water layer forming under the membrane, interfering with the charge exchange at the solid/membrane interface.

Modern ISE technology is based on Liquid-Membrane Solid-Contact (LMSC) electrodes, in which the complications of internal charge transfer have been reduced. Radiometer has patented a way of dispensing the membrane cocktail onto a specific substrate[17]. This method, called thick film printing, is much more suited for automation and, although the substrate properties are not entirely understood[18], this is rarely a problem.

The LMSC electrode will be described in detail in section 3.3.

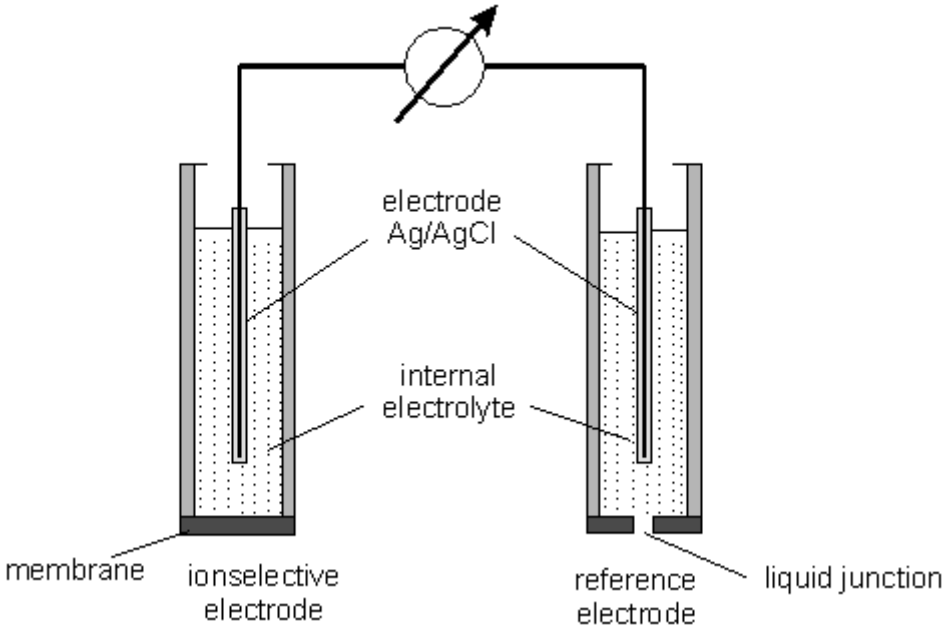

Figure 3.1: Ion Selective Electrode, Conventional Construction.

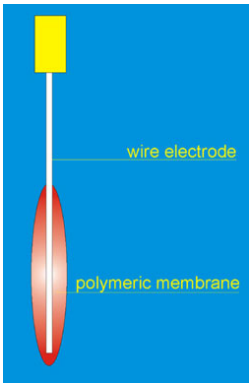

Figure 3.2: Coated Wire Electrode (CWE)

3.1.3 Alternative Electrode Principles

The ISE's described so far, have all been of the *Potentiometric* type. To illustrate the versatility of polymeric-membrane based sensors, several alternative working principles will be described briefly in this section.

Potentiometric Sensors

These are the main focus of this thesis.

In a Potentiometric Sensor there is no current, so the charge difference

builds up between the sensing membrane and a reference membrane, until an electrochemical equilibrium is reached. The charge difference is then related to the activity of the desired ion through for example the Nernst Equation, as described in section 2.1.1.

Amperometric Sensors

The amperometric sensors measures a current between the sensor and a reference electrode.

This current may originate from a production of charge within the membrane, for example hydrogen peroxide coming from an enzymatic degradation of glucose.

The sensor measures the current when this is steady, and relates the current to the rate of charge production, which in turn is related to the concentrations of metabolites and enzymes.

The steady current breaks with the assumption of zero current (no. vii) in section 2.1.3), so models must be altered or redeveloped to account for this type. However, the system can be assumed to be in a steady state, so thermodynamic modeling may still be used to describe the effects.

Optical Sensors

Optical sensors use an ionophore that changes its light absorption spectrum when it complexes with an ion. Shining light through the membrane, the change can be observed, and related to the ion concentration. These are generally slower than potentiometric sensors, as the entire membrane must be in equilibrium for the spectrum change to be visible.

Alternating Current Sensors

In these sensors, a AC-current is imposed on the membrane, and the impedance and resistivity is measured. Instead of measuring equilibrium states, it is used for measuring relaxation phenomena, i.e. rates of change. It has for example been used to measure the change in surface transfer rates of sodium, on a membrane covered with the non-ionic surfactant BRIJ-35[19].

Reference Electrodes

The reference electrode should be impervious to changes in sample concentration. This is not easily accomplishable, and to date the best electrodes are based on the liquid junction principle, as described in section 2.2.2, although some research has been put into developing a solid-state or liquid-membrane reference electrode[20]. The reference electrode used by Radiometer is described in detail in section 3.4.

3.2 Applications

The technology of ISE's has been implemented to analyze substances in a wide range of scientific fields. A selection of applications is shown here to emphasize the versatility of the method.

3.2.1 Analytical Chemistry

Within analytical chemistry, the ability to measure single ion activity at practically any concentration has had tremendous influence. Modern ISE's have been shown to span a staggering 8 orders of magnitude in concentration[6, p.72].

The traditional *Stick Electrode* is versatile and can measure on a variety of solutions with great ease. The pH-electrode is typically of this construction. A selection of stick electrodes can be seen in figure 3.3.

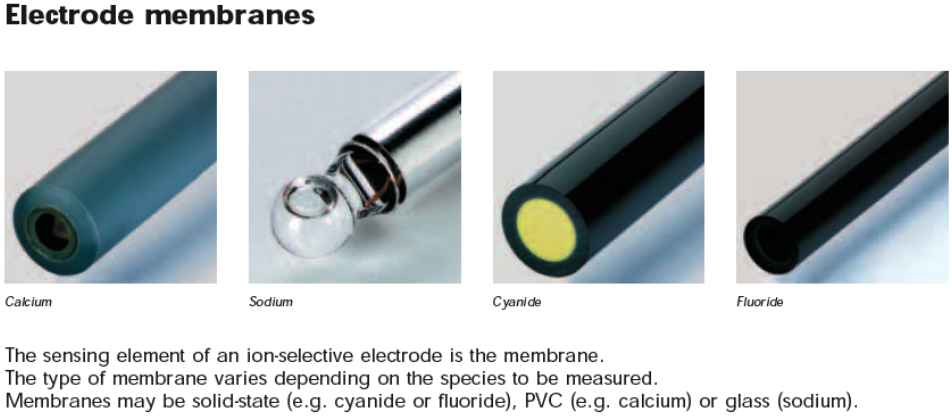

Figure 3.3: A selection of stick electrodes. Source: Radiometer Analytical Product Catalog[21]

With these sensors, it is possible to measure on a wide range of different solutions, from aqueous samples and oil to beer or curdled milk.

3.2.2 Biomedicine and Medico-Technical

The ability to measure on whole blood, instead of having to separate the plasma, add buffer, etc., has had a tremendous influence on the applicability within biomedicine. Technology and engineering has made it possible to put several different sensors in an array, where they measure simultaneously on the same blood sample. Miniaturization has even made it possible to measure intracellular concentrations[6].

In biomedicine, the detection range is not as important as the reproducibility of the results, since physiological concentrations seldom vary more than one order of magnitude.

The solid-contact polymer-membrane electrodes are durable enough to last for several weeks of use, or several hundred blood measurements.

The new generation of apparatus from Radiometer, as shown in figure 3.4, contains 8 different sensors, making it able to measure the concentration/activity of up to 8 different analytes in a blood sample of less than 0.2ml, in less than two minutes. These platforms are now a standard feature of emergency rooms and intensive care units, where the first measurement is taken to establish a "baseline" for a patient, and subsequent measurements are taken to detect changes.

Figure 3.4: Radiometers ABL80, a fully automated platform for measuring on whole blood.

3.2.3 Environmental

In environmental science, the low detection limit (down to attomole) makes it possible to detect trace amounts of analytes. This has been implemented in sea-water and waste-water analyzers. Electrodes have even been constructed that detect non-ionic substances through their interactions with, and influence upon, the regular membrane components[7].

3.2.4 Other

The *Chemical Nose* is an example of a different approach. It consists of an array containing a large number of ISE's, with only slightly different compositions. Instead of predicting a response theoretically, the Nose is subjected to a large number of different chemical samples (e.g. 10000), and a neurological network is trained to relate the resulting potentials to substances and their concentrations in the samples.

3.3 Liquid Membrane Solid Contact Electrode

One example of a modern ISE-electrode for blood gas analysis is the Liquid Membrane Solid Contact Electrode (LMSC-electrode). A basic construction can be seen in figure 3.5.

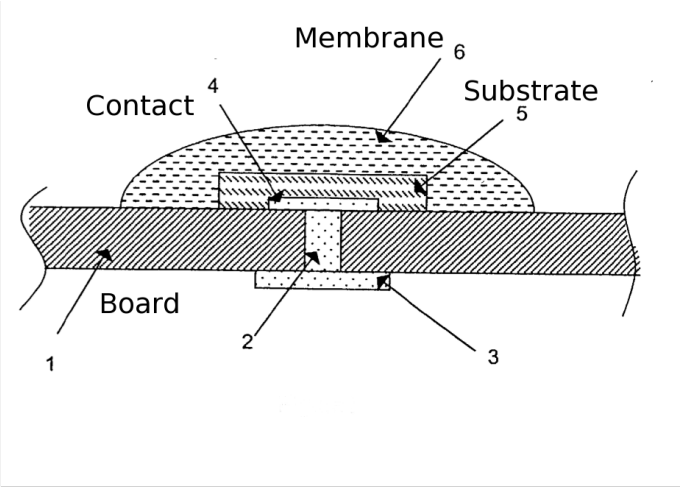

Figure 3.5: Liquid Membrane Solid Contact electrode. Example from [17].

This electrode is constructed by dispensing the *membrane cocktail* onto a solid, conducting substrate. In the terminology introduced in section 2.1 this means that the membrane potential can be described as $E_M = E_S + E_D + E_B$, where E_D is the diffusion potential, which is assumed to be constant. The total potential of the ISE circuit is then:

$$E_{Total} = E_1 + E_2 + E_3 + E_4 + E_B + E_J + E_S, \tag{3.1}$$

where $\sum_{i=1}^{5} E_i = E_0$ is assumed constant, E_B is the boundary potential between the aqueous sample and the hydrophobic membrane phase, E_J is the liquid junction potential of the reference electrode and E_S is a Solid/Membrane potential between the substrate and the membrane.

The boundary potential of this electrode type is described very well by the Phase Boundary Potential Model.

Each potential will be described in section 3.3.2, after a description of the components used in the construction of the electrode.

Some of the advantages of the solid state contact liquid membrane electrode are, in random order:

i) Long lifetime out of solution, i.e. before first use[22]

ii) Low diffusion potential

iii) No ion interchange with an internal solution

iv) Very low lower detection limit, down to attomole [23]

3.3.1 Construction

The general construction of the sensor used in this thesis is described in this section. The specific components of the membrane is described in section 3.3.3.

Substrate

A good substrate must respond to changes in potential and concentration like a conventional reference electrode. Furthermore it must be hydrophobic, have a stable potential, a fast response, be insensitive towards oxidizing and reducing substances and be insensitive to substances with acid/base properties.

Radiometers LMSC electrode technology implements a suitable substrate.

For details regarding this substrate, consult [17] and/or Appendix H.

Dispensing

After mixing the membrane cocktail, it is poured into a syringe, and around 0.5μg is dispensed as a drop in a cavity in an insulating material, with substrate on the bottom.

Sensor Board

A sensor board is a plate with room for several sensors. Each sensor has it's own cavity, as well as electronic connections on the backside of the board. In this thesis the sensor boards have three sensors each.

3.3.2 Potentials

This construction of the electrodes introduces the following phase-interfaces, each of which may generate a potential that is dependent on the sample.

Membrane Boundary Potential

This is the potential that should measure the activity of a specific ion. It is usually described by the Phase Boundary Potential model.

Liquid Junction Potential

In the reference electrode, there is a liquid junction potential between the sample and the internal electrolyte. This potential is assumed to be constant, which is true as long as the concentration of the inner electrolyte is

sufficiently high. The reference electrode and it's potential is described in section 3.4.

Solid/Membrane Interface Potential

The formation of the solid/membrane interface potential for the specific substrate is not generally understood. It does, however, seem to be stable.

3.3.3 Membrane Components

In this section, the components of a typical membrane for a Liquid Membrane Solid Contact electrode will be described.

The solution of membrane components is called a *membrane cocktail*.

Solvent

A solvent is added to dissolve all the other components and lower the viscosity of the membrane cocktail before dispensing on a substrate. Is assumed to evaporate completely, yet trace amounts may still be contained in the membrane. A solvent is shown in figure 3.6. The sensors are dried at around

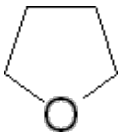

Figure 3.6: THX, a typical solvent used for membrane cocktails

60°C, for around 18 hours, after dispensing, ensuring that the solvent evaporates without boiling or denaturalization of any components.

Polymer

In most cases, regular PVC is used as the basic polymer. It is called the *Polymer-Matrix* of the membrane, and acts as a kind of sponge for the plasticizer and other components. The viscosity of the membrane is dependent on the average length of the PVC molecules.

For special membranes other PVC variants have been tried. PVC with ethoxylated groups have been tested to develop a more hydrophilic membrane, for example. Another example is mentioned in Kisiel et al. [20], where the polymerisation happens by UV exposure after dispensation.

The chemical company Fluka recommends a PVC content of a finished membrane of around 30 weight-percent.

Plasticizer

The plasticizer is added to make the PVC membrane gel-like. Plasticizers are relatively small molecules. Two examples of plasticizers used in this thesis can be seen in figure 3.7.

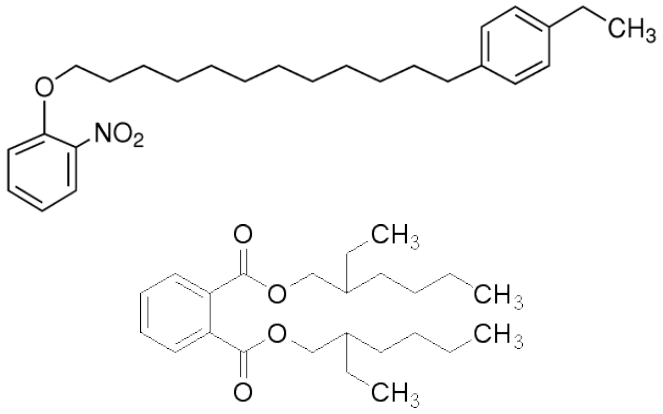

Figure 3.7: Top: ETH8045; The plasticizer recommended by Fluka for Mg-sensitive membranes. Bottom: DOP; The plasticizer recommended for Ca-sensitive membranes.

Although plasticizers ideally have no other purpose than to allow diffusion (of charge, carrier etc.) within the membrane, some plasticizers may have functional groups, making them act as ionophores or carriers. The plasticizers may also increase the polarity of the membrane, making it easier for ions in the aqueous phase to dehydrate and enter the membrane.[6]

The Mg^{2+}-ion is quite difficult to dehydrate and the right choice of plasticizer is non-trivial, as it is thought to help in the dehydration process.

It is important to note that although the membrane is often thought of as solid, it is actually a gel-like liquid, allowing interchange of components with the samples, including larger molecules.

Ionophore

Ionophores in general are described in section 2.4.1.

For magnesium sensors, several ionophores exist, yet none are very selective.

They have a variety of shapes. A few examples can be seen in figure 3.8

The difference in shape illustrates the difficulty in designing an ionophore.

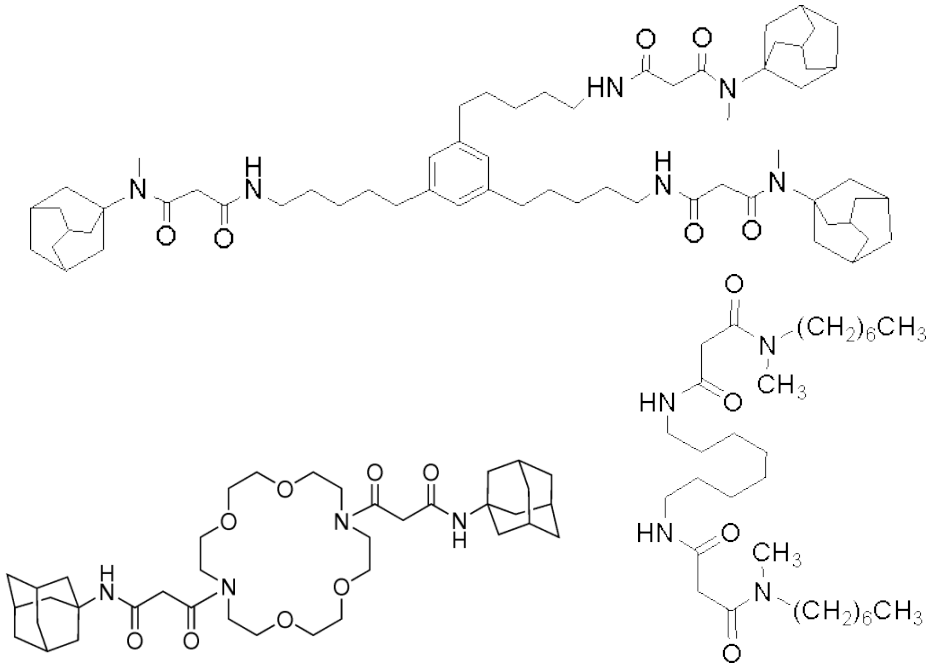

Figure 3.8: Top: Magnesium Ionophore ETH5506; Left: Magnesium ionophore VI, K22B5. Right: Magnesium ionophore III, ETH 4030

Lipophilic salt

As described in section 2.4.2, the amount of lipophilic counterions may have a large influence on the response of the sensor, due to the exchange dynamics of the membrane. Having the right ratio of ionophore to lipophilic salt can decrease the interference from ions with different valencies than the primary ion.

In general, Tetra-Phenyl-Borate, and variations of it, are used as lipophilic anion. See figure 3.9 for variations.

For some more information on the role of lipophilic salt consult Appendix H In Magnesium sensors, tetra-chloro-phenyl-borate is thought to catalyze the dehydration of Mg^{2+}-ions, by folding around the ion at the water/membrane interface. This hypothesis is to some extent substantiated by an internal technical study at Radiometer of a membrane with the bulkier tri-flouro-methyl TPB, shown in figure 3.9, which showed a significantly lower sensitivity to Mg^{2+}.

Ratio of Components

The ratio of components, as recommended in the Fluka catalogue, can be seen in table 3.1.

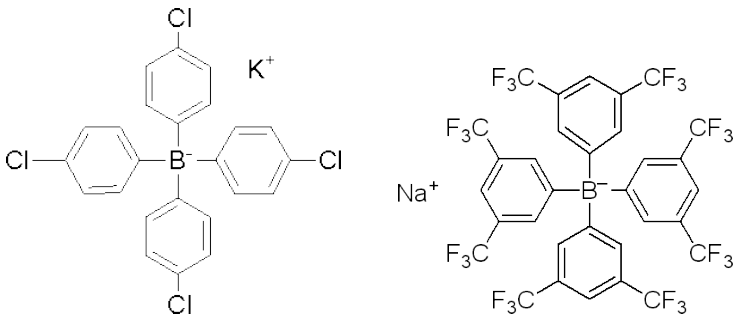

Figure 3.9: Left: Potassium Tetra-chloro-phenyl-borate (Fluka 60591); Right: Sodium TPB-tri-fluoro-methyl (Fluka 72017). Lipophilic salts used in membranes.

Table 3.1: Recommended ratios of components in membranes.

Component	Example	Weight Percent
Polymer	PVC	30%
Plasticizer	ETH8045	68%
Ionophore	ETH5506	1%
Lipophilic Salt	TPB-Cl	1%

3.4 Reference Electrode

The reference electrode is based on the liquid junction principle, which can be estimated through the Henderson Formalism, as described in section 2.2.2.

3.4.1 Radiometers Reference Electrode

Radiometers reference electrode is constructed as depicted in figure 3.10. The reference electrode itself is a silver rod covered with silver chloride, and the charge transfer is defined by the equilibrium reactions:

$$AgCl \leftrightharpoons Ag^+ + Cl^- \tag{3.2}$$

$$Ag^+ + e^- \leftrightharpoons Ag_{solid} \tag{3.3}$$

A bridge electrolyte is added to the chamber, and contained by a set of membranes that reduce unwanted interaction between the sample and the bridge electrolyte. The Cl concentration of the bridge electrolyte is adjusted to the Cl concentration of the rinse liquid, to minimize diffusion of Cl from the electrode.

The membrane separating the internal electrolyte from the sample contains three layers.

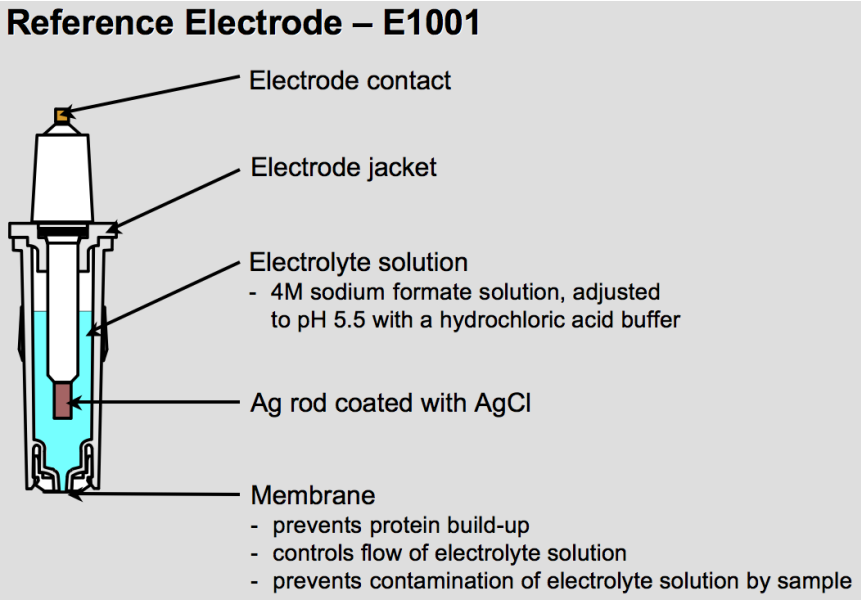

Figure 3.10: The reference electrode as constructed by Radiometer[24]. The membrane is a porous diaphragm that hinders flow, but it is not ion selective.

i) The inner layer limits diffusion

ii) The middle layer prevents protein diffusion

iii) The outer layer reduces cross-membrane flow of Na^+ and $COOH^-$

3.4.2 Experimental Consequences

The useful lifetime of a reference electrode is determined by the concentration of the bridge electrolyte. For details regarding the durability of the Radiometer reference electrode, consult Appendix H.

Although it is theoretically possible to calculate the actual liquid/liquid interface potential, through the Henderson Formalism (2.31), doing so requires knowledge of the ionic concentrations of the inner electrolyte at the time of the experiment. Since these concentrations cannot be measured (without removing the reference electrode from the system), and the development of the concentrations over time is highly dependent on the use of the machine in the meantime, it is assumed that the potential is constant, and the reference electrode is changed accordingly.

3.5 Calibration

Each sensor produced behaves a little differently. Since the target is to estimate the concentration of an ion from a sample, knowing only the potential

between the sensor and the reference electrode, a calibration is necessary.

A calibration uncovers the primary parameters of a sensor, as described later, as well as defining the regime in which measurements can be trusted. These parameters are also important when several sensors are compared, or a single sensor is tested under different circumstances.

In potentiometric ISE's there are two main parameters to estimate:

i) Sensitivity

ii) Interference

3.5.1 Sensitivity

The sensitivity is related to the ideal nernstian behaviour of a sensor, as described in section 2.1.1. A nernstian response has the form of

$$E_M = E_0 + \frac{RT}{F}\frac{1}{z_i}\ln(a_i) \approx 2.303 \cdot \frac{RT}{F}\frac{1}{z_i}\log(a_i'), \tag{3.4}$$

which is a linear response to the logarithm of the activity, with a slope of $S = 2.303 \cdot RT/Fz_i$mV pr. decade concentration change. In a real sensor, one can normally find a activity range in which the response is indeed linear, yet the slope is often different. The sensitivity is defined as the slope of the linear part.

A graph of the response of a sensor is shown in figure 3.11.

3.5.2 Interference

Describing the interference of other ions is no easy matter. As can be seen in section 2.2.1, the correct response to a solution containing several valencies of ions is not easy to calculate. For practical purposes the semiempirical Nikolsky-Eisenmann equation (2.17) is used, in the form:

$$E_M = E_0 + S\ln\left(a_i + K_{ij}^{pot} a_j^{z_i/z_j}\right). \tag{3.5}$$

The interference coefficient between two ions is identified as K_{ij}^{pot}, and it is assumed that several different ions in the solution will simply add up in the form:

$$E_M = E_0 + S\ln\left(a_i + \sum_j K_{ij}^{pot} a_j^{z_i/z_j}\right). \tag{3.6}$$

A graph illustrating the interference from other ions can be seen in figure 3.12.

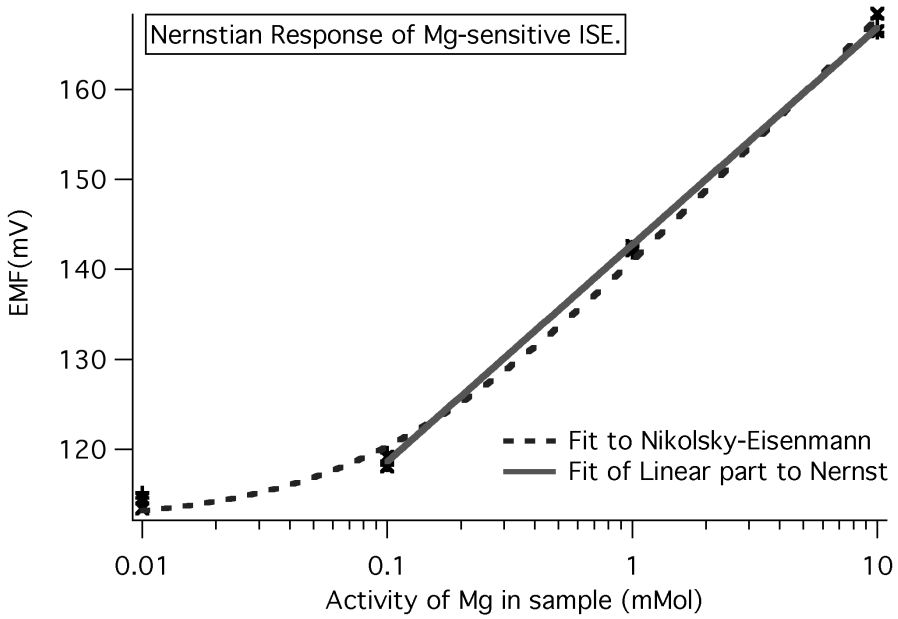

Figure 3.11: Example of the response of a Mg-sensitive electrode to samples containing only $MgCl_2$ at different concentrations. Experiment performed according to method described in section 6.1.1. The gray solid line is a fit of the linear part (assumed to be from 0.1mmol to 10mmol Mg^{2+}), to the Nernst equation: $E = E_0 + S\log(a_i)$. The dotted line is a fit to an extended Nernstian equation of the form $E = E_0 + S\log(a_i + K)$. The fits give the same sensitivity-slope of $S \approx 25m\text{V/mol}$, compared to the theoretically predicted $30.6m\text{V/mol}$.

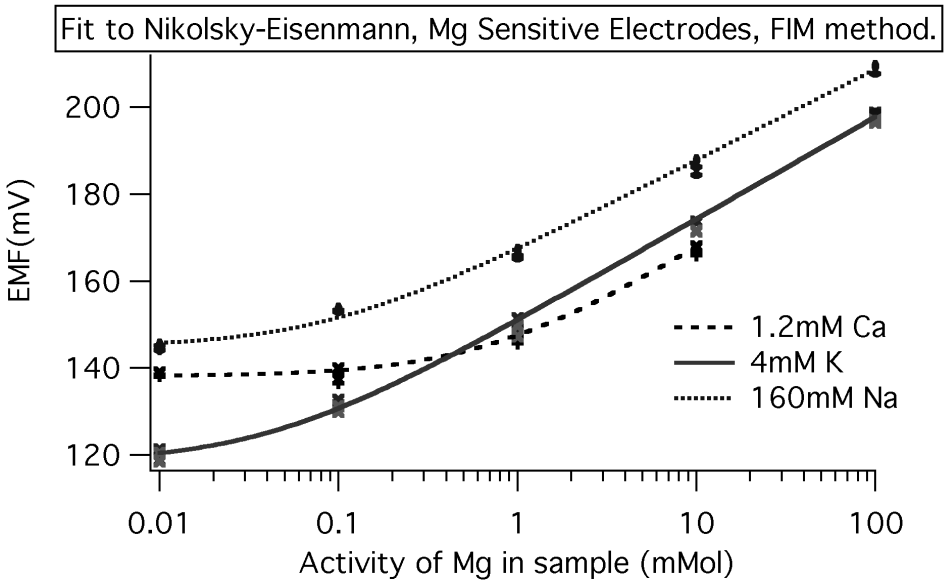

Figure 3.12: Example of the response of a Mg-sensitive electrode to samples containing $MgCl_2$ at different concentrations and a constant background of an interfering ion a a different concentration. The experimental procedure is described in section 6.4.2. The lines show the Nikolsky-Eisenmann equation, fitted to datapoints from measurements with different interfering ions, at constant activity, and with primary ion (Mg^{2+}) at concentrations form 0.01mMol to 100mMol. The gray solid line is a fit to samples with 160mMol Na^+ as background. The dashed line is a fit to samples with 1.2mMol Ca^{2+} as background. The dotted line is a fit to samples with 4mMol K^+ as background.

3.6 Conditioning

Ion selective electrodes are generally conditioned in a solution containing their primary ion before being used for measurements, in order to decrease interference from other ions.

The conditioning should be performed at concentrations close the desired samples, to reduce the diffusion potential when measuring.

In practical medicotechnical applications, the membranes are often prepared with no primary ions in the membrane cocktail, so a conditioning must take place after insertion of the sensor into the apparatus.

This conditioning is done in the apparatus by the calibration and rinse liquids. There will typically be a potential drift ranging from a few hours to several days, as can be seen in figure 3.13.

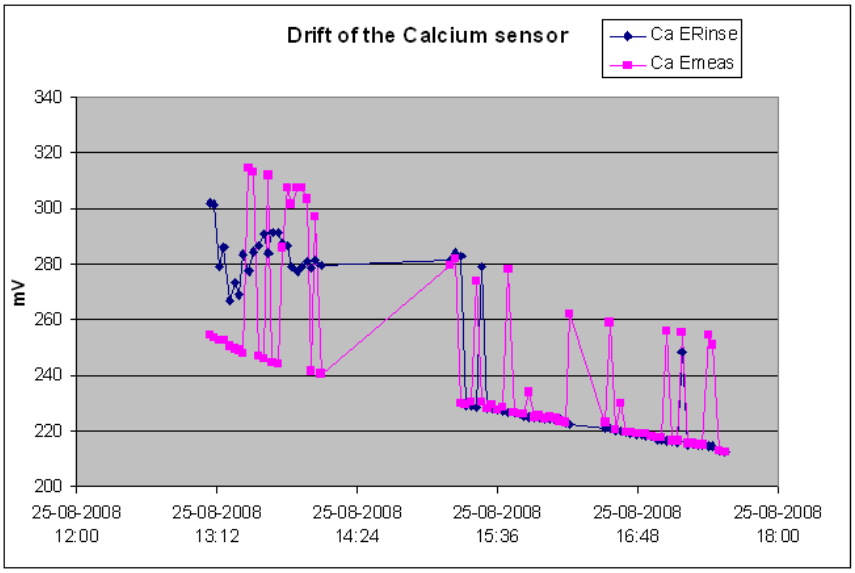

Figure 3.13: Example of the drift of an ISE over the first hours in the analyser. Each dot represents a separate measurement on the same sample. The drift in the potential appears linear, and has a rate of approx. $-7,5\text{mV/hour}$. The noise on the signal is presumably due to air bubbles forming on the membrane surfaces.

3.6.1 Rinse liquid

Since there are several sensors in a sensor array, the rinsing and calibration liquids contain the primary ions of each sensor, which may cause interference in others. Additionally, some other components are added, e.g. surfactants to reduce surface tension and disinfectant to avoid microbacterial growth.

The relevant contents of the rinse liquid used in this thesis can be seen in table D.1 in Appendix D.

3.7 Durability

LMSC-electrodes can last a long time before first use. This has been verified during the work of this thesis by keeping the sensors under the strictly uncontrolled storage conditions of a plastic box on my desk. A set of sensors was produced in June and worked equally well when inserted into the analyser in July and January.

After being mounted in the analyser, LMSC-electrode lifetime is strongly dependent on sample rate, type of membrane etc. – and may vary from a few days to several months.

A sensor is termed "dead" when the sensitivity S drops below a certain threshold, or when the interference coefficient towards other ions becomes too high. The actual value of the thresholds are determined for each electrode according to the analytical requirements.

This section describes the most common phenomena that can result is malfunctioning of the sensor.

3.7.1 Leaching of Membrane Components

Since the active components of a membrane must be able to coordinate with a metal ion, they have parts that are polar, which means that these parts are hydrophilic. They are often bound covalently to highly hydrophobic parts, to reduce leaching of membrane compontents into the samples and rinse solution.

The effects can be separated into the following:

i) The leaching of carrier molecules (ionophores) from the membrane. Below a critical concentration, a breakdown of the selectivity is observed.

ii) Extraction of plasticizer from the membrane, increasing viscosity, thus lowering diffusion rates and slowing down the membrane response, or even killing it.

iii) Extraction and/or degradation of mobil ionic salt additives (lipophilic salt), causing increased impedance. Selectivity may also be affected since interference is dependent on the ratio of ionophore to ionic sites, as described in section 2.4.2.

Spichiger-Keller [25] has made a study which relates the partition rate of a molecule between oil and water, with it's rate of leaching from a membrane. This makes it possible to estimate lifetimes of specific membranes.

The partition rate of the lipophilic salt may also play a role in the lifetime.

3.7.2 Internal Water Layer

As mentioned in section 3.1.2, early the Coated Wire Electrodes suffered from water layers forming between the membrane and the solid state contact (the wire). Although the substrate for a modern electrode is designed to reduce this effect, it may still occur. If not by direct diffusion of water through the membrane, some chemical reactions may occur at the interface causing the formation of water molecules, or simply dislodging the membrane from the substrate. Any changes at this interface may interfere severely with the mechanism of the sensor.

3.7.3 Pollution of Membrane

In blood sample measurements, the sensors are exposed to proteins and other macro-molecules with highly hydrophobic parts. These proteins may block the surface of the sensor and prevent ion uptake. The phenomena regarding blood pollution of membranes are not generally understood.

The surfactant in the rinse liquid may also have an effect. Numerous studies show that the surfactant Triton X-100, shown in figure 4.1 on 47, has a high influence on a number of different sensors types. In some cases the sensors "die" after only one sample containing Triton X-100.

Some of these effects may be due to surface effects, while others may be caused by a polution of the bulk of the membrane. The identification of the phenomena causing these effects, is the main goal of this thesis. Therefore it is necesary to know more about surfactants and their properties in general. This will be adressed in the next chapter.

Chapter 4

Surfactants and Ion-Selective Electrodes

In this chapter a very brief introduction to previous studies of surfactant interference will be given.

There will be a brief introduction into the role and importance of surfactants in practical applications of ISE technology.

The basic properties of surfactants will be described, introducing the structures and relevant properties and comparing different types of surfactants.

The class of non-ionic surfactants called acetylenic diols will be introduced, and the special properties will be described.

The chapter concludes with an analysis of acetylenic diols as surfactants in the model of Surfactant Interaction presented in section 2.5.

4.1 Surfactants Role and Position in ISE Systems

4.1.1 Reasons for Having Surfactants in the System

Surfactants are added to the rinse liquid for a number of reasons. Among these are:

- Avoid that bubbles forming in the system get stuck on sensors or in tubes
- Fast wetting of sensors
- Prevent blood components from adhering too strongly to membranes and flow wall surface

These can be summarized into two phenomena:

i) Lowering of surface tension
ii) Emulsification of blood components

The lowering of surface tension facilitates bubble-dislodging from hydrophobic surfaces, and reduces the chances of them forming in the first place.

4.1.2 Problems and Challenges

Although surfactants are necessary, several problem may also arrise. Here is a list of known issues.

- Coordination with ions in aqueous phase ($\Rightarrow$ lowering of $a_{aq,ion}$)
- Partitioning into organic phase
- Coordination with ions in organic phase ($\Rightarrow$ Change in $\mu_{0,org,ion}$)
- Problems with proteins

The nature of the problems is highly dependent on the structure of the surfactant. Many studies have been made to describe these phenomena, but there has not been performed a throrough comparative study relating surfactant structures and phenomena.

This also means that the choice of surfactant for an ISE system is not easy, as it is a balancing of several properties, and since many properties cannot be predicted.

4.2 Molecular Structure

A surfactant is a molecule with a polar, or hydrophilic, part and an apolar, or hydrophobic, part. The properties of surfactants are effects of hydrophobic/hydrophilic interactions with the solvent/interface. As a consequence, surfactants with different chemical composition may have very similar properties, if their hydrophobic/hydrophilic geometry is similar.

Surfactants can be divided into groups depending on their geometry:

4.2.1 Ionic surfactants

An ionic molecule is, by it's very nature, polar. Ionic surfactants have a head group that is charged and an apolar tail as the hydrophobic part.

The apolar part is typically a non-branched carbon chain, but can also be branched. Long carbon chains can cause cooperative effects between surfactant molecules.

4.2.2 Non-ionic Surfactants

Non-ionic surfactant do not have a charge to provide polarity. Instead of a charged headgroup, they typically have a chain of polar molecules, i.e. ethoxylates, a chain of $[CH_2CH_2O]$-links. In such a chain, the oxygen atoms will have a free electron pair, that can form hydrogen bonds with water. This

effect is much smaller than for a charged head group, so the chains need to be rather long to get a hydrophilic surfactant.

If the hydrophobic part is highly branched, the surfactants can look like ‘ìnverted” surfactants with a hydrophobic head and hydrophilic tail. As an example of this, the non-ionic surfactant Triton X-100 can be seen in figure 4.1.

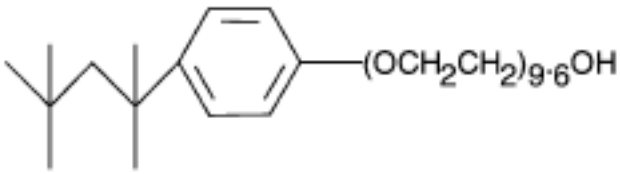

Triton® X-100

Figure 4.1: Molecular structure of Triton X-100. The surfactant Triton X-100 was used extensively until it was found that it caused interference effects, i.e. Malinowska[26]. A very similar molecule has been tested as a Barium ionophore[14], shown in figure 2.7.

4.2.3 Gemini surfactants

Gemini surfactants, or twin surfactants, are surfactants where two “regular” surfactants (ionic or non-ionic) are attached to each other by a *spacer*, typically by a carbon chain connecting the two head groups. The primary difference between gemini surfactants and natural lipids with two carbon chains, is that gemini surfactants have a rotational freedom around the central chain, whereas the carbon chains of lipids are fixed and parallel.

The structure causes several new phenomena, but it is not easy to predict or model behavior, since it is no longer rotationally symmetric, and since the molecule can rotate around the spacer[27].

In general, however, they tend to lower surface tension at a much lower concentration than their corresponding single surfactants.

4.3 Secondary Structure

Due to the hydrophobic and hydrophilic parts of surfactant molecules, they can form structures involving many molecules. Transitions between different

phases are dependent on a number of circumstances, aside from concentration of surfactant;

- Temperature
- pH
- Ionic Strength of aqueous phase (especially in the case of charged headgroups)
- Pressure

In the apparatus used in this thesis, the temperature is kept constant at $37°C$, and the pressure is assumed to be 1 atm, although the pumping may temporarily cause pressure fluctuations.

4.3.1 Monolayer

The defining secondary structure of surfactants is the monolayer arising at the interface of a polar and an apolar phase, i.e. water and air. Surfactants will gather at the surface, and form a compact monolayer, as shown in figure 4.2.

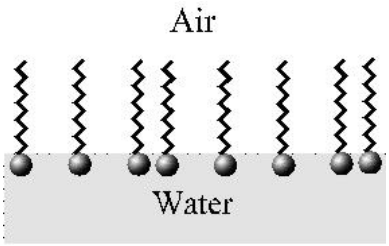

Figure 4.2: Monolayer of surfactants at water/air interface.

It is generally assumed that the surfactant molecules not at the interface are distributed evenly in the aqueous phase due to distributional entropy. The monolayer can thus be treated as a thermodynamic system in contact with a reservoir of molecules, i.e. the bulk phase.

Some molecular dynamics simulations indicate that gemini surfactant molecules may form complex three-dimensional structures at the interface, when the monolayer becomes too closely packed. This is illustrated in figure 4.3.

4.3.2 Bilayer

Some surfactants, especially biological lipids, may form bilayers, where two monolayers of surfactants shield their hydrophobic chains from water with their head groups. The bilayer behaviour is caused by cooperative effects between non-branched carbon chains. While this process and structure is

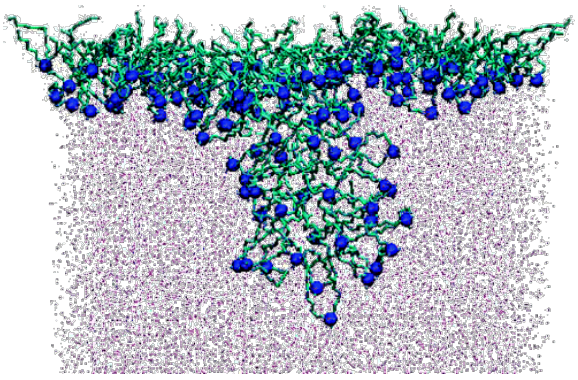

Figure 4.3: Monolayer of Gemini surfactants, with complex 3D structure. Calculated by molecular dynamics by Khurana et al. [28].

very important in biological reactions, the concentration of surfactants in ISE applications is generally too low to form bilayers.

4.3.3 Micelles

At a certain concentration, surfactants may congregate in balls where the hydrophilic head groups shield the hydrophobic chains. Such a ball is called a micelle. The number of surfactants in a micelle depends on the geometry of the surfactant. For simple surfactants, the number of surfactants in each micelle can be predicted, and the concentration at which the micelles first form, called the *Critical Micelle Concentration* (CMC) can be predicted. If the surfactants are dissolved in oil, inverse micelles can form, where the

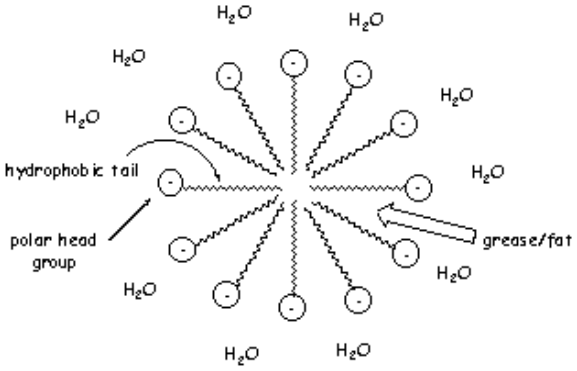

Figure 4.4: Micelle formed from surfactants.

hydrophilic headgroups are shielded by the hydrophobic tails.

4.3.4 Emulsions

Emulsions are caused by a monolayer forming around a bubble of i.e. oil, covering it in hydrophilic head-groups, so it can be dissolved in the aqueous phase instead of sticking to a hydrophobic surface. This is the effect of normal dish washer soap. This is also the effect that allows a surfactant to

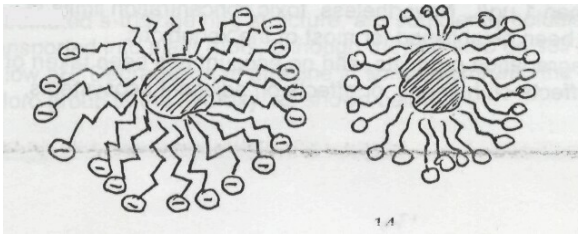

Figure 4.5: Emulsification of a drop of oil by surfactants.

rinse blood components off membrane surfaces.

Inverted emulsions are droplets of water shielded by surfactants and dissolved in oil. An article by Marco et al. [29] demonstrated that a water layer could form under a polymeric membrane. The water could be transported through the membrane by nanoliter droplets of water encased in surfactants.

4.4 Interfacial Phenomena

One of the primary roles of surfactants in ISE systems, is to ensure fast and complete wetting of the membrane. A rough surface may not be wetted by a drop of water if the surface tension is high. If the surface tension is lowered, the drop will fill the irregularities in the surface.

4.4.1 Contact Angle

The underlying concept of this behavior is the *contact angle*. This is the angle between a surface and a drop of water. It is defined in figure 4.6.

The contact angle is described by the Young equation:

$$\cos(\theta) = \frac{\gamma_{SV} - \gamma_{SL}}{\gamma_{LV}}, \tag{4.1}$$

which balance the surface tension, γ, of the three involved interfaces: Solid/-Vapor, Solid/Liquid and Liquid/Vapor. For a good wetting, a low value of γ_{SL} and γ_{LV} is required, which is achieved by monolayers of surfactant forming at the respective interfaces.

The surface tension is directly related to the Gibbs Free Energy pr. Area of the interface. Surfactants at the interface between liquid and solid will lower the surface tension.

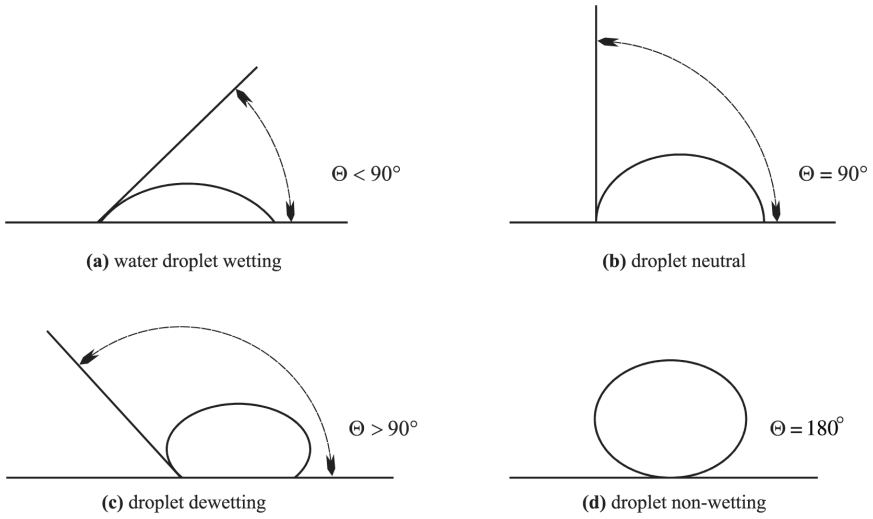

Figure 4.6: Several figures illustrating the contact angle principle. Contact angle goes from wetting (a) to non-wetting (d).

It is not generally possible to calculate the surface tension of an interface, or more specifically, to calculate the change in surface tension from the structure of a surfactant.

The dislodging of bubbles that have adsorbed at the surface is also easier to do with a lower contact angle. The role of the contact angle in a capillary tube like the hoses of the Radiometer platform, can be seen in figure 4.7:

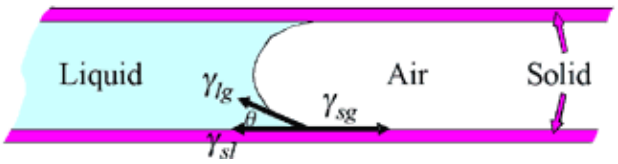

Figure 4.7: The contact angle in a capillary system. A high contact angle increases the likelyhood of air bubbles forming as the liquid progresses through the tube.

4.4.2 Adsorption Isotherms

The reduction in surface tension is directly related to the density of the monolayer of surfactant on the interface. An *adsorption isotherm* relates the concentration of free surfactant in the liquid with the density of surfactant molecules at the interface. Traditionally, the Langmuir isotherm has been used to describe the relation between surface coverage and concentration of

free molecules:

$$C_{free} = \frac{1}{K_0} \frac{\theta}{1-\theta} \tag{4.2}$$

where $\theta = \Gamma/\Gamma_{max}$ denotes the surface coverage fraction, and K_0 is a binding constant.

The Langmuir isotherm, however, assumes no interaction between molecules, and essentially allows full surface coverage.

A more physically correct isotherm is the *van der Waals isotherm*[30]:

$$C_{free} = \frac{1}{K_0} \frac{\theta}{1-\theta} \exp\left(\frac{\theta}{1-\theta}\right), \tag{4.3}$$

Through these isotherms it is possible to define a range of free surfactant concentration, in which the surface density changes significantly. This range is called the *Dynamic Range* of the surfactant.

4.5 Surfactant Interference

Interference from surfactants has been documentes for a wide range of surfactants.

Giannetto et al. [31] defined the interference of a range of non-ionic surfactants according to their influence on the sensitivity of a calcium-sensitive ISE. The results can be seen in figure 4.8.

Malinowska et al. [26] document a direct potential change as a consequence of changed surfactant concentration in an aqueous sample containing ions at physiological values. The results are shown in figure 4.9.

They concluded that the large interference from Triton-X100 was caused by complexation, due to the long ethoxylated chain.

Recently, researchers at Radiometer discovered interference from ethoxylated acetylenic diols, even though the number of links in the ethoxylate chain was too low to form complexes.

A representative of this class was chosen as the subject of this thesis. It will be introduced in the next section.

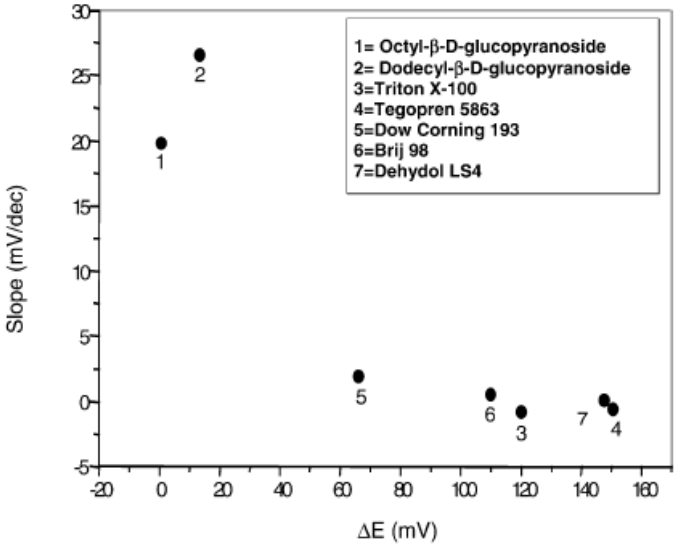

Figure 4.8: Classification of surfactants. The potential change of the sensor when exposed for one hour to a solution containing 100ppm surfactant, vs. the Nernst slope towards Ca^{2+} after exposure. The interfering surfactants are characterized by long ethoxylate chains.[31]

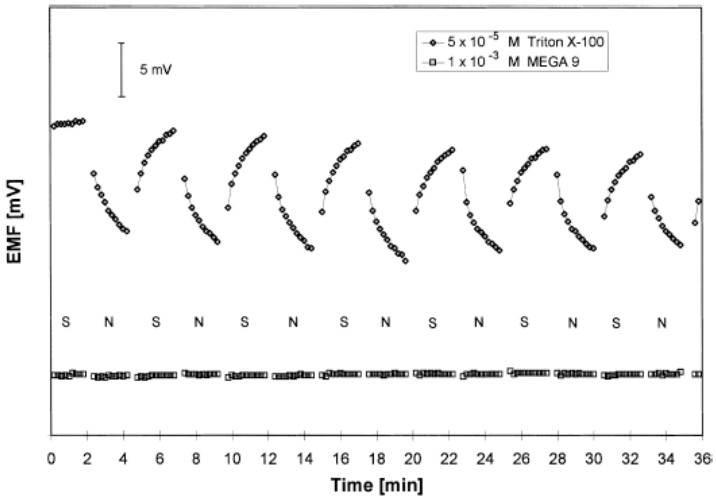

Figure 4.9: Dynamic EMF response profiles of magnesium-selective polymeric membrane electrodes when the sample solution, of physiological composition (140 mM NaCl, 5 mM KCl, 0.6 mM MgCl2 and 1 mM CaCl2; 0.05 M Tris/HCl buffer, pH 7.4), was changed from one containing surfactant (S) to one without surfactant (N) and vice versa. The concentrations of nonionic surfactants used in these experiments were: $5 \cdot 10^{-5}$ M for Triton X-100 and $1 \cdot 10^{-3}$ M for MEGA 9. [26]

4.6 Ethoxylated Acetylenic Diols

Interference behavior was observed by Radiometer on some acetylenic diols, even though the ethoxylate chains of these are considered too short to complexate.

Interference from this class of surfactants has not been documented before. I have chosen to investigate a single representative. It will be referred to as AD throughout this thesis.

The properties of surfactants based on ethoxylated acetylenic diols are not well documented. This section is based on a study by Musselman and Chander [32], which investigates and compares several of these surfactants. It contains studies of adsorption and surface organisation and orientation, onto lampblack (graphite). In lack of more focused studies, It is assumed that the main results can be transferred to liquid PVC-membranes.

4.6.1 Molecular Structure

Acetylenic diols are a subgroup of gemini surfactants. They have the shortest possible spacer, only a Carbon triple bond. A very simple version is shown in figure 4.10.

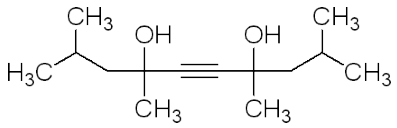

Figure 4.10: Molecular structure of Surfynol 104, a basic molecule of many acetylenic diols. Variations may be made by ethoxylating the oxygen atoms, i.e. attaching several $[CH_2CH_2OH]$ links at each of the two oxygen atoms, or by longer carbon chains in the hydrophobic part.

They exist in a number of variations, i.e. with a different number of ethoxylate links or different number of carbon atoms in the hydrophobic chains.

AD has a total of 4-5 links on average, varying between 1 and 7, making it unlikely to form complexes between a single ethoxylate chain and an ion. Due to the short chains, AD is not very hydrophilic and it is only possible to dissolve around 150ppm pr. liter.

Due to the high uncertainty in molecular size, the amount of AD in samples will be measured in ppm (parts pr. million, or mg/kg).

The exact formula of AD is proprietary. Information may be found in the confidential Appendix H.4, or by contacting the author.

4.6.2 Secondary Structures

AD is special when it comes to secondary structures. It does not form micelles in aqueous solutions. This may be due to:

- Rotational freedom around triple-C bond.
- Hydrophobic and hydrophilic parts very similar in size.
- Low solubility.

4.6.3 Dynamic Range

As defined in section 4.6.3, the *Dynamic Range* of a surfactant, is the range in which a change in free concentration will cause a change in surface concentration.

The close-packed surface layer of AD has a concentation of $\Gamma_m = 2.21\mu\text{mole} \cdot m^{-2}$, which gives an area pr. molecule of $0.75nm^2$. The corresponding C_{free} is $0.3m\text{mol}/l$, which means that at concentrations below this limit, any change in surfactant concentration will be reflected in a change in surface coverage, and consequently in a change in surface tension.

The surfactant concentration in the rinse liquid studied in this thesis is within the dynamic range, which is confirmed by a *sessile drop* contact angle experiment. It is observed that pure rinse liquid has a contact angle of 90° on a membrane surface, while rinse liquid containing 100ppm AD has a contact angle of 50°, see figure 4.11 for details.

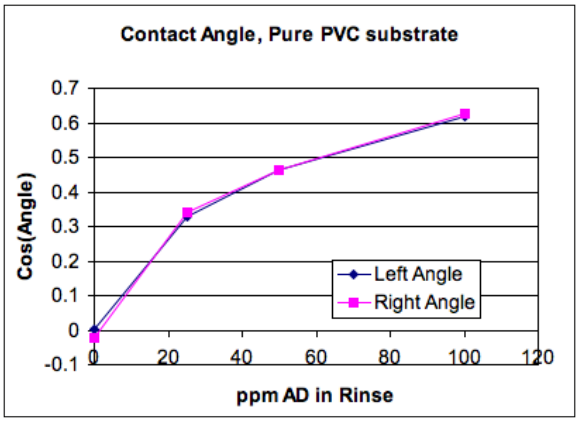

Figure 4.11: Measurements of contact angle of Rinse Liquid containing between 0 and 100ppm surfactant, on pure PVC substrate. It is seen that the contact angle changes dramatically within the concentration range of the surfactant.

4.6.4 Surface Orientation

An important observation made by Musselman and Chander [32] is that exthoxylated acetylenic diols orient themselves at the surface in vertical positions with the ethoxylated chains into the water. This is like an inverted version of the monolayer shown in figure 4.2.

They also conclude that at low surface coverage fractions, the ethoxylate chains attach to the surface, instead of pointing into the water.

4.6.5 Dynamic Adsorption

The adsorption isotherms above describe the surface coverage at equilibrium. However, it is relevant to know how fast this surface coverage occurs.

Ferri and Stebe [33] measures the dynamic surface adsorption rate of Surfynol 104, and extrapolates that a complete surface cover is built on a timescale of milliseconds with a free concentration of only $0.01m$mol pr. liter. At the concentrations of AD present in the samples used in this thesis the surface coverage can be assumed to have reached equilibrium nearly instantaneously.

4.6.6 Theoretical Challenges

Normal modelling assumes that the interface is between an aqueous phase and a solid or air, neglecting the effects of partitioning of surfactant between polar and apolar phases. As a consequence, the following phenomena are not described, to the best of my knowledge. Developing these models is beyond the scope of this thesis, but would be an excellent focus of future research.

i) Surface distribution in case of partitioning
ii) Bulk distributions of surfactants between immiscible phases
iii) Adsorption Isotherms when surfactants may adsorb from both sides of the interface
iv) Effects at very low diffusion rates, i.e. in a polymeric membrane
v) General behavior and distribution of surfactants in polymeric membranes

The diffusion constants of surfactants are much lower in a polymeric membrane than in the aqueous phase. This means that at short time scales, one can use the models and isotherms developed in this section, but at longer time scales, partitioning may play a role. In later experiments, it is shown that there are two seperate phenomena, one occuring on a timescale of seconds, the other on a timescale of several minutes.

4.7 Applicability of Surfactant Interaction Model

In section 2.5 a model for a surfactant selective electrode was proposed. The model relied on two key phenomena:

i) A pseudo-cationic complex is formed between surfactant and an ion

ii) The pseudo-cationic complex forms sparingly soluble salt with TPB in the membrane

By careful choosing of the membrane components, they can keep the concentrations within the membrane constant, which gives a Nerstian response to concentration changes in the aqueous phase.

4.7.1 Complexation

AD may form pseudo-cationic complexes with ions in the solution or at the surface of the membrane. While the extholylated chains of AD are too short to form a complex like the one described by Sak-Bosnar et al. [7], the gemini-structure may make it possible to form complexes with two shorter chains.

The geometry of acetylenic diols does not indicate a stable complex, however, due to the rotational freedom around the triple-carbon bond. At surfaces ethoxylated acetylenic diols orients with both chains parallel[32], making complexation more likely.

Whether this the surfactant-ion complex partitions into the membrane is unclear.

4.7.2 Sparingly Soluble Salt

It is not known whether AD might form a sparingly soluble salt with TPB, but it is possible.

4.7.3 Constant Concentrations

The constant concentrations within the membrane are not initially true for the sensors researched in this thesis. However, all components necessary are in the solutions or the membranes. It is conceivable that the sensor is "conditioned" by the surfactant in the Rinse.

In the model, one of the assumptions is that the free concentration of the complexing ion, $[J^{z_J}]$, is constant. The concentration of AD is up to $\approx 0.235\text{m}mol$ pr. liter. The concentration of ions in the Rinse and other samples is consistently significantly higher. This means that for chemical equilibrium purposes, the concentration/activity of free ion can be considered to be constant.

4.7.4 Summary

Although there are many unknown factors when transferring the phenomena of their model, I believe it can provide information about the interference mechanism.

Chapter 5

Experimental – General Considerations

This chapter documents the procedures used for experiments in this thesis.

All experiments in this thesis are performed on the same experimental platform: A modified version of Radiometers ABL700 analyser.

This chapter describes the general experimental platform and the procedure for the experiments performed in this thesis.

It consists of the following parts:

Implementation Overview of the construction of the analyser

Procedure The procedure followed when making a measurement/-experiment and the terminology is described.

Samples The composition and methods of preparing the samples used.

Compositions Overview of the membranes used in the thesis. Details of their components and their composition. An overview of the samples used.

Data Collection Description of how the data are measured, collected and summarized for each measurement.

Data Treatment Description of how data are fitted to models to yield parameters. The Non-Linear Fit Method is explained.

Degassed Liquids An experimental procedure to reduce the amount of bubbles in the analyser is described.

5.1 Overview of Radiometer Experimental Platform

Radiometer has implemented the LMSC-electrode onto a sensor board that fits into a modified version of their older ABL700 analyser. It has automatic sample transport, membrane rinse and calibration programs. This makes sample measurement and data collection easier. The construction principle can be seen in figure 5.1.

There are room for 6 different sensors in the measurement chamber, and each will be measured simultaneously. They are connected to a reference electrode, constructed like the reference electrode described in section 3.4.

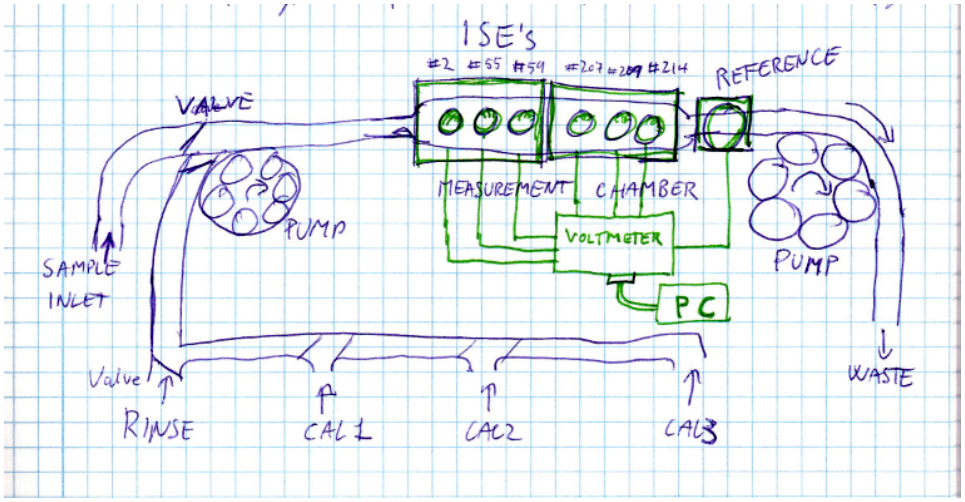

Figure 5.1: Sketched diagram of the ABL700 adapted for LMSC-sensorboards. The measurement chamber contains 6 ISE's.

5.1.1 Measurement Chamber

The measurement chamber is always heated to 37°C, to keep it at the same temperature as blood. Samples and other liquids are assumed to equilibrate in temperature before entering the chamber. For this reason, all samples should be at least room temperature before insertion.

5.1.2 Sensor Board

The sensor boards are constructed with three sensors on each board. Two of these boards fit into the measurement chamber.

Each ISE sensor has a reference number for data collection, see figure 5.2.

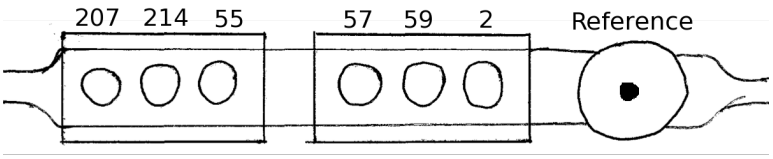

Figure 5.2: Sketched diagram of a Sensor Board. Flow direction is from left to right.

5.1.3 Simultaneous Measurements

Since there are six sensors in the measurement chamber, it is possible to have the same ISE on two or more positions. This reduces the need for repeated experiments, and makes it possible to estimate the reliability and stability of a given composition, since the experimental conditions during a single sample measurements can be assumed to be equal for two positions on the board.

One possible exception is the effect of prolonged surface flow for the first sensors in the chambers, as described in section 2.3.

It may cause some confusion when referring to the data from a measurement on a sample. The terminology is defined in section 5.2.

5.1.4 Liquid Flow During Measurement

Between measurements the measurement chamber is filled with rinse liquid.

When a syringe containing a sample is put at the inlet, the platform first measures on the rinse liquid already present in the chamber. Then the rinse liquid is pumped out, and the sample is pumped into the chamber. The potential is measured while the sample is stagnant. The sample is then expunged, and replaced with rinse liquid. The rinse is then measured again. Between each liquid phase is an air gap, to hinder mixing between samples and rinse liquid.

There is generally a remnant of the previous liquid present in the chamber. When replacing this, not all may be removed. The liquid left from the previous, after replacement, is called the "Carry-Over". It is generally considered to be around 1-3%. Increased sample size or rinse amount can reduce the Carry-Over.

5.1.5 Bubbles

Small air bubbles may form in the tubes and attach at the sensor surfaces.

At the measurement chamber the circular tube, in which the liquid flows, spreads out into a flat form with curved corners. This change in shape may

induce formation of bubbles. Similarly, the irregularities at the edges of the sensors may induce or trap bubbles.

This problem is especially relevant when measuring on samples with no surfactants. The problem is analyzed in section 5.7.

5.1.6 Data collection

A PC is built into the analyser. An I/O card samples the potential difference between a sensor and the reference electrode. the measurements are taken once pr. second.

The data is stored for 10 seconds of the rinse liquid in the measurement chamber before the sample. For 30 seconds while the sample is stagnant within the chamber. And for 10 seconds on the rinse liquid that replaces the sample. It does not sample while liquids are being changed (see figure 5.3).

This is done to be able to use the rinse liquid as reference, as E_0 of a sensor may drift significantly over time (Recall the conditioning effect shown in figure 3.13).

It is possible to measure once a second without pauses, through the use of a special program, but this method simply samples the potential, without noting sample changes etc.. This makes data analysis on data of this format highly elaborate, and beyond the scope of this thesis.

5.1.7 Consequences of construction

- 6 simultaneous experiments performed
- Possible remnants of rinse-liquid when measuring sample (carry over effect)
- Possible carry-over between samples
- Rinse and other liquids may be present in tubes some time after changing the bottles supplying them.
- Possible transport of components from one sensor to another
- Possible bubble formation in tubes and at the surface of sensors.
- Exact times of exposure unknown, as the analyser measures in intervals while the liquid is stagnant
- Conditioning happens slowly, and after sensors are inserted into apparatus. E_0 may drift significantly during the run of an experiment (7.5mV/hour was measured for the Ca sensor).
- All experiments are performed at 37°C, and 1 atm pressure.

5.2 Procedure and Terminology

Each experiment contains the following elements:

i) Sensor Board, containing 6 ISE's
ii) Rinse Liquid
iii) Planned sequence of samples.

The planned sequence of samples is called a measurement series. Each of the elements may be changed during an experiment, but for practical reasons each change of Sensor Board of Rinse Liquid is considered a new experiment.

One *physical measurement* is one sample measured in parallel on the six ISE's of one sensor board with one Rinse Liquid composition, and contains data from each sensor.

5.2.1 Logical Data Structure

The data from one physical measurement are logically divided into *ISE-measurement's*.

One *ISE-measurement* contains $30 + 2 \times 10$ time-resolved measurements (see section 5.1.6). These are summarized into E_{real} and E_{ref} for the sample and the rinse, respectively. One ISE measurement is characterized by a list of the known parameters of the physical measurement, i.e.

i) Membrane Composition
ii) Membrane Position (in chamber)
iii) Rinse Composition
iv) Sample Composition

Several ISE-measurements can then be grouped according to a similarity of one of these parameters, e.g. Rinse Composition. Such a grouping is called a *setting*.

Each ISE-measurement is assumed to be uncorrelated with previous measurements.

5.2.2 Experiment Preparation

Sensors in measurement chamber are replaced if necesary. Reference electrode is replaced if necesary. The different rinse and calibration liquid containers are changed if necesary.

The time of sensor insertion is noted, to be able to measure conditioning effects.

5.3 Sample preparation

All experiments are performed with aqueous samples, even though the technology is developed to measure on whole blood. This choice is made to reduce the number of unknown factors in the system.

Since the ISE's measure activities of ions, and not concentrations, care has to be taken when mixing samples. The calculation of activity of ions is explained in Appendix B.

Unless explicitly mentioned, samples "Containing AD" contain 100ppm AD pr. liter.

5.4 Membrane Compositions

In this thesis three membrane compositions are analysed in detail. Other compositions are introduced for comparison.

As an example of a membrane composition with a very marked response towards AD, a commercially available Magnesium sensitive membrane is chosen[34]. It contains the ionophore ETH5506 (Fluka 63112), the plasticizer ETH8045 (Fluka 46092), the lipophilic salt potassium tetrakis(4-chlorophenyl)borate (Fluka 60591), and regular PVC as polymer matrix.

Structural diagrams of these components can be found in Appendix A.

To isolate the effect of ionophore and lipophilic anionic sites, membranes with similar compositions but without ionophore and/or lipophilic salt are introduced. These membranes are not selective. The membranes are named "Pure", "Salt" and "Mg". Their compositions can be seen in table 5.1, along with sensors used for comparison purposes.

Exact membrane compositions may be obtained from the author.

Table 5.1: Compositions of membranes. This table relates the name used for the membrane in this thesis, the components of the membrane cocktail and an internal ID tag. All membranes investigated in this thesis are included.

Name	Salt	Ionophore	Plasticizer	Description	ID
Mg	+	ETH 5506	ETH8045	Mg^{2+} Selective	Mg097
Mg	+	ETH 5506	ETH8045	Mg^{2+} Selective	Mg098
Salt	+	–	ETH8045	Plasticizer + Salt	Mg159
Pure	–	–	ETH8045	Pure PVC/Plasticizer	Mg160
Ca	+	ETH1001	DOP	Ca^{2+} Selective	M1217
Ca	+	ETH1001	DOP	Ca^{2+} Selective	M1443
DOP-Salt	+	–	DOP	Different Plasticizer, Salt	Mg162
DOP-Pure	–	–	DOP	Different Plasticizer	Mg161

5.5 Data Format and Data Collection

Since the sensor may need some time to equilibrate, the potential is measured once a second for 30 seconds.

The data is measured as described in section 5.1.6.

The data extraction program relates the measurements with an ID number of the measurement, and relates each measurement to a log book.

The data for each sensor is divided into two parts; Numbers summarizing the entire measurement, and a series of time-dependent measurements. E_{real} has the value of the last measurement on the sample. E_{ref} has the value of the last measurement on the rinse.

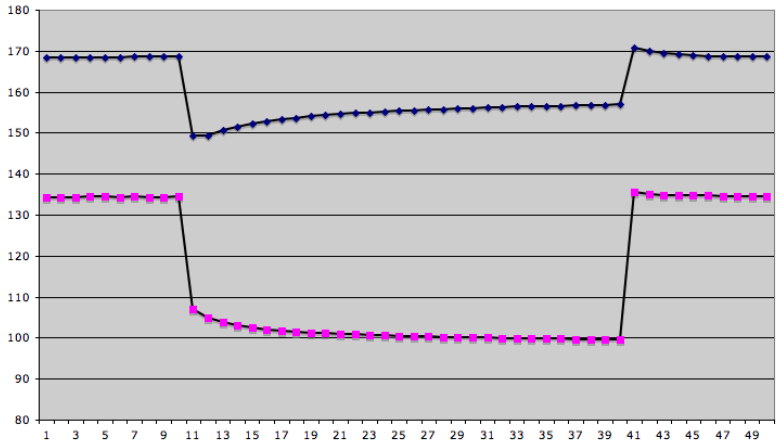

Figure 5.3: Potential of Timeresolved measurements from two ISE-sensors on the experimental platform described in section 5.1.

5.6 Data Analysis

Some of the experiments are performed according to standard procedures, in order to obtain key parameters in different models.

To fit the data to the different models describing the response of the ISE's, i.e. Nernstian response (2.8) or Nikolskii-Eisenmann (2.17), the experimental data are fitted to the model using Excel's non-linear optimisation package "Solver". This method has been tested and approved by Walsh and Diamond [35] and Kane and Diamond [36].

The method minimizes a value that one can relate to the difference between the measured data and the model, i.e. *Sum of Squared Residuals*

(SSR)

$$\mathrm{SSR} = \sum_k \left((E_{model,k} - E_{meas,k})^2 \right), \tag{5.1}$$

for all datapoints k, by fitting any number of parameters.

If the datapoints are assumed to be normally distributed around the ideal response, with fixed variance, then SSR will be an unbiased estimator of the parameters. This is not generally true for non-linear models, yet for practical reasons, I choose to assume that the bias is negligible in this case.

The values from fits performed by the graphing software Igor Pro are obtained by the same procedure. The resulting parameters are listed plus/minus one standard deviation.

Data points which are obviously far from the model, due to e.g. bubbles, are treated as NaN, not a number, and disregarded in the fit. This happens in very few measurements.

A detailed description of the data analysis performed is included in the chapters describing the experiments.

5.7 Degassed Liquids

When performing experiments without surfactants in the system, many small bubbles were observed in the measurement chamber. If one of these bubbles attached to a sensor surface, the electrical circuit is broken, and the potential reads as -600V. To alleviate this problem and get reliable measurements without adding surfactant, a method was developed to reduce the amount of air absorbed in the liquids and samples. This is thought to reduce the number of bubbles formed within the tubing and measurement chamber.

The method is very low-tech, but quite efficient.

i) A syringe is filled halfway with the liquid in question.

ii) All air within is removed by pushing the piston.

iii) The nozzle is plugged.

iv) The piston is withdrawn, causing the pressure within the syringe to drop.

v) The syringe is shaken vigorously, and bubbles form and rise to the surface.

vi) The piston is gently released.

vii) The plug is removed, and the "new" air is removed by pushing the piston.

viii) The process is repeated until no bubbles form.

The liquids are then carefully poured into their bottles, and it is assumed that air will not be absorbed in significant amounts during the run of an experiment. Both samples and Rinse Liquid are degassed before an experiment.

It is estimated by comparing the position of the piston before and after, that $40ml$ of rinse liquid releases $1ml$ of air.

The method is illustrated in figure 5.4.

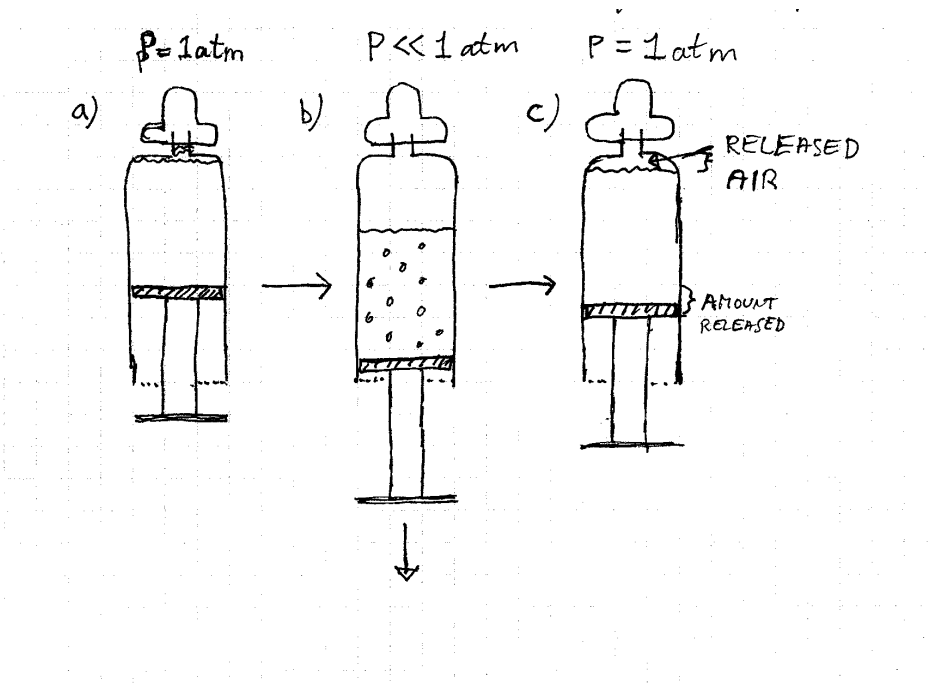

Figure 5.4: Illustration of the procedure used to degas samples and rinse liquids. The procedure is explained in section 5.7.

Chapter 6

Experimental – Standard Response of Electrode

The purpose of the experiments described in this chapter is to evaluate the effect of the surfactant AD on standard parameters of the membrane, i.e.

Sensitivity Defined through the Nernst Slope

Selectivity Defined through the interference coefficient K_{ij}^{Pot}

If the sensitivity of, or selectivity against, an interfering ion changed dramatically as a consequence of the presence of AD , this could account for the change in potential.

Furthermore, these experiments substantiates and illustrates the theoretical models presented in Chapter 2. The Magnesium sensitive sensors ("Mg"), described in section 5.4, are tested and compared with "dummy" sensors of a similar composition, but without ionophore ("Salt"), or without ionophore and lipophilic salt ("Pure"). These variations were chosen since early experiments demonstrated that a sensor without ionophore still responded to changes in AD concentration.

6.1 Experiment Series Overview

All experiments in these series are performed with the sensor array seen in table 6.1.

6.1.1 Sensitivity

One series of experiments determine the sensitivity of the sensors towards Mg, Ca, K and Na, respectively. The sensitivity S is then calculated according to the definition by the Nernst Equation:

$$E = E_0 + S \ln a_i \tag{6.1}$$

Table 6.1: Sensor Array of the membranes used for Sensitivity and Selectivity experiments. The flow direction in the measurement chamber is from top to bottom of the table. Compositions can be seen in table 5.1

Name	Position
Salt	207
Salt	214
Pure	55
Mg	57
Mg	59
Pure	2

or an extended Nernstian response with a $E = E_0 + S\ln(a_i + K)$, where K is introduced to facilitate calculation of S and represents the lower detection limit etc., but does not have a direct physical interpretation.

6.1.2 Selectivity

Another series of experiments determine the interference coefficient K_{ij}^{Pot} between the primary ion Mg^{2+} and the interfering ions Ca^{2+}, K^{+} and Na^{+}. This is done by the Fixed Interference Method (FIM), in which the concentration of the primary ion is varied, while each interfering ion in turn is kept constant. The response is then fitted to the Nikolsky-Eisenmann equation (2.17):

$$E_M = E_i^{\circ} + \frac{RT}{2F}\ln\left(a_i' + K_{ij}^{Pot} a_j'^{z_i/z_j}\right) \tag{6.2}$$

6.1.3 Settings

Each of these series of experiments are then repeated under different conditions regarding the surfactant:

No AD This is the setting used to evaluate reference-values. The sensors have never been in contact with any surfactant before, as there might be a long term effect of the surfactants. In this setting, bubbles are a problem (recall that surfactant is added to reduce bubble formation). To avoid bubbles, the rinse liquid is degassed, as described in section 5.7.

AD in Rinse In this setting, the rinse liquid contains AD , but the samples do not. It is expected that some AD will be released from the tubing and chamber walls into the samples during measurements.

AD in All In this setting, there is AD in both rinse liquid and samples. This supposedly reduces bubbles and makes the samples flow more smoothly.

Where AD is present, the concentration is 100ppm pr. liter.

6.2 Sample Preparation

As mentioned in section 2.1.3, the sensors measure single ion activities, not concentrations.

Since a logarithmic dependence between potential and activity is expected, the concentrations of the samples are varied logarithmically.

The samples are made from distilled water by adding a certain amount (weight) of salt, calculated according to Appendix B, to get the sample with the highest concentrations. This is then diluted in steps, until all samples are finished. In cases where all samples contain the same amount of a given substance (i.e. ion or AD), this is added to the distilled water used for dilution.

6.2.1 Sensitivity

For the sensitivity experiment, the samples seen in table 6.2 were mixed. The

Table 6.2: Samples used for the sensitivity experiment. Activities are measured in mmol. The samples are made by adding pure chloride salts to distilled water. A similar set containing a background of 100ppm AD pr. liter was also prepared.

Ion	0.01	0.1	1	10	100	1000
Mg	+	+	+	+	+	−
Ca	+	+	+	+	+	−
Na	−	−	+	+	+	+
K	−	−	+	+	+	+

activities are chosen so they are distributed around the lower detection limit of the Magnesium sensitive sensor. These values are known from previous studies by Radiometer.

6.2.2 Selectivity

For the experiment with interference, samples were prepared with 0.01, 0.1, 1, 10 and 100mmol Magnesium, and with background concentrations of: 1.2mmol Ca, 4mmol K, 160mmol Na. Due to the circumstanceous mixing procedure, no sample series with AD was mixed.

6.3 Measuring Procedure

For each experiment, a series of samples are measured. The samples were measured from low concentrations to high, to avoid problems with equilibration times, as described in section 2.3.

Each sample was measured twice, and a Rince Program was executed between each sample, to reduce correlation between measurements. Between each experiment, several Rinse Programs were executed.

6.3.1 Rinse Change

To change the conditions of the experiments to "AD in Rinse", the Rinse Liquid container was changed to one containing AD , and several rinses were run to replace the rinse liquid in the tubing.

6.4 Data Analysis

These experiments evaluate standard parameters for accepted models. The data are fitted to these models using non-linear Least Squares fitting, as described in section 5.6

6.4.1 Sensitivity

Since the Nernst equation in the form:

$$E_M = E_0 + S \log (a_i) \tag{6.3}$$

only fits to the linear part of the response, the definition of this linear part would have to be a subjective choice. This is hardly trustworthy with only 5 data-points, so instead the data are fitted to an Extended Nernstian Response on the form:

$$E_M = E_0 + S \log (a_i + K). \tag{6.4}$$

The sensitivity coefficients calculated by the two methods are similar, as can be seen in figure 3.11 on page 39, although the physical interpretation of the parameter K is less clear than in e.g. the Nikolskii-Eisenman equation.

The ideal value of S is $S = 2.303RT/Fz_i = 61.57\,m\mathrm{V}/z_i$ at $T = 37°\mathrm{C}$.

A graphical representation of the response to magnesium in three different settings can be seen in figure 6.1.

In some cases the response is nearly constant, and no fitting is possible.

The results are summarized and evaluated/discussed in section 6.5

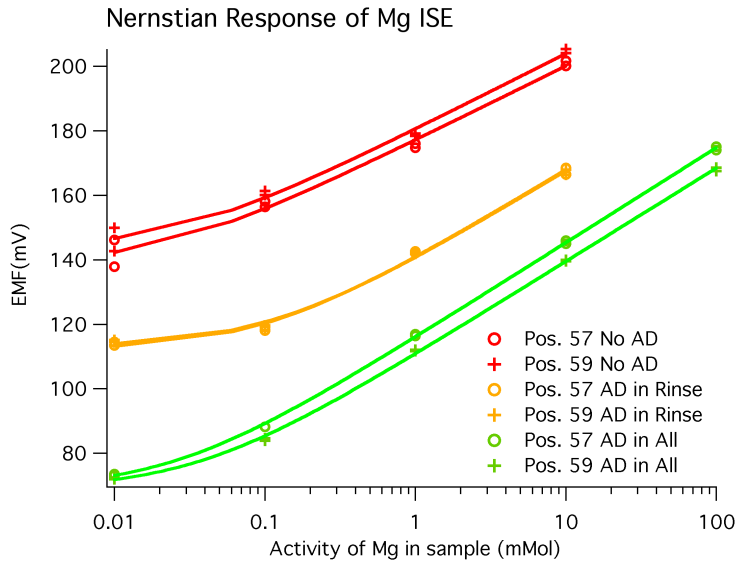

Figure 6.1: Response of the regular Mg-sensitive electrode to samples containing only $MgCl_2$ at different concentrations. As can bee seen, there is quite a difference in E_0 under the different conditions, yet S is approximately unchanged. The data has been fitted to an extended Nernstian Response of the form $E = E_0 + S\log(a_i + K)$. Fit coefficients can be seen in table 6.3.

6.4.2 Selectivity

The selectivity experiment was performed by the Fixed Interference Method (FIM), where the selectivity is measured by varying the concentration of the primary ion against a background caused by an interfering ion at constant concentration.

The selectivity coefficients of each sensor towards each interfering ion is calculated by fitting to the Nikolsky-Eisenmann equation:

$$E_M = E_0 + S\ln\left(a_i + K_{ij}^{pot} a_j^{z_i/z_j}\right). \tag{6.5}$$

The SSR is minimized, fitting the parameters E_0, S and K_{ij}^{pot}, using a_i as variable, and $a_j^{z_i/z_j}$ is a constant for each experiment. A high precision is required for the numerical fitting, since the value of K_{ij}^{pot} can be very close to zero, and may vary with several orders of magnitude.

The results are summarized and discussed in section 6.5.2.

6.5 Results

The results from the two series of experiments are explained here.

There was a drift in E_0 for all sensors over time. This drift may be due to conditioning effects. I do not find it justified to claim that it is caused by the presence of AD .

6.5.1 Sensitivity

The goal of the sensitivity experiments was to determine if the presence of AD changed the fundamental sensitivity of the sensors towards any of the four tested ions. If it increases the sensitivity towards an ion noticeably, this could account for the interfering effect.

Six sensors of three different compositions are tested, and their sensitivity towards four ions under three different conditions is calculated . This gives a total of 72 values to evaluate. I choose to spare the reader of the tediousness of graphs and tables, and document only the most interesting results here. Additional tables for the interested reader, can be found in Appendix E.

Mg Sensor

The response can be seen in figure 6.1, and parameters from the fit are listed in table 6.3.

The sensitivity of the Mg sensor towards Mg^{2+} increased slightly, from around $23mV$ to $28mV$, when exposed to AD . The sensitivity towards Ca^{2+} changed similarly. In other words, the sensor became slightly more sensitive with AD present. The sensitivity towards Na^{+} and K^{+} did not change.

Table 6.3: Values of parameters from fitting the response of Mg sensors towards Mg^{2+} under different conditions to an extended Nernstian response, equation (6.4). Notice the change in sensitivity, S, with increased AD exposure. The graph of the fit can be seen in figure 6.1.

AD in:	ISE	E_0	S	K
None	Mg, Pos. 57	177.1±1.5	23.1±2.1	2.11E-02±1.56E-02
Rinse	Mg, Pos. 57	139.8±1.3	28.0±1.8	1.02E-01±3.15E-02
All	Mg, Pos. 57	115.8±0.41	29.5±0.3	2.5E-02±2.87E-03
None	Mg, Pos. 59	180.4±1.5	23.5±2.0	2.66E-02±1.67E-02
Rinse	Mg, Pos. 59	139.5±1.4	27.9±1.8	1.12E-01±3.46E-02
All	Mg, Pos. 59	110.5±0.5	29.0±0.4	3.64E-02±4.80E-03

Salt and Pure Sensor

For the other membrane compositions (Salt and Pure), the sensitivity towards the divalent ions was very low in all cases. The results were non-

conclusive at best. It seems that ion concentrations generally are below their lower detection limit.

The sensitivity of these sensors towards Na^+ and K^+ was unchanged.

6.5.2 Interference

Mg Sensor

Table 6.4 shows the values of fits. It is shown that the interference towards Ca^{2+} is high (from 0.38 to 0.77), and that it increases with "AD in Rinse". The interference from Na and K were lowered a bit, but not significantly.

The increase in sensitivity seen in the Sensitivity experiment is not apparent here.

Table 6.4: Mg sensor. Effect of AD on Interference from other ions. The value of K_{ij}^{pot} is the important parameter. FIM method used, see section 6.4.2.

AD	Pos.	E_0	S	K_{ij}^{pot}	SSR
$a_j = 1.2$ mMol Ca^{2+}					
No AD	57	173.57	24.57	0.39	22.03
	59	175.20	25.14	0.58	18.61
AD	57	141.25	25.85	0.63	11.12
In Rinse	59	138.39	26.70	0.77	10.27
$a_j = 4$ mMol K^+					
No AD	57	192.51	22.21	5.38E-06	4.75
	59	194.67	22.50	6.96E-06	6.22
AD	57	166.61	21.09	3.64E-06	14.40
In Rinse	59	165.80	18.89	2.86E-06	48.40
$a_j = 160$ mMol Na^+					
No AD	57	178.23	25.40	4.23E-03	7.58
	59	181.57	25.59	4.43E-03	4.7
AD	57	150.70	23.54	2.61E-03	13.71
In Rinse	59	148.57	23.79	3.31E-03	14.12

6.5.3 Salt and Pure

The Salt and Pure sensors were non-selective as predicted.

All the fitted parameters are documented in Tables in Appendix E.2.

6.6 Summary

The experiments described in this chapter demonstrate that:

- The Mg sensor is indeed Magnesium selective, and behaves according to the extended Nernstian equation.
- The sensitivity of the Mg sensor towards Mg^{2+} may change a little when AD is in the system, before or during the measurement.
- The interference from Calcium appeared to increase slightly when AD has been present in the system.
- The "Salt" sensor sensitive but non-selective, and adding AD did not change the selectivity.
- The "Pure" sensor was generally unresponsive.

No decisive causes for AD interference could be found in these experiments.

Chapter 7

Experimental – Surfactant Sensitivity

The purpose of the experiments described in this chapter is to measure the relation between potential and surfactant concentration in samples.

Since there is no established theory of the influence of surfactants, there are no "standard parameters" to evaluate or compare. These experiments are not based on any established procedure, and are explorative in nature.

The experiments are performed with varying concentrations of surfactant (from 0ppm to 100ppm). The concentration of surfactant is varied, while the ionic concentrations of the system are kept constant, at the level of the rinse liquid.

The response measured previously by Radiometer, was linear and symmetric, meaning that the slope of an ISE measurement series was the same whether the individual samples were measured in increasing or decreasing order of concentration.

It is attempted to reproduce this result and correlate the responses of different sensors.

7.1 Experiment Series Overview

It was observed that the response of the "Salt"-sensor was highly dependent on the number of days the sensor had been in contact with AD . Consequently, the data analysis is divided into series in which the sensors are:

New i.e. have had only very little contact with AD

Old i.e. have been conditioned in AD for several days

In each of these cases, the samples are measured first in increasing concentrations then in decreasing concentrations.

7.1.1 Settings

The experiments are performed under the following conditions:

No AD in Rinse In this setting there is only AD in samples, and no AD in rinse. It is only performed with "new" sensors, so the sensors have had no previous contact with AD .

AD in All In this setting, there is AD in both rinse liquid and samples. The sensors get exposed to AD between each measurement.

7.2 Samples

The samples all have the same ionic content as the rinse liquid, listed in Appendix D. It contains various ions at physiological concentrations.

The amount of AD in samples is measured in ppm (Parts Pr. Million = 1mg/kg), since AD has quite large variations in molecular size, which introduces a high uncertainty on the molar weight, as described in section 4.6.1.

A linear response was expected, so sample concentrations are equidistant.

A concentration series of AD in rinse solution was obtained by mixing a 0ppm and a 100ppm solution in different ratios. The resulting samples have an AD concentration of 0, 10, 25, 50, 75, and 100ppm, with identical background concentration of ions.

It was not possible to dissolve more than 100ppm AD .

7.3 Sensors Analysed

The sensors analyzed and their role are described in table 7.1. The specific sensors used for experiments under a given setting, will be listed in the relevant sections.

Table 7.1: Sensors used for measurement of the linearity of the response towards AD . Their compositions can be found in table 5.1.

Name	Purpose
Mg	Detailed Analysis
Salt	Detailed Analysis
Pure	Detailed Analysis
Ca	Control
DOP	Comparison
DOP–Salt	Comparison

7.4 Measurement Series

In each experiment each sample is measured three times, to evaluate the stability and reproducibility of each measurement. First in increasing concentration, then in decreasing concentrations.

The measurements of a measurement series are generally taken immediately after each other, i.e. as soon as the platform is ready to measure again.

A typical measurement series is shown in figure 7.1. Note that each marker denotes an ISE measurement.

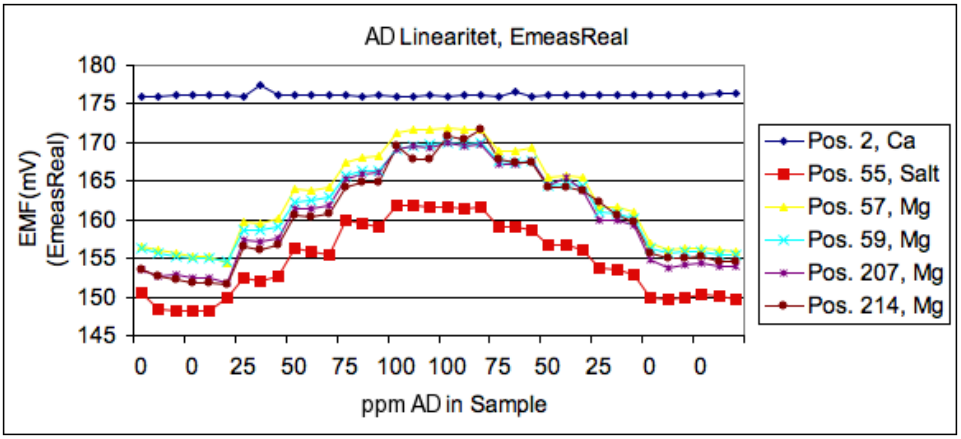

Figure 7.1: A typical measurement series on the Setting AD in All, Old Sensors. Each mark denotes an ISE measurement. Each sample of 0, 25, 50, 75 and 100ppm AD are measured 3 or 6 times. It is seen directly that even a sensor without ionophore (Pos. 55), experiences the effect of AD . The Calcium sensor (Pos. 2) is entirely unaffected.

7.5 Data Analysis

There is no previous theory to base the data analysis on.

The first task is therefore to describe and identify responses and phenomena, and their dependence on membrane composition. This will be done in section 7.6.1.

Some of the responses appear fit to recognizable functions, e.g. a linear response. These are analyzed by Non-Linear Fit method as introduced in section 5.6.

7.5.1 Sensors Responding

The first task is to identify which sensors respond to a change in AD concentration, and whether there is a difference under different settings.

The responses are plotted, and the sensor responses are analyzed and compared by visual inspection.

The symmetry of upwards and downwards concentration profile of the measurement series is analysed.

7.5.2 Non-Linear Model Fitting

Since no general theory exist, I have chosen the following models:

Linear Response

The data are fitted to a linear response since this was the observation by Radiometer.

$$E = E_0 + s[D] \tag{7.1}$$

where s is the slope of the linear response and $[D]$ is the concentration of AD .

Nernstian Response

The model in section 2.5 predicts a Nernstian response due to complexation of the surfactant.

The data are fitted to an extended Nernstian of the form used in the previous chapter, in section 6.1.1:

$$E_D = E_D^0 + S_D \log([D] + K), \tag{7.2}$$

where D denotes AD , and the sensitivity coefficient is defined through equation (2.45) as:

$$S_D = \frac{x}{z_J} \cdot 2.303 \frac{RT}{F}. \tag{7.3}$$

7.6 Results

Since these experiments were explorative in nature, the results are both qualitative and quantitative.

7.6.1 Sensors Responding

First it is identified which sensors respond at all. The results are shown in table 7.2. Where applicable, the difference between the potential at 100ppm and 0ppm AD will be noted.

The numbers for each sensor measured are summarized in Appendix F.2.

Table 7.2: Sensor response to AD . Characteristic potential differences between 0ppm and 100ppm AD are noted. All sensors except the Calcium ISE responded. DOP-Pure and DOP-Salt have only been measured under "No AD " conditions.

	Setting	
Sensor	AD in All Old sensors	No AD New Sensors
Mg	15mV	12mV
Salt	13mV	120mV
Pure	5mV	15mV
Ca	1mV	1mV
DOP-Pure	-	70mV
DOP-Salt	-	40mV

The variations between sensors of the same composition are quite big. The numbers do not indicate whether the potential variation is correlated with the AD concentration of the samples, or whether it is just measurement errors or noise. A detailed analysis of sensors will be described in section 7.7.

7.6.2 Interpretation

Here the different responses will be interpreted.

Mg Sensor

The Mg sensor does dot respond immediately towards AD . The sensitivity is acquired over several days. Technical studies at Radiometer have shown that the Mg sensor gradualy becomes more sensitive within the first 5-10 days.

Salt sensor

When the Salt sensor first encounters AD it responds very strongly. A change of 120mV corresponds to a 100-fold concentration change for monovalent ions, or 1000-fold for divalent ions. This response appears to be Nernstian, and will be analyzed in section 7.7.3. The response of DOP-Salt sensors is much less pronounced, which may indicate a plasticizer-specific AD interaction.

The sensor responds less strongly on old sensors, and with an apparent linear response profile for both ascending and descending concentration changes. This is analysed in section 7.7.1.

Calcium Sensor

The Calcium sensor is not sensitive to AD at all. Research at Radiometer shows that the Ca-sensor *does* show interference, if there is no Calcium in the sample. This may indicate that the sensor is too selective for Calcium to notice anything else.

Pure Sensor

The Pure sensors do not respond very strongly, compared to "Salt". This may be caused by the very high impedance of these sensors, or indicate that the effect is caused by a specific interaction between AD and Tetra-Phenyl-Borate.

7.7 Analysis of Sensitivity

As will be demonstrated in this section, there was a marked difference in the response of some of the sensors under different settings.

The analysis will focus on whether the response towards ascending or descending concentrations in samples is symmetric.

The following cases will be analysed:

Symmetry of Response	Assuming linarity, slopes at upwards and downwards concentration changes will be compared.
Downward Concentration Changes	This response seemed linear for all sensors. Their responses will be compared and analyzed.
AD in Samples, New sensors	Different fit functions will be compared. Apparent Nernstian behavior will be analysed.

7.7.1 Symmetry of Response

Some sensors showed a nearly symmetric response, while others had a response that was clearly not symmetric. The difference is illustrated in figure 7.2 and figure 7.3.

Inspection of the conditions of the experiments determined that the symmetric response only occured under the setting " AD in All", on sensors that had spent more than 48 hours in the apparatus with AD in the Rinse liquid.

The experiments performed under these conditions will now be analyzed.

As can be seen, the response appeards linear, and although E_0 differs from sensor to sensor, the slope of a linear fit does not show a significant difference. The coefficients of such fits are summarized in table 7.3. Representative graphs for the analysis of symmetry can be found in Ap-

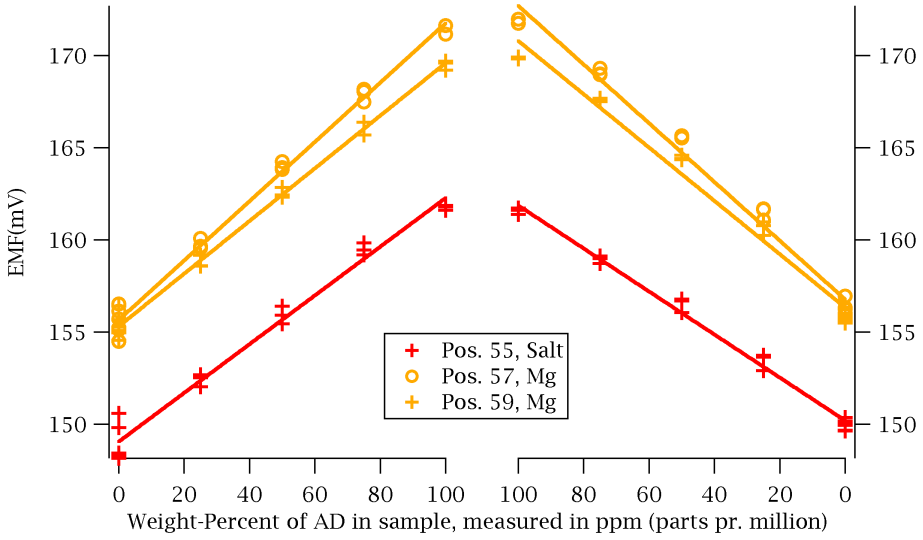

Figure 7.2: Plot of the measured potential of different sensors of Salt and Mg composition, at different AD concentrations. The symmetry measuring from low to high, and from high to low, is clear. The Setting is AD in All, so the sensors have been conditioned in AD -containing rinse for several days. The potential is fitted to a linear function. Values of these parameters can be seen in table 7.3.

Table 7.3: Slope of linear responses on old sensors. Clearly symmetrical.

		Up	Down
		mV/ppm AD	mV/ppm AD
Ca	Pos. 2	-0.001±0.002	-0.001±0.001
Salt	Pos. 55	0.132±0.005	0.117±0.003
Mg	Pos. 57	0.161±0.003	0.159±0.005
Mg	Pos. 59	0.143±0.005	0.145±0.005
Mg	Pos. 207	0.169±0.003	0.161±0.007
Mg	Pos. 214	0.162±0.004	0.159±0.006

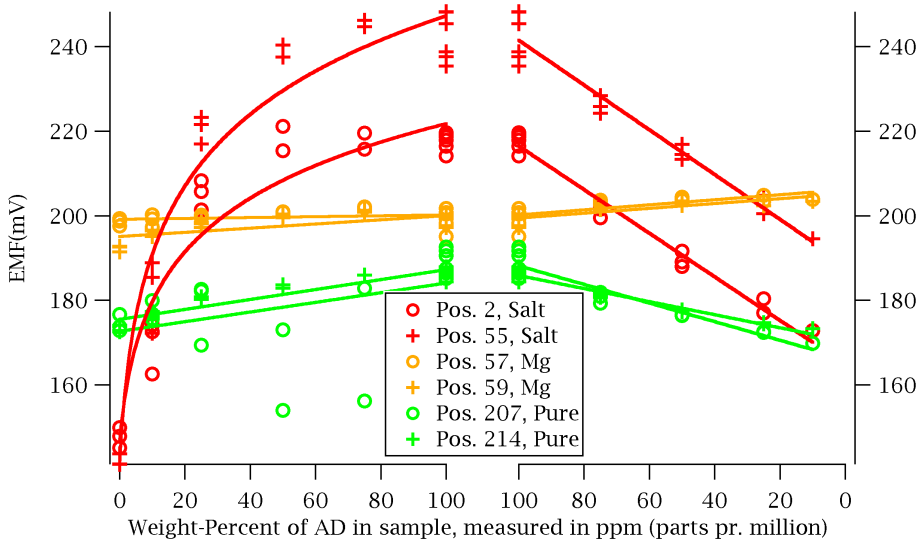

Figure 7.3: This graph illustrates the lack of symmetry on sensors when they first are exposed to AD . Plot of the measured potential of different sensors at different AD concentrations. The setting is "New Sensors". It is clear that there is not symmetry between from low to high, and from high to low. The potentials are fitted to a linear function, except Pos.2, Salt and Pos.55, Salt on the right. These are fitted with an extended Nernstian response.

pendix F.

7.7.2 Downwards Concentration Profile

This response seemed linear for all sensors. Their responses will be compared and analyzed. In table 7.4 the results for the "Salt" sensors are summarized. There is a large difference between new and old sensors. In table 7.5 the results for "Mg" sensors are summarized. The tendency is the same as for "Salt" sensors.

Table 7.4: Comparison of Downwards slope of Salt sensors. There is a big difference between new and old sensors.

Sensor	Slope
Old	0.117±0.003
New	0.649±0.049
	0.529±0.035
	0.571±0.024
	0.515±0.022

Table 7.5: Comparison of Downwards slope of Mg sensors. There is a big difference between new and old sensors.

Old	New
0.159±0.005	0.049±0.025
0.145±0.005	0.052±0.022
0.161±0.007	-0.060±0.017
0.159±0.006	-0.057±0.011

7.7.3 Initial Response of New Sensors

The very big response on "New" Salt sensors is very interesting.

The nature of this response is apparently Nernstian-like, as can be seen in figure 7.4, which shows the responses that form the basis of this analysis.

The important results are:

Reproducibility

All experiments performed on Salt sensors under similar conditions appear to be of the same type. This means that the response is is not simply a measurement error or fluke. It also indicates that the results are reproducible.

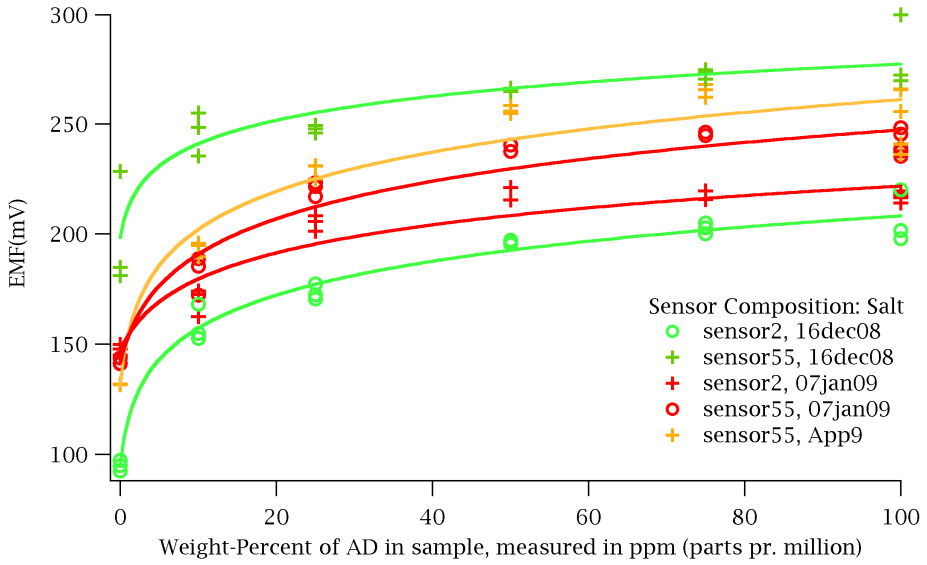

Figure 7.4: Plot of the measured potential of different sensors of the Salt composition, at different AD concentrations. The Setting is No AD , so it is the first time the sensors register AD . The potential is fitted to a Nerstian-like function of the form $E = E_0 + S\log(c_{AD} + K)$, where E_0, S and K are the fitting parameters. Values of these parameters can be seen in table F.2.

Recognizable Response

The responses can all be fitted to the same function with three free parameters. Although the values of the fitted parameters vary from sensor to sensor, the fact that a single function can be fitted to all responses indicate that this function is representative of the phenomena.

Apparent Nernstian Response

The responses fit to the function

$$E = E_0 + S\log([AD] + K). \tag{7.4}$$

This can be fitted by an Extended Nerstian Fit. Table F.2 in Appendix F contains values of fitted parameters.

This response was predicted by the model introduced in section 2.5.

Assuming that AD is charged, i.e. through complex formation with ions in solution, the relation between the fitted S and corresponding stoichiometry/charge relationship x/z_i, can be calculated from the relation given by equation (2.45): $S_D = \frac{x}{z_i} \cdot 2.303\frac{RT}{F} = \frac{x}{z_i} \cdot 61.57mV$

The results from these calculations are shown in table 7.6, and give a value of x/z_i between 0.5 and 1. This is equivalent to 1-2 AD molecules pr.

charge of the ion.

Table 7.6: Relation between the fitted S and corresponding stoichiometry/charge relationship x/z_i, calculated from the relation equation (2.45): $S_D = \frac{x}{z_i} \cdot 2.303 \frac{RT}{F} = \frac{x}{z_i} \cdot 61.57$

Parameter	S	x/z_i
Pos. 2, 16dec08	52.27±5.07	0.849±0.085
Pos. 55, 16dec08	37.23±10.63	0.604±0.179
Pos. 2, 07jan09	45.89±7.64	0.745±0.128
Pos. 55, 07jan09	60.17±7.53	0.977±0.127
Pos. 55, App9	60.60±9.36	0.984±0.157

7.8 Summary

In this chapter several experiments were performed, and the results from Radiometer were reproduced:

- The linear and symmetric response of "Old" Mg ISE's was reproduced, with slopes around $0.15mv$/ppm AD .
- This response was also observed on "Old" sensors without Ionophore, i.e. "Salt", with similar slope.
- No response was observed on the Ca sensor.
- "New" Mg sensors did not respond to changes in AD concentration.

For "New" sensors many phenomena were observed for the first time.

- The potential difference of "Salt" sensors was a big as 170mV between 0 and 100ppm AD
- The responses of all the "Salt" sensors could be fitted to a Nernstian-like response. Values of sensitivity were between 35 and 60.
- The Salt sensors all showed a linear reponse for the downwards concentration profile. Slopes were around $0.55m$V/ppm AD .

Finally, the results of the fitting to the model proposed by Sak-Bosnar et al. [7] yielded complexation stoichiometry which seem reasonable. This indicates that AD indeed complexates at the surface.

In the setting with AD in All, the potential of consecutive measurements on samples with 0ppm AD appears to drop slightly for each. This may indicate a memory-effect in the sensors, and a seperate experiment is performed to analyze this effect. This experiment is described in section 8.1.

Chapter 8

Experimental – Clarifying Experiment

Visual inspection of responses like the one demonstrated in figure 7.1 indicated a common trend, i.e. that the potential was lowered consistently for repeated samples without surfactant. To clarify this effect, the following experiment was performed.

8.1 Memory Effect

8.1.1 Procedure

To test whether there was a memory effect, an experiment was performed where 10 samples at 100ppm were measured, and then 10 samples without AD . Immediate data analysis indicated that an equilibrium had not been reached, and 8 more samples without AD were measured half an hour after the last.

Just before the experiment, the rinse with AD was changed to a rinse without AD .

The same samples as in Chapter 7 were used.

8.1.2 Sensor Array

The sensor array used is described in table 8.1.

Table 8.1: Sensor Array. The flow direction in the measurement chamber is from top to bottom of the table.

Name	Number	Description	ID
Ca	207	Ca^{2+} selective electrode	M1217
Mg	214	Mg^{2+} selective electrode	Mg098
Salt	55	Mg^{2+} selective electrode, without Ionophore	Mg097
Mg	57	Mg^{2+} selective electrode	Mg098
Mg	59	Mg^{2+} selective electrode	Mg098
Salt	2	Mg^{2+} selective electrode, without Ionophore	Mg097

8.2 Data Analysis

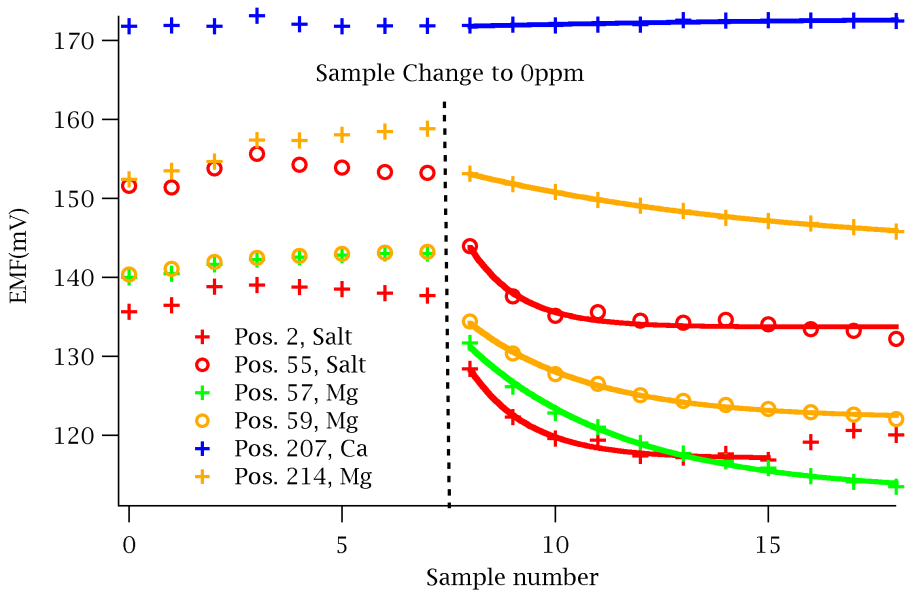

Figure 8.1: Long memory effect when changing from samples with 100ppm AD to samples with 0ppm AD , when there is no AD in rinse.

As can be seen from Figure 8.1 there is a very pronounced effect. This indicates that it takes several cycles of rinsing and measuring to remove the AD from a sensor. The process appeared to behave like an exponential decay, and it was fitted to an exponential of the form:

$$E = E_0 + A \cdot \exp\left(\frac{x - x_0}{\tau}\right) \tag{8.1}$$

where x is the sample number and x_0 is the first sample after changing to

samples without AD .

The results of the fit can be seen in table 8.2. As shown in figure 8.1, there

Table 8.2: Coefficients for fit of $E = A\exp((x - x_0)/\tau)$ on E_{meas}.

Sensor	Position	E_0	A	τ
Mg	Pos. 214	143.48±0.38	9.58±0.34	7.28±0.53
Salt	Pos. 55	133.72±0.33	10.06±0.85	1.19±0.23
Mg	Pos. 57	112.78±0.51	18.39±0.52	3.64±0.29
Mg	Pos. 59	122.18±0.21	12.04±0.27	2.80±0.17
Mg	Pos. 2	117.12±0.35	11.21±0.60	1.39±0.19
Salt	Pos. 2	118.46±0.51	10.05±1.42	0.96±0.32

is a very pronounced memory effect, lasting the duration of the experiment, around 30 minutes.

After the first samples, initial data analysis showed that the responses had not flattened out entirely, and I decided to try to get the last part of the "tail". The results surprisingly showed that the potential had increased while the platform was unused. Without AD in the Rinse. The potential dropped again when the measurements started. A graph of the entire experiment can be seen in figure G.1.

The fit coefficients, calculated as previously, are seen in table 8.3. The

Table 8.3: Coefficients for fit of $E = A\exp((x - x_0)/\tau)$ on Second Round, measurements 19-28.

Sensor	Position	Range	E_0	A	τ
Mg	Pos. 214	[19,28]	141.52±0.24	4.69±0.22	5.34±0.58
Salt	Pos. 55	[19,28]	134.28±0.09	6.36±0.22	1.04±0.09
Mg	Pos. 57	[19,28]	112.78±0.10	7.33±0.23	1.23±0.09
Mg	Pos. 59	[19,28]	122.92±0.10	2.99±0.25	1.10±0.22
Salt	Pos. 2	[19,28]	121.00±0.07	4.88±0.15	1.65±0.12

τ-values are not quite the same, but the result is qualitatively the same.

8.2.1 Results

This experiment clearly shows that there is a memory effect in the AD response.

The results indicate that this effect has the form of an exponential decay, with a "halftime" between 1 and 7 measurements. Closer inspection of the time-resolved data (not shown) reveals that the potential only drops when liquid is flushed through the chamber.

Furthermore the potential increases while the system is undisturbed, i.e. when it is not exposed to additional AD through samples or Rinse.

The consequences of this will be discussed in section 9.3.2.

Chapter 9

Discussion and Conclusion

This chapter summarizes the observed results from the experiments and discusses possible explanations. Areas for possible future research are introduced.

At the end my final hypothesis will be presented.

9.1 Conclusion

An ion selective electrode is a complex system, in which a large number of phenomena may occur. To describe the potential response of an electrode, several quite complex models have been developed. These models have ignored/neglected the effect of (non-ionic) surfactants. This thesis, however, demonstrates a case in which said effects cannot be ignored.

For a non-ionic surfactant of the "acetylenic diol"-type, a linear response to surfactant concentration is measured, while every model predicts a logarithmic response to linear changes in ion concentration/activity. This indicates a qualitative difference in the underlying phenomena.

For one class of sensors; "New" sensors not containing ionophore, the response was Nernstian, and fitted to a model proposed by Sak-Bosnar et al. [7].

Long term effects are also observed.

While several mechanisms may be proposed to account for the phenomena observed in systems containing surfactants, none have yet given a satisfying explanation.

9.2 Summary of Results

The main results of the thesis are summarized below:

9.2.1 Influence on Standard Parameters

The experiments that yielded information on the standard characteristic parameters of the sensors, and researched the influence of surfactant on these, found behavior of the sensors to be as expected, but no decisive causes for AD interference could be found from this analysis.

9.2.2 Surfactant Sensitivity

The experiments with direct measurement of sensitivity of the membrane towards concentrations of the surfactant reproduced the linear and symmetric response observed by Radiometer, with slopes around $0.15m$V/ppm AD $\approx 60m$V/$m$mol. This was also observed for sensors without ionophore, but not for sensors without lipophilic salt.

However, it was only reproduced for sensors that had been exposed to AD for several days.

"New" sensors demonstrated a different response:

- "New" Mg sensors did not respond to changes in AD concentration.
- "New" Ionophore-free sensors ("Salt"), responded in a Nernstian-like fashion, when first exposed to AD
- The total response these "Salt" sensors was a big as 170mV between 0 and 100ppm AD
- When samples were measured from high to low concentration, the response appeared linear, with slopes around $0.55mv$/ppm AD .

Fitting of the Nernst-like response to a model relating the potential to formation of ion-surfactant complexes, yielded a stoichimetry of 1-2 AD molecules pr. charge of ion.

None of these observations lead to a conclusive explanation of the AD interference.

The highly selective Calcium sensor did not show interference. This indicates that a highly selective ionophore reduces or eliminates surfactant interference.

9.2.3 Memory Effect

The clarifying experiment clearly showed that there was a memory effect in the AD response.

The results indicate that this effect has the form of an exponential decay, with a "halftime" between 1 and 7 measurements. Furthermore, the potential would rise between measurements, even without aditional exposure to AD , indicating that the phenomena is not simple to understand.

9.3 Discussion

The key findings and their consequences will be discussed in this section.

9.3.1 Time scales

The experiments demonstrated that while on one hand the sensors responded immediately to changes in AD concentration, there was also a second phenomena, happening on a much longer timescale.

I believe these two to be a surface-adsorption-related phenomena and a bulk partitioning phenomena, respectively.

9.3.2 Reversibility and Memory Effect

The researchers at Radiometer assumed that the effect of AD was Reversible due to the symmetric response described in section 7.7.1. The long time scale demonstrated in section 8.1, indicates that reversibility cannot be examined on shorter timescales. To research true reversibility, one would have to measure on a sensor before exposure to AD , expose it to AD for at least 48 hours (or more depending on the number of measurements performed in that period), until the AD sensitivity of the Mg sensor reached a steady value, and then measure on it after a very long period without AD .

9.3.3 Symmetric Response

The symmetric response in itself can be explained by assuming that the rinse between two measurements brings the sensors back to a ground state (i.e. full surface coverage and equilibrium bulk membrane partitioning of AD).

Each experiment "merely" measures a rate of desorption of AD from the sensor, rather than waiting for a true steady state.

This also means that it is not possible to conclude that there is a linear relation between AD concentration and EMF-response, but merely that there is a linear relation between the potential and the adsorption/desorption/partitioning as a function of concentration.

9.3.4 Nernstian-like Response

The data from "New" Salt sensors show a response that fits very well with the model proposed by Sak-Bosnar et al. [7]. The resulting stoichiometry of x/z_i between 0.5 and 1, seem reasonable.

However, the key assumptions of that model, i.e. that

i) The surfactant form a stable pseudo-cationic complex
ii) This complex form a hardly dissolvable salt in the membrane
iii) The membrane concentrations of pseudo-cationic complexes and salt are constant

are not well founded for a description of the system found in this thesis.

9.3.5 Surfactant Structure

From the Nernstian-like response it is natural to assume that AD complexates with ions.

However, the rotational freedom around the central triple-carbon bond makes this unlikely in the aqueous phase.

The structure is fixed on the surface, with parallel exthoxylate chains, which leads to the conclusion that AD can and does complexate at the surface.

In organic phase, one would expect the ethoxylate chains to shield the polar parts with the apolar parts. Whether this stabilizes the structure and allows complexation is a good question.

The irregular behavior could be caused by AD being present in both sample and bulk of the membrane, but only complexating at the surface.

9.4 Future Research

9.4.1 Surfactant Analysis

Acetylenic Diols are special, since they lower surface tension at a very low concentration, both under static and dynamic conditions. I believe this to be due to the geometry of AD . Specifically the Gemini-structure with very small hydrophobic and hydrophilic parts, would allow fast dynamics.

Unfortunately, the Gemini-structure might be what causes the interference, as it may invite complexation with ions (at least on the surface). If this complexation happens on the surface only, the response becomes dependent on the surface concentration of AD , which changes rapidly with concentration of samples.

Acetylenic Diols

It could be of great interest in understanding the phenomena, to research other ethoxylated acetelynic diols, e.g. the Surfynol family.

These are available with different ethoxylate chain lengths, and a correlations between the chain length and phenomena could provide valuable insight into the phenomena.

Alternative Surfactants

An alternative surfactant, which would have to be synthesized, could be a acetylenic-diol, with maltosides on the oxygen atoms, instead of ethoxylated chains, since Maltosides are not complexing agents[26]. This would have

approximately the same geometry as AD with regards to hydrophobic/hydrophilic parts, and the properties could then be investigated, to identify "ethoxylate"-specific phenomena.

Acetylenic Diols based surfactants with polyethylene amide chains (chains with NH-groups instead of O-atoms), could be researched. The geometry would be similar to the one investigated in this thesis, and complexation behaviour could be identified.

9.4.2 Analysis of Time Resolved Measurements

Interesting phenomena were observed, but are not documented here. It was observed that the sensor had an equilibration time of several seconds, in which the potential rose. Further analysis of this would be of great interest.

Since AD adsorbs to equilibrium surface coverage nearly immediately from aqueous solutions, the behaviour could be caused by adsorption from the bulk of the membrane, which has a much higher diffusion constant.

9.4.3 Theoretical Challenges

To understand this phenomena, I believe it is necesary to build an understanding of the following aspects:

Adsorption Isotherms The partitioning into the membrane phase means that adsorption to the surface can happen from both sides of the interface. Prediction of equilibrium surface cover fractions would be very useful for understanding the response of the sensors.

Partitioning Rates and equilibrium rates for partitioning of surfactants into the membrane phase

Stability of Complexes General stability of the complex that might be formed from an ion and the two short ethoxylated chains. This analysis should take into account the three different phases surfactant is present in, in the system:

- Dissolved in aqueous phase
- Dissolved in membrane phase, and
- Monolayer on surface

9.5 Final Hypothesis

At the end, I will introduce my final hypothesis of the phenomena:

- The AD interference is caused by surfactant-ion complexation at the surface only.

- AD adsorbs immediately to surface when concentration is raised in sample.
- AD partitions slowly into the membrane.
- AD can diffuse within the membrane, but with a low rate of diffusion,
- AD partitions into the membrane, without complexating to an ion, due to electroneutrality, as ionophores present in the membrane will already have complexated their primary ion.
- During a measurement without AD , AD is flushed of the membrane surface. However, it diffuses (slowly) from the bulk of the membrane to the surface, where it complexates with ions.
- Repeated measurements without AD gradually depletes the membrane bulk concentration of AD

This model could account for the two different timescales.

Appendix A

Chemical Names and Structures

Table A.1: Chemicals and Molecules

Abbreviation	Trivial Name	CAS number
DOP	Bis(2-ethylhexyl) phthalate	117-81-7
Triton X-100	4-(1,1,3,3-tetramethylbutyl)phenyl-polyethylene glycol	
Surfynol	2,5,8,11-tetramethyl-6-decyn-5,8-diol	
PVC	$(CH_2CHCl)_n$, poly(vinyl chloride)	9002-86-2
ETH 8045	[12-(4-Ethylphenyl)dodecyl] 2-nitrophenyl ether	155056-63-6
TPB	tetra-phenyl-borate	
3F-TPB	Tetrakis[3,5-bis(trifluoromethyl)phenyl] borate	105560-52-9
THF	Tetra-hydro-furan	109-99-9

A.1 Chemical Substances

Structural diagrams of some of the chemical substances used in the ISE technology.

Unless mentioned, the images are from Flu [34].

A.1.1 Surfactants

The surfactant Triton X-100, which was used extensively until it was found that it caused interference effects, i.e. Malinowska[26]. A very similar molecule has been tested as a Barium ionophore[14].

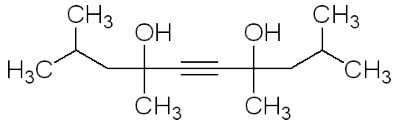

Figure A.1: Molecular structure of Surfynol.

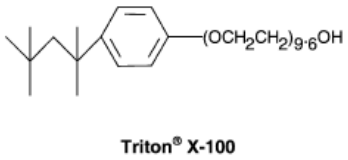

Figure A.2: Molecular structure of Triton X-100. n≈ 10

A.1.2 Ba Ionophore

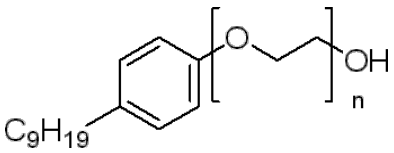

Figure A.3: Molecular structure of the Barium ionophore Igepal 890. $n \approx 40$. Notice the similarity with Triton X-100. CAS: 68412-54-4, linear formula: $(C_2H_4O)_n \cdot C_{15}H_{24}O$

A.1.3 Plasticizers

Here are the two plasticizers used in the membrane cocktails.

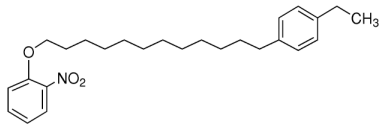

Figure A.4: ETH8045; The plasticizer used in the Mg-selective membranes.

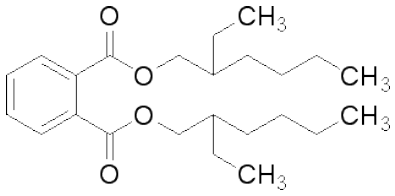

Figure A.5: DOP; The plasticizer used in the Ca-selective membranes.

A.1.4 Lipophilic salts

The lipophilic salts used in ISE's are generally derivatives of Tetra-phenyl-borate, which can be seen in figure A.6

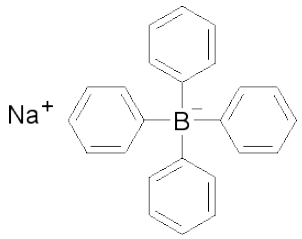

Figure A.6: TPB (Fluka 72018); A lipophilic salt.

A.1.5 A selection of Mg Ionophores

Magnesium ionophores.

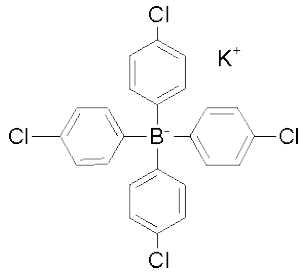

Figure A.7: Potassium tetra chlorophenyl borate (Fluka 60591); The lipophilic salt used in the magnesium membrane.

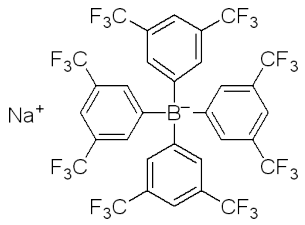

Figure A.8: TPB-TriFluoroMethyl (Fluka: 72017). A lipophilic salt. Used in some sensors.

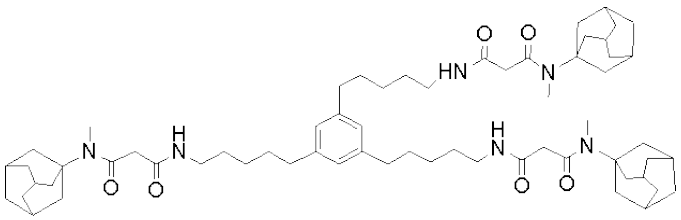

Figure A.9: Magnesium Ionophore ETH5506 (Fluka 63112.

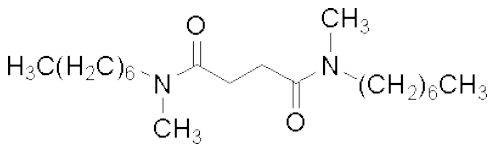

Figure A.10: Magnesium ionophore I, ETH 1117

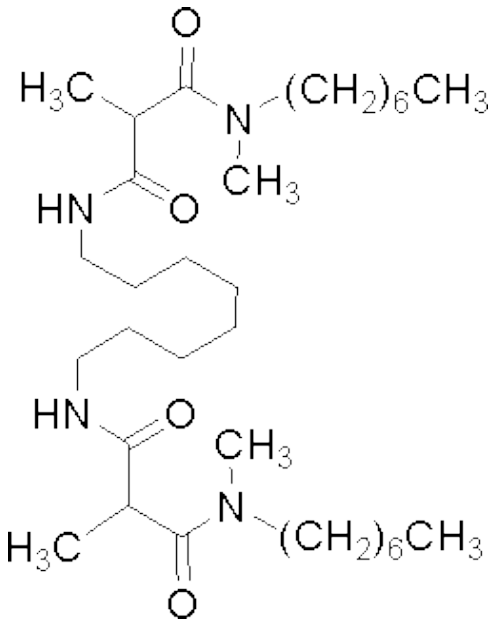

Figure A.11: Magnesium ionophore II, ETH 5214

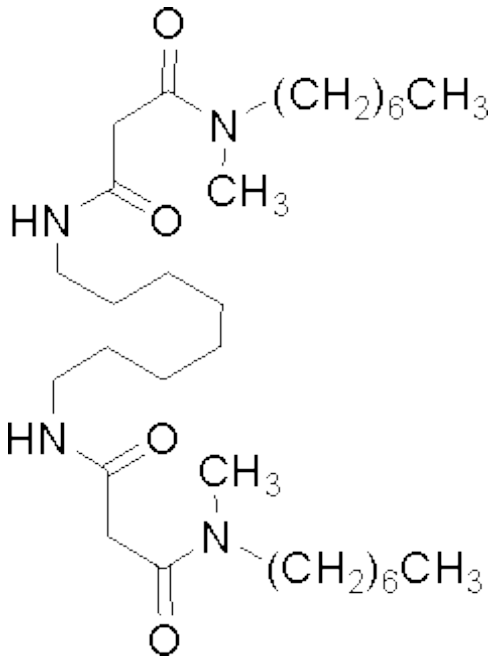

Figure A.12: Magnesium ionophore III, ETH 4030

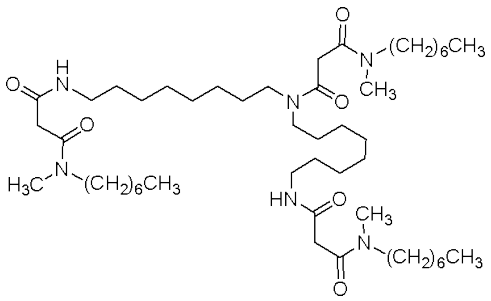

Figure A.13: Magnesium ionophore IV, ETH 7025

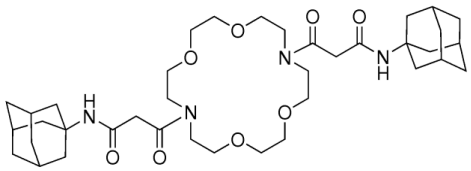

Figure A.14: Magnesium ionophore VI, K22B5

Appendix B

Single Ion Activity

B.1 Single Ion Activity

The section is based on [2, chap. 1, pp. 13-19], and references contained therein.

Membranes measure Single Ion Activities, not mean activities . It is possible to calculate this single ion activity in several cases, using different approximations, whose validity depends on the concentration, the ionic strength and the hydration degree of the ions.

The challenge is separating the mean activity, $\gamma_{\pm}$, into single ion activities γ_- and γ_+. The mean activity can be predicted from Debye-Hückel theory, and in the simple case of aqueous 1:1 electrolytes at $C \leq 0.1$M, it has the form:

$$\log \gamma_{\pm} = \log f_{DH} = -\frac{A\sqrt{I}}{1 + Ba\sqrt{I}},$$

where A and B are constants, and a is the ionic size parameter .

Ions of higher valencies, and at higher concentrations, can be described as developed by Stokes and Robinson [2, ref. 53],

$$\log \gamma_{\pm} = |z_+ z_-| \log f_{DH} + C'm, \tag{B.1}$$

which is a reduced form of the complete form

$$\log \gamma_{pm} = |z_+ z_-| \log f_{DH} - \frac{h}{\nu} \log a_w - \log\left(1 - 0.018(h - \nu)m\right), \tag{B.2}$$

which also takes the effects of hydration into account.

At low concentrations (C $\leq$ 1M), the Debye-Hückel convention holds [2, ref. 57,58]:

$$\log \gamma_+ = |z_+/z_-| \log \gamma_{\pm} \tag{B.3}$$

$$\log \gamma_- = |z_-/z_+| \log \gamma_{\pm} \tag{B.4}$$

At higher concentrations, the hydration of the ions must be taken into account, as by the Stokes-Robinson-Bates convention [2, ref. 59].

$$\log \gamma_+ = z_+^2 \log f_{DH} - h_+ \log a_w - \log\left[1 - 0.018(h - \nu)m\right] \tag{B.5}$$

$$\log \gamma_- = z_-^2 \log f_{DH} - h_- \log a_w - \log\left[1 - 0.018(h - \nu)m\right] \tag{B.6}$$

This formulation also makes it possible to tabulate values.

Appendix C

Ionic Mobilities

Table C.1: Mobilities

Ion	Equivalent ionic conductivity at infinite dilution, $\Lambda_i[\Omega^{-1}cm^2\text{equiv.}^{-1}$	Absolute Mobility, according to eqrefeq 4.27 i Morf $u_i \cdot 10^9[cm^2s^{-1}J^{-1}mol]$
H^+	350	37.6
Li^+	39.5	4.24
Na^+	50.9	5.47
K^+	74.5	8.00
Mg^{2+}	54	2.90
Ca^{2+}	60	3.22
Ba^{2+}	65	3.49
OH^-	192	20.6
Cl^-	75.5	8.11
I^-	76.0	8.16
NO_3^-	70.6	7.58

Appendix D

Recipe for Rinse

Table D.1: Recipe for the Rinse liquid used as base for surfactant sensitive experiments. The ionic concentrations correspond to physiological concentrations.

Content	Cal1/ Rinse
pH	7.3
pCO2 [mmHg]	35
pO2 [mmHg]	180
cK+ [mM]	4
cNa+ [mM]	150
cCa2+ [mM]	0.5
cCl- [mM]	95
Mg [mM]	0.15
NH4+ mM	3
HCO3- mM	17.8
buffer mM	70
Biocide [g/kg]	0.3
Ionic Strength [mM]	167

Appendix E

Results from Experimental – Standard Parameters

E.1 Tabulated Results from Sensitivity Experiments

Table E.1: Values resulting from non-linear fit of data to equation (6.4). Separate solutions are used as samples, as described in section 6.2

ID Number	2	55	57	59	207	214
Composition	Mg097	Mg098	Mg159	Mg160	Mg161	Mg162
$a_i = \{0.01, 0.1, 1, 10\}$mmol Mg						
No AD in System (28nov08						
E_0	78.93	92.23	178.65	182.32	92.50	86.53
S	0.00	1.67	19.49	19.36	0.00	2.71
SSR	140.74	294.21	91.96	96.18	216.50	773.08
AD in Rinse (01dec08						
E_0	56.47	56.04	144.81	144.79	69.81	67.50
S	0.00	0.40	18.42	18.02	1.28	0.00
SSR	126.62	186.85	244.56	251.74	433.25	212.99
AD in All (09dec08)						
E_0	43.76	38.36	117.16	115.24	35.42	40.93
S	6.88	8.14	27.23	24.73	6.05	4.69
SSR	195.76	207.91	956.35	207.01	117.94	65.13

E.2 Tabulated Results from Interference Measurement

This section contains the results from the data analysis performed in section 6.4.

Table E.2: Mg sensors interference from other Ions. FIM method used, see section 6.4.2

Background	$a_j = 1.2$ mMol Ca^{2+}		$a_j = 160$ mMol Na^+		$a_j = 4$ mMol K^+	
Position	57	59	57	59	57	59
Composition	Mg	Mg	Mg	Mg	Mg	Mg
No AD in System						
E_0	173.57	175.20	192.40	194.67	178.23	181.57
S	24.57	25.14	22.24	22.50	25.40	25.59
$K^{pot}_{i,j}$	0.39	0.58	5.49E-06	6.96E-06	4.23E-03	4.43E-03
SSR	108.54	18.61	4.68	6.22	7.58	4.69
AD in Rinse						
E_0	141.25	138.39	166.61	165.80	150.70	148.57
S	25.85	26.70	21.09	18.89	23.54	23.79
$K^{pot}_{i,j}$	0.63	0.77	3.64E-06	2.86E-06	2.61E-03	3.31E-03
SSR	11.12	10.27	14.40	48.40	13.71	14.14

Table E.3: Values resulting from non-linear fit of data to equation (6.5). FIM method used, see

ID Number	2	55	57	59	207	214
Composition	Mg097	Mg098	Mg159	Mg160	Mg161	Mg162
$a_j = 1.2$ mMol Ca^{2+} background						
No AD in System						
E_0	81.47	92.23	173.57	175.20	92.50	81.47
S	2.00	1.67	24.57	25.14	0.00	2.00
$K^{pot}_{\mathrm{Mg,Ca}}$	0.51	0.03	0.39	0.58	3.40	0.51
SSR	108.54	89.20	22.03	18.61	470.17	391.94
AD in Rinse						
E_0	43.50	24.97	141.25	138.39	80.19	70.85
S	15.25	28.42	25.85	26.70	19.62	0.00
$K^{pot}_{\mathrm{Mg,Ca}}$	7.03	12.25	0.63	0.77	0.08	0.47
SSR	25.80	47.23	11.12	10.27	2717.30	1026.30

Table E.4: Values resulting from non-linear fit of data to equation (6.5). FIM method used, see

ID Number	2	55	57	59	207	214
Composition	Mg097	Mg098	Mg159	Mg160	Mg161	Mg162
$a_j = 160$ mMol Na^{+} background						
No AD in System						
E_0	159.43	173.00	192.40	194.67	150.49	150.00
S	1.37	1.05	22.24	22.50	3.05	2.00
$K^{pot}_{\mathrm{Mg,Na}}$	7.24E-01	2.13E+00	5.49E-06	6.96E-06	5.32E+00	5.07E-01
SSR	34.74	37.71	4.68	6.22	1709.98	10857.67
AD in Rinse						
E_0	145.18	148.27	166.61	165.80	155.38	119.82
S	0.18	0.00	21.09	18.89	1.43	13.68
$K^{pot}_{\mathrm{Mg,Na}}$	6.52E-01	1.62E+00	3.64E-06	2.86E-06	5.10E-05	1.34E-02
SSR	54.92	53.78	14.40	48.40	70.02	38.10

Table E.5: Values resulting from non-linear fit of data to equation (6.5). FIM method used, see

ID Number	2	55	57	59	207	214
Composition	Mg097	Mg098	Mg159	Mg160	Mg161	Mg162
$a_j = 4$ mMol K^+ background						
No AD in System						
E_0	159.43	109.49	178.23	181.57	92.50	81.47
S	1.37	0.00	25.40	25.59	0.00	2.00
$K^{pot}_{\mathrm{Mg,Na}}$	7.24E-01	77.16	4.23E-03	4.43E-03	3.40	0.51
SSR	35763.02	42.33	7.58	4.69	5810.34	9981.19
AD in Rinse						
E_0	70.80	0.00	150.70	148.57	91.33	102.35
S	10.18	39.59	23.54	23.79	9.37	4.63
$K^{pot}_{\mathrm{Mg,Na}}$	1.50E+00	1.47E+01	2.61E-03	3.31E-03	4.84E+00	2.2E-01
SSR	26.00	17.53	13.71	14.12	84.26	13.28

Appendix F

Results from Experimental – Surfactant

F.1 Symmetry Plots of AD Sensitivity

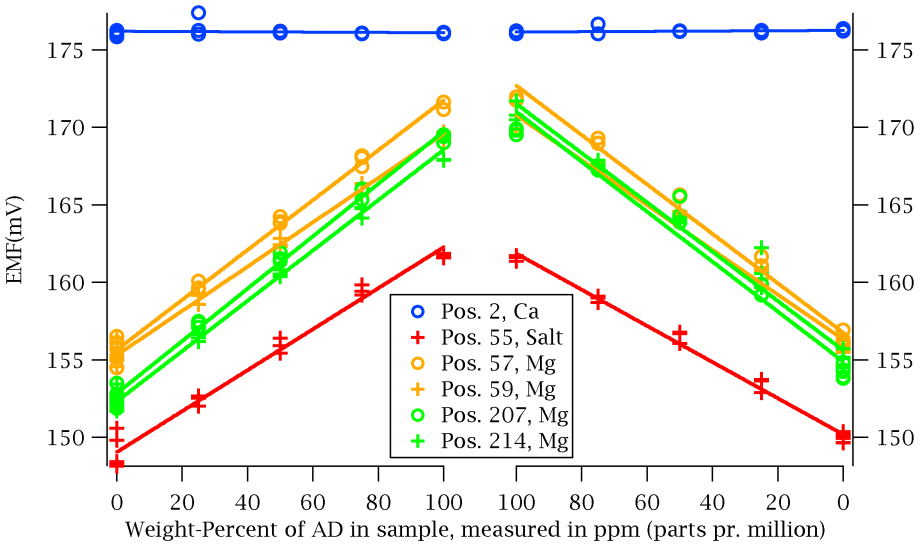

Figure F.1: AD Interference, and fit to linear response. Illustration of symmetry or lack thereof when increasing vs. decreasing sample order. ADLinSymmetry18jun08.png.

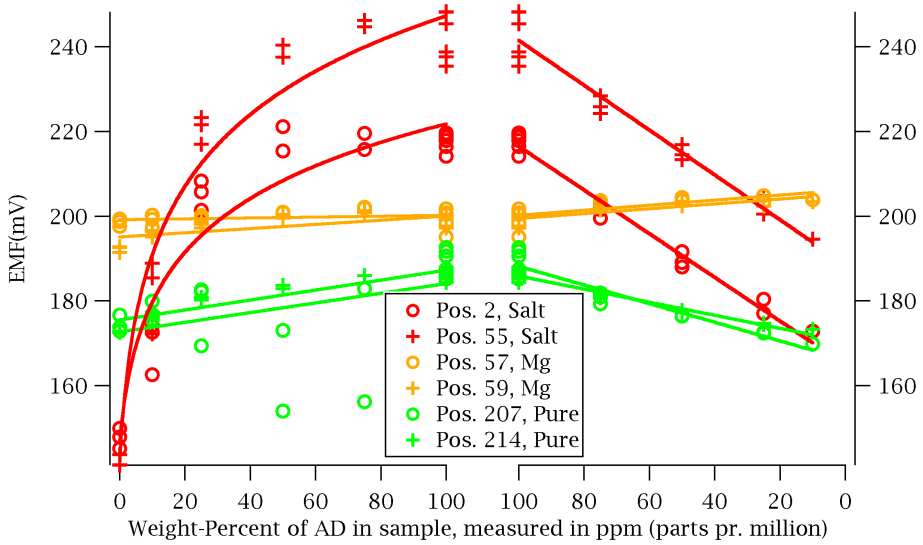

Figure F.2: AD Interference, and fit to linear response. Illustration of symmetry or lack thereof when increasing vs. decreasing sample order. ADLinSymmetry07jan09.png.

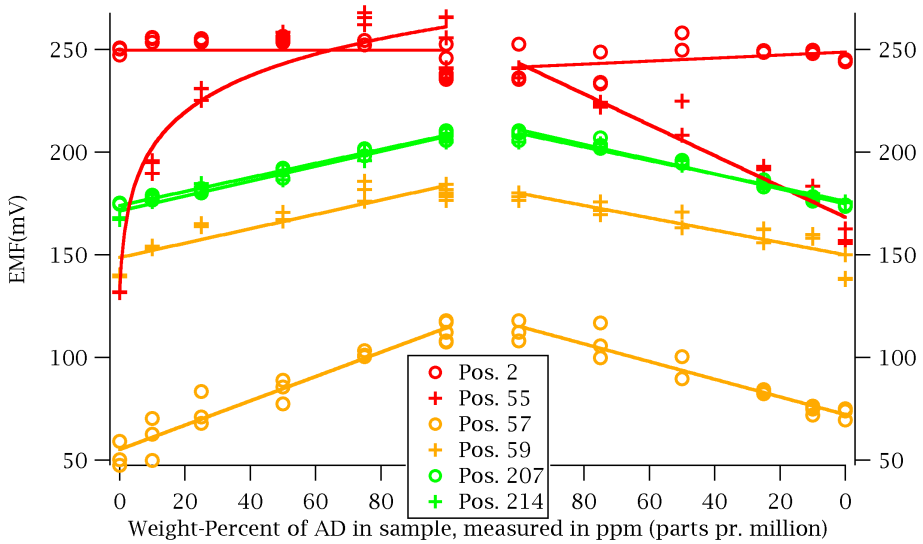

Figure F.3: AD Interference, and fit to linear response. Illustration of symmetry or lack thereof when increasing vs. decreasing sample order. ADLinSymmetry07jan09App9.png.

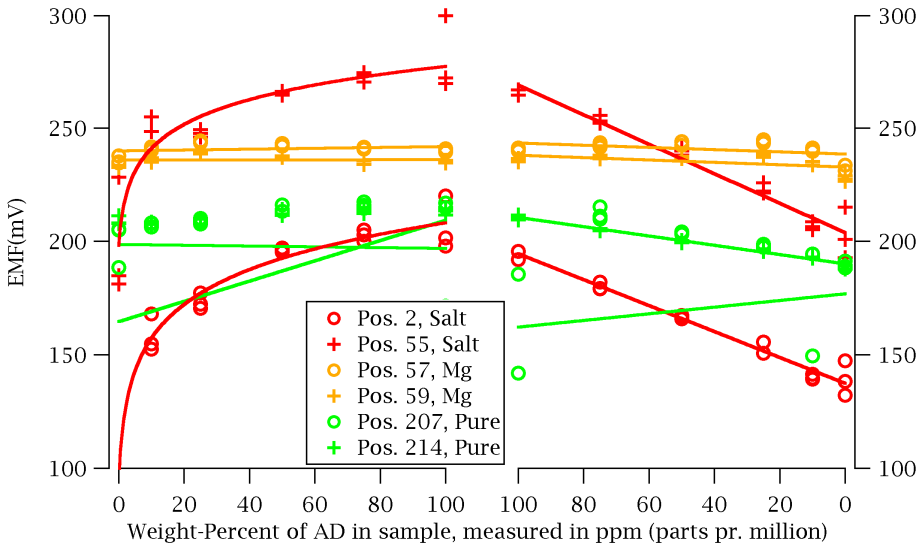

Figure F.4: AD Interference, and fit to linear response. Illustration of symmetry or lack thereof when increasing vs. decreasing sample order. A lot of noise in these measurements, presumably caused by bubbles. ADLinSymmetry16dec08.png.

F.2 Table with Sensor Response

Table F.1: Sensor response to AD . Maximum and minimum value of response noted. Some data points are ignored, as they lie outside of pattern.

Sensor Responses						
	Ca	Salt	DOP-Pure	DOP-Salt	DOP-Salt	DOP-Salt
07jan09	2	55	57	59	207	214
Emax	258.0	267.9	117.9	185.7	210.5	209.1
Emin	233.1	131.6	47.5	137.9	173.5	167.2
DeltaE	24.9	136.2	70.4	47.8	37.0	41.9
	Salt	Salt	Mg	Mg	Pure	Pure
07jan09	2	55	57	59	207	214
Emax	221.1	248.2	204.8	203.8	192.6	187.9
Emin	145.2	141.2	195.1	191.5	169.4	172.6
DeltaE	76.0	107.0	9.7	12.3	23.2	15.3
	Salt	Salt	Mg	Mg	Pure	Pure
16dec08	2	55	57	59	207	214
Emax	220.1	299.5	244.8	239.2	217.4	214.8
Emin	92.5	181.2	231.1	226.6	141.9	187.9
DeltaE	127.6	118.3	13.7	12.6	75.5	26.9
	Salt	Salt	Mg	Mg	Pure	Pure
09dec08 OLD	2	55	57	59	207	214
Emax	134.6	132.8	143.2	140.2	133.6	133.5
Emin	128.2	125.2	134.9	132.2	128.7	129.1
DeltaE	6.4	7.6	8.3	8.0	5.0	4.4
	Ca	Salt	Mg	Mg	Mg	Mg
16jun08 OLD	2	55	57	59	207	214
Emax	177.4	161.9	172.0	169.9	169.9	171.7
Emin	175.8	148.1	154.5	154.6	151.9	151.7
DeltaE	1.5	13.7	17.5	15.4	18.0	20.0

F.3 Fit Value tables

Table F.2: Results from fitting the response of "New" Salt sensors to an extended Nernstian Response. Results described in section 7.7.3.

Parameter	E_0	S	K
Pos. 2, 16dec08	103.53±8.55	52.27±5.07	0.68±0.30
Pos. 55, 16dec08	202.59±17.98	37.23±10.63	0.76±0.99
Pos. 2, 07jan09	129.51±13.94	45.89±7.64	2.36±1.51
Pos. 55, 07jan09	126.46±13.54	60.17±7.53	1.77±0.90
Pos. 55, App9	139.64±16.39	60.60±9.36	0.73±0.54

Appendix G

Results from Experimental – Clarifying Experiments

G.1 Figures

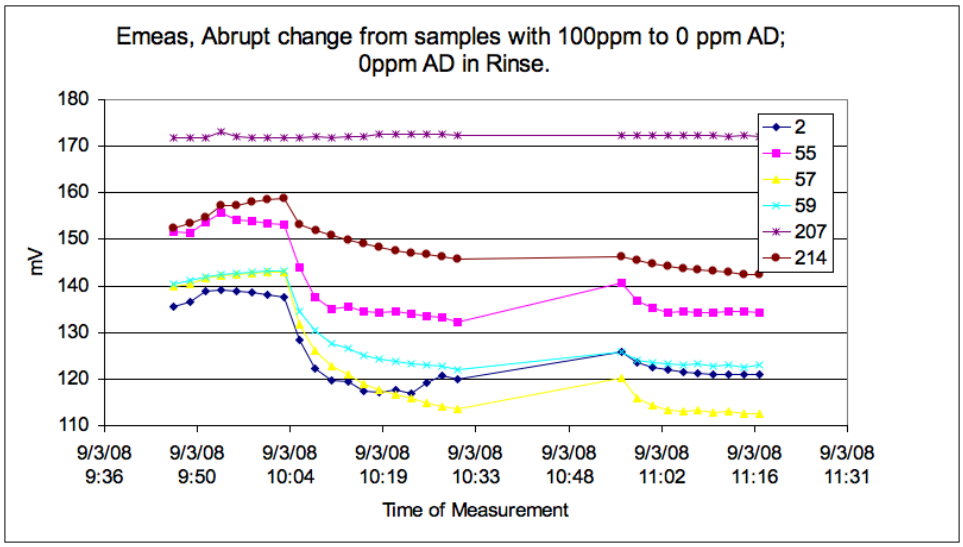

Figure G.1: Long memory effect when changing from samples with 100ppm AD to samples with 0ppm AD , when there is no AD in rinse. Notice the rise in potential between the two measurement series.

G.2 Tabulated Results

Table G.1: Coefficients for fit of $E = A\exp((x - x_0)/\tau)$ on the Rinse Liquid potential E_{rinse}.

Sensor	E_0	A	τ
Pos. 2[8-15]	119.03±2.83	19.55±4.32	1.61±0.91
Pos. 55[8	141.29±0.93	14.51±2.44	1.09±0.43
Pos. 57[8	115.08±1.56	27.80±1.72	3.29±0.57
Pos. 59[8	124.98±1.20	18.43±1.64	2.65±0.62
Pos. 207[8	521.64±Inf	-351.46±Inf	-13891.00±Inf
Pos. 214[8	148.73±1.19	13.43±1.19	3.70±0.93

Table G.2: Coefficients for fit of $E = A\exp((x - x_0)/\tau)$ on E_{meas}.

Sensor	Position	Range	E_0	A	τ
Ca	Pos. 207	[8,18]	172.94±0.93	-1.15±0.86	8.69±11.8
Mg	Pos. 214	[8,18]	143.48±0.38	9.58±0.34	7.28±0.53
Salt	Pos. 55	[8,18]	133.72±0.33	10.06±0.85	1.19±0.23
Mg	Pos. 57	[8,18]	112.78±0.51	18.39±0.52	3.64±0.29
Mg	Pos. 59	[8,18]	122.18±0.21	12.04±0.27	2.80±0.17
Salt	Pos. 2	[8,15]	117.12±0.35	11.21±0.60	1.39±0.19
Salt	Pos. 2	[8,18]	118.46±0.51	10.05±1.42	0.96±0.32

Table G.3: Coefficients for fit of $E = A\exp((x - x_0)/\tau)$ on Second round, measurements 19-28.

Sensor	Position	Range	E_0	A	τ
Ca	Pos. 207	[19,28]	164±331	8.4136±331	335.89±1.34e+04
Mg	Pos. 214	[19,28]	141.52±0.245	4.6933±0.22	5.3417±0.577
Salt	Pos. 55	[19,28]	134.28±0.0915	6.3646±0.226	1.0498±0.0897
Mg	Pos. 57	[19,28]	112.78±0.103	7.332±0.237	1.2348±0.0943
Mg	Pos. 59	[19,28]	122.92±0.103	2.9873±0.25	1.1019±0.22
Salt	Pos. 2	[19,28]	121±0.079	4.8846±0.151	1.6545±0.122

Appendix H

Confidential Appendix

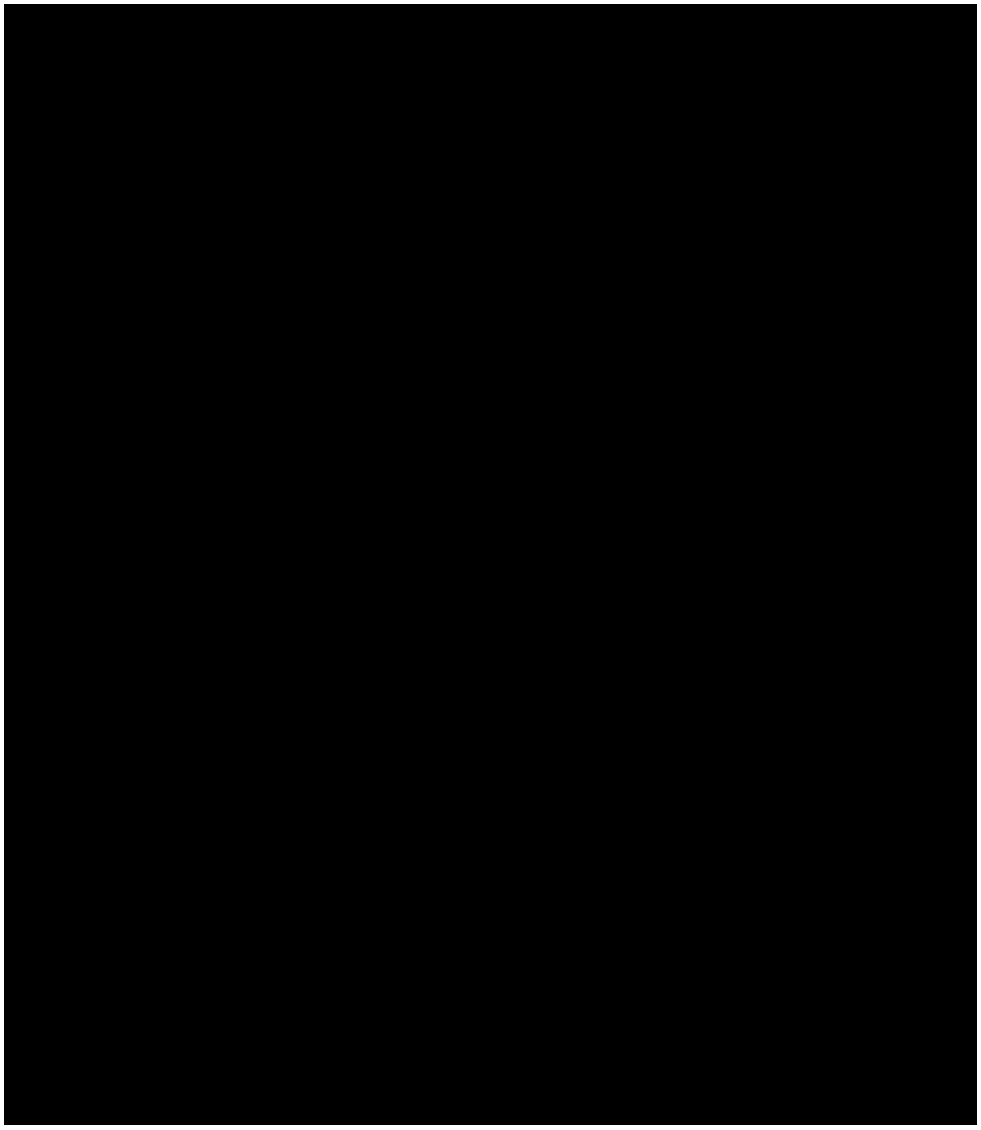

H. Confidential Appendix

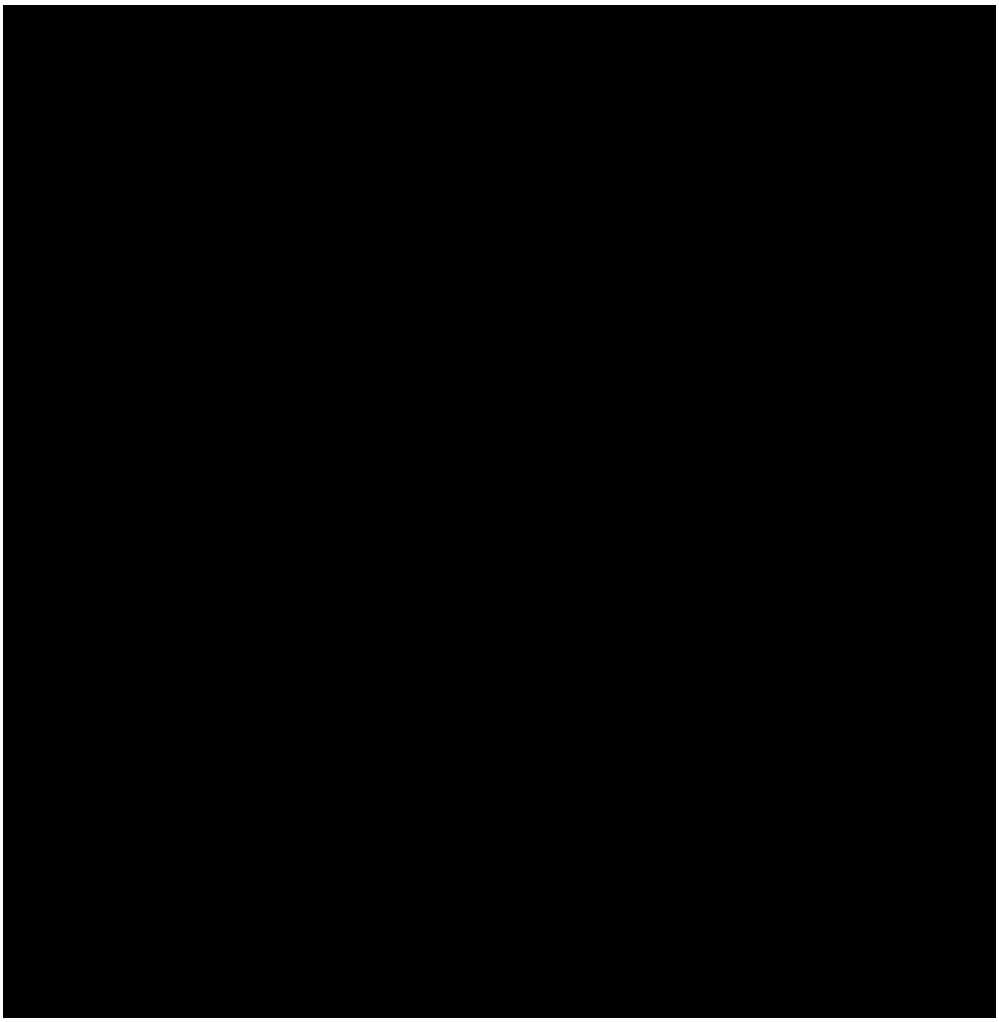

Bibliography

[1] Ernö Buck, Richard P.and Lindner. Recommendations for nomenclature of ionselective electrodes (iupac recommendations 1994). *Pure Appl. Chem.*, 66(12):2527–2536, 1994. doi: doi:10.1351.

[2] W E Morf. *The principles of ion-selective electrodes and of membrane transport*. Elsevier Scientific Publishing Company, 1981.

[3] Brian L. Silver. *The Physical Chemistry of Membranes*. The Solomon Press, 1985.

[4] E. Bakker, P. Buhlmann, and E. Pretsch. Carrier-based ion-selective electrodes and bulk optodes. 1. general characteristics. *Chemical Reviews*, 97(8):3083–3132, 1997. ISSN 0009-2665. URL http://pubs3.acs.org/acs/journals/doilookup?in_doi=10.1021/cr940394a.

[5] Erno Pretsch. The new wave of ion-selective electrodes. *TrAC Trends in Analytical Chemistry*, 26(1):46–51, 2007. URL http://www.sciencedirect.com/science/article/B6V5H-4MC71B8-1/2/a1effaae501042e2d283d65ce46e8d5f.

[6] Sergey Makarychev-Mikhalov, Alexey Shvarev, and Eric Bakker. *Electrochemical Sensors, Biosensors and their Biomedical Applications*, chapter New trends in ion-selective electrodes, pages 71–109. Academic Press, 2008.

[7] Milan Sak-Bosnar, Dubravka Madunic-Cacic, Ruzica Matesic-Puac, and Zorana Grabaric. Nonionic surfactant-selective electrode and its application for determination in real solutions. *Analytica Chimica Acta*, 581(2):355–363, 1 2007/1/9. URL http://www.sciencedirect.com/science/article/B6TF4-4KNV2P1-5/2/b01bc6c5d49c15e8be37f957f3af8ccd.

[8] Israel Rubinstein. Fundamentals of physical electrochemistry. In Israel Rubinstein, editor, *Physical Electrochemistry: principles, methods, and applications*. Marcel Dekker, Inc., 1995.

[9] Eric Bakker, Philippe Buhlmann, and Erno Pretsch. The phase-boundary potential model. *Talanta*, 63(1):3–20, 2004. URL http://www.sciencedirect.com/science/article/B6THP-4CB0JS6-1/2/92ffa34805bb8ca03fd10dd668e894f3.

[10] Yoshio Umezawa. *Liquid Interfaces in Chemical, Biological, and Pharmaceutical Applications.*, volume 95 of *Surfactant Science Series.*, chapter Liquid Membrane Ion-Selective Electrodes: Response Mechanisms Studied by Optical Second Harmonic Generation and Photoswitchable Ionophores as a Molecular Probe, pages 439–468. Marcel Dekker, Inc., 2001. doi: 10.1021/ja015249a. URL http://pubs.acs.org/doi/abs/10.1021/ja015249a.

[11] Mathias Nagele, Eric Bakker, and Erno Pretsch. General description of the simultaneous response of potentiometric ionophore-based sensors to ions of different charge. *Analytical Chemistry*, 71(5):1041–1048, 1999. doi: 10.1021/ac980962c. URL http://pubs.acs.org/doi/abs/10.1021/ac980962c.

[12] Roland Glaser. *Biophysics.* Springer Verlag, 4th edition, 1996.

[13] Stephen W. Feldberg. On the dilemma of the use of the electroneutrality constraint in electrochemical calculations. *Electrochemistry Communications*, 2(7):453–456, 2000. URL http://www.sciencedirect.com/science/article/B6VP5-40PGR9W-1/2/fc19f16681f4023c9e885ab1d918902b.

[14] P. Buhlmann, E. Pretsch, and E. Bakker. Carrier-based ion-selective electrodes and bulk optodes. 2. ionophores for potentiometric and optical sensors. *Chemical Reviews*, 98(4):1593–1688, 1998. ISSN 0009-2665. URL http://pubs3.acs.org/acs/journals/doilookup?in_doi=10.1021/cr970113+.

[15] Rudolf. Eugster, Ursula E. Spichiger, and Wilhelm. Simon. Membrane model for neutral-carrier-based membrane electrodes containing ionic sites. *Analytical Chemistry*, 65(6):689–695, 1993. doi: 10.1021/ac00054a007. URL http://pubs.acs.org/doi/abs/10.1021/ac00054a007.

[16] Richard P. Buck and Ernö Lindner. Tracing the history of selective ion sensors. *Analytical Chemistry*, 73(88), February 2001. doi: 10.1021.

[17] Poul Ravn Sørensen and Birgit Zachau-Christiansen. Electrode device with a solid state reference system. US 2004/Patent number: 6,805,781 B2, August 2004.

[18] Poul Ravn Sørensen. Ion-selective electrodes with sodium vanadium oxide as the internal reference element. In *The 14th European Conference on Solid-State Transducers (EUROSENSORS XIV). August 27-30, 2000, Copenhagen, Denmark*, 2000.

[19] Qingshan Ye, A. Vincze, G. Horvai, and F. A. M. Leermakers. Partial blocking of ion transport at the interface of an ion-selective liquid membrane electrode by neutral surfactants: Experiments and computer simulation. *Electrochimica Acta*, 44(1):125–132, 1998. URL http://www.sciencedirect.com/science/article/B6TG0-3VGV20K-J/2/3f3f550f4029aef1375371c4d913d9b7.

[20] Anna Kisiel, Agata Michalska, Krzysztof Maksymiuk, and Elisabeth A. H. Hall. All-solid-state reference electrodes with poly(n-butyl acrylate) based membranes. *Electroanalysis*, 20(3):318–323, 2008. URL http://dx.doi.org/10.1002/elan.200704065.

[21] *Electrode Catalogue, Radiometer Analytical SAS*, 2006. URL http://www.radiometer-analytical.com/pdf/meterlab/Electrode_Guide_en.pdf.

[22] R. W. Cattrall and Henry. Freiser. Coated wire ion-selective electrodes. *Analytical Chemistry*, 43(13):1905–1906, 1971. doi: 10.1021/ac60307a032. URL http://pubs.acs.org/doi/abs/10.1021/ac60307a032.

[23] Adam Malon, Tamas Vigassy, Eric Bakker, and Erno Pretsch. Potentiometry at trace levels in confined samples: ion-selective electrodes with subfemtomole detection limits. *Journal of the American Chemical Society*, 128(25):8154–8155, 2006. URL http://pubs.acs.org/doi/abs/10.1021/ja0625780.

[24] *ABL 700 Reference Manual*. Radiometer.

[25] Ursula E. Spichiger-Keller. Ionophores, ligands and reactands. *Analytica Chimica Acta*, 400(1-3):65–72, 1999. URL http://www.sciencedirect.com/science/article/B6TF4-3XX6871-9/2/be8cfeffa8759677e64d427e0a50ba5a.

[26] Elzbieta Malinowska, Angelo Manzoni, and Mark E. Meyerhoff. Potentiometric response of magnesium-selective membrane electrode in the presence of nonionic surfactants. *Analytica Chimica Acta*, 382(3):265–275, 1999. URL http://www.sciencedirect.com/science/article/B6TF4-3VX9XPY-4/2/a6542435df8530133ce8b73e46738c0f.

[27] Haim Diamant and David Andelman. Models of gemini surfactants. In R. Zana and J. Xia, editors, *Gemini Surfactants: Interfacial and Solution Pahse Behavior*. Marcel Dekker, New York, 2003.

[28] Ekta Khurana, Steven O. Nielsen, and Michael L. Klein. Gemini surfactants at the air/water interface; a fully atomistic molecular dynamics study;. *The Journal of Physical Chemistry B*, 110(44):22136–22142, 2006. doi: 10.1021/jp063343d. URL http://pubs.acs.org/doi/abs/10.1021/jp063343d.

[29] Roland De Marco, Jean-Pierre Veder, Graeme Clarke, Andrew Nelson, Kathryn Prince, Erno Pretsch, and Eric Bakker. Evidence of a water layer in solid-contact polymeric ion sensors. *Physical Chemistry Chemical Physics*, 10(1):73–76, 2008. doi: 10.1039/b714248j.

[30] Thomas Heimburg. *Thermal Biophysics of Membranes*. Tutorials in Biophysics. Wiley-VCH, 2007.

[31] Marco Giannetto, Claudia Minari, and Giovanni Mori. Potentiometric determination of non-ionic surfactants by liquid membrane electrodes. *Electroanalysis*, 15(20):1598–1605, 2003. URL http://dx.doi.org/10.1002/elan.200302727.

[32] S. W. Musselman and S. Chander. Wetting and adsorption of acetylenic diol based nonionic surfactants on heterogeneous surfaces. *Colloids and Surfaces A: Physicochemical and Engineering Aspects*, 206(1-3):497 – 513, 2002. ISSN 0927-7757. doi: DOI:10.1016/S0927-7757(02)00055-9. URL http://www.sciencedirect.com/science/article/B6TFR-45D15S5-3/2/b13335b05212486e55f1522dea89244c.

[33] James K. Ferri and Kathleen J. Stebe. A structure-property study of the dynamic surface tension of three acetylenic diol surfactants. *Colloids and Surfaces A: Physicochemical and Engineering Aspects*, 156(1-3):567–577, October 1999. ISSN 0927-7757. URL http://www.sciencedirect.com/science/article/B6TFR-3X94KT9-1R/2/1364bd1e7e6f7f6081feda5a3a02f69b.

[34] Fluka online product catalogue. URL http://www.sigmaaldrich.com/technical-service-home/product-catalog.html.

[35] S. Walsh and D. Diamond. Non-linear curve fitting using microsoft excel solver. *Talanta*, 42(4):561 – 572, 1995. ISSN 0039-9140. doi: DOI:10.1016/0039-9140(95)01446-I. URL http://www.sciencedirect.com/science/article/B6THP-3YS8N5R-6N/2/894e2a6ee7c632cd4c1f2f82997a379a.

[36] Paddy Kane and Dermot Diamond. Determination of ion-selective electrode characteristics by non-linear curve fitting. *Talanta*, 44(10):1847–1858, 1997/10. URL http://www.sciencedirect.com/science/article/B6THP-3ST28MG-M/2/e646e26377de6c092973ca1210f5794a.